

Aus dem
CharitéCentrum 14 für Tumormedizin
Klinik für Hämatologie, Onkologie und Tumorummunologie
Direktor: Prof. Dr. Ulrich Keller

Habilitationsschrift

Die Entwicklung T-Zell basierter Immuntherapien durch optimierte Isolation und Analyse von HLA Liganden

zur Erlangung der Lehrbefähigung
für das Fach Experimentelle Hämatologie und Onkologie

vorgelegt dem Fakultätsrat der Medizinischen Fakultät
Charité-Universitätsmedizin Berlin

**von Dr. med. Martin Gunther Klatt
geboren in Kitzingen**

Eingereicht: Januar 2024

Dekan: Prof. Dr. med. Joachim Spranger

Inhaltsverzeichnis

Abkürzungsverzeichnis	3
1. Einleitung	4
1.1 Molekulare Grundlagen der Präsentation von HLA Liganden	4
1.2 Immunpeptidomik als Goldstandard der Targetidentifikation	6
1.3 Untergruppen von tumorspezifischen Zielantigenen	10
1.4 Therapeutische Ansätze für T-Zell basierte Immuntherapien	13
2. Eigene Arbeiten	15
2.1 Fragestellung	15
2.2 Optimierung und Standardisierung der HLA Liganden Isolation	16
2.2.1 Optimierung der HLA Liganden Isolation	16
2.2.2 Standardisierung der HLA Liganden Isolation	27
2.3 Pharmakologische Modulation des Immunpeptidoms	35
2.3.1 Epigenetische Modulatoren	35
2.3.2 Modulation durch Tyrosinkinaseinhibitoren	51
2.4 Entwicklung einer tumoragnostischen TZR-imitierenden CAR-T-Zelle	65
3. Diskussion	80
3.1 Absolute Sensitivität und Spezifität von T-Zell basierten Therapien	80
3.2 Limitationen der Therapie und der Wirkstoffentwicklung	82
3.3 Zukünftige Herausforderungen	84
4. Zusammenfassung	87
5. Literaturverzeichnis (eigene diskutierte Arbeiten)	89
6. Literaturverzeichnis (andere Arbeiten)	90
7. Danksagung	96
8. Erklärung	97

Abkürzungsverzeichnis

ACN	Acetonitril
ALK	ALK Tyrosin Kinase Rezeptor
CAR	Chimeric Antigen Receptor = Chimärer Antigen Rezeptor
CGA	Cancer Germline Antigen
CTG1B	Cancer Testis Antigen 1
CDK4/6	Cyclin Dependent Kinase 4/6 = Zyklin abhängige Kinase 4/6
CHAPS	3-[(3-Cholamidopropyl)dimethylammonium]-1-propansulfonat
CNBr	Cyanobromid
CTC	Circulating Tumor Cell = Zirkulierende Tumorzelle
DDA	Data Dependent Acquisition = Datenabhängige Messung
DIA	Data Independent Acquisition = Datenunabhängige Messung
DLBCL	Diffuse Large B-Cell Lymphoma = Diffus großzelliges B-Zell-Lymphom
ERAP1	Endoplasmatisches Retikulum Aminopeptidase 1
EZH2	Histon-Lysin N-Methyltransferase EZH2
HLA	Humanes Leukozyten Antigen
HPLC	Hochleistungsflüssigchromatographie
IFN- γ	Interferon gamma
KRAS	Kirsten Rat Sarcoma Onkogen
LOH	Loss of Heterozygosity = Verlust der Heterozygotie
LTR	Long Terminal Repeat = lange endständige Sequenzwiederholung
MAGE-A3	Melanom assoziiertes Antigen A3
MAGE-A4	Melanom assoziiertes Antigen A4
MAGE-A12	Melanom assoziiertes Antigen A12
MS/MS	Tandem-Massenspektrometrie
OPG	<i>n</i> -Octyl- β -D-glucoopyranosid
pHLA	Peptid:Humanes Leukozyten Antigen Komplex
PRAME	Präferenziell exprimiertes Antigen in Melanomen
PSMC1	26S Proteasom regulatorische Untereinheit
RET	RET Tyrosin Kinase Rezeptor
scFv	Single Chain Variable Fragment
TZR	T-Zell Rezeptor
TAP1	Antigen Peptid Transporter 1
TIL	Tumor infiltrierender Lymphozyt
TP53	Tumor Protein 53

1. Einleitung

Mit der Zulassung des Checkpoint-Inhibitors Ipilimumab 2011 wurde der große Erfolg der T-Zell vermittelten Immuntherapien eingeleitet (1). Seither haben sich viele Behandlungskonzepte der Onkologie grundlegend verändert und folgerichtig wurde diese bahnbrechende Entdeckung 2018 mit dem Nobelpreis für Physiologie und Medizin für Tasuku Honjo und Jim Allison honoriert. Checkpoint-Inhibitoren verdeutlichten wie keine andere Therapie zuvor das Potenzial von T-Zellen für die Therapie von metastasierten Tumorerkrankungen. Im Zentrum dieser Therapie steht die unspezifische Aktivierung von T-Zellen und daraus resultierend die Interaktion von T-Zell-Rezeptoren (TZR) und Peptiden, welche auf humanen Leukozytenantigenen (HLAs) den T-Zellen präsentiert werden.

Seitdem hat die Entwicklung und Zulassung von Immuntherapien rasant zugenommen und neben den unspezifischen Immuntherapien rücken immer mehr auch spezifische Immuntherapien in den Mittelpunkt der Forschung und der klinischen Praxis. Den vorläufigen Höhepunkt erlangte diese Entwicklung mit der Zulassung von Tebentafusp (2), einem Fusionsmolekül, welches einerseits das Peptid YLEPGPVTA aus dem Melanom-assoziierten Protein gp100 im Kontext von HLA-A*02:01 mit Hilfe eines TZR erkennt und mit der zweiten Hälfte des Moleküls T-Zellen über deren CD3 Antigen bindet. Dies führt zur Aktivierung der T-Zellen, welche dann über die Freisetzung zytotoxischer Substanzen wie Granzyme und Perforine die Tumorzellen zerstören. Dieses Medikament stellt die erste zugelassene Therapie dar, welche mittels eines TZR Tumorzellen erkennen und zerstören kann und zu einem verlängertem Gesamtüberleben von Patient:innen mit metastasiertem Aderhautmelanom gegenüber der Standardtherapie mit Chemotherapie führt (3). Dies verdeutlicht, dass die weitere Entwicklung von TZR basierten Immuntherapien ein wichtiges Forschungsfeld der Onkologie darstellt, welches in den kommenden Jahren hoffentlich weiter zur Verbesserung der klinischen Versorgung von Patient:innen mit Tumorerkrankungen beitragen wird.

1.1 Molekulare Grundlagen der Präsentation von HLA Liganden

Für den Erfolg der oben genannten Therapien ist es unumgänglich, dass die erkannten Zielpeptide, welche zur Aktivierung der T-Zellen führen, an der Oberfläche der Tumorzellen präsentiert werden. Die Präsentation von Peptiden auf HLA Komplexen kann hierbei auf zwei unterschiedlichen Unterformen von Komplexen stattfinden, HLA Klasse I und Klasse II. Da die Expression von HLA Klasse II Proteinen in erster Linie antigenpräsentierenden Zellen vorbehalten ist und viele Tumorarten somit keine HLA Klasse II Präsentation aufweisen, beschränkt sich diese Arbeit auf die Peptide, welche auf HLA Klasse I präsentiert werden. HLA Komplexe der Klasse I wiederum finden sich auf allen kernhaltigen Zellen des

menschlichen Körpers sowie auf Thrombozyten und sofern kein funktioneller Verlust vorliegt auch auf allen Arten von Tumorzellen.

Der klassische Präsentationsmechanismus verläuft dabei in Grundzügen folgendermaßen (4): Wenn Proteine nicht mehr benötigt werden oder bei deren Produktion ein Fehler aufgetreten ist, werden diese Proteine ubiquitiniert und über das Proteasom degradiert. Die resultierenden Peptide werden über einen Transporter TAP1 (peptide transporter involved in antigen processing 1) in das endoplasmatische Retikulum eingebracht und dort nach eventueller Kürzung der Peptide durch Aminopeptidasen im endoplasmatischen Retikulum (ERAP1) mit Hilfe von Chaperonen auf HLA Komplexe geladen. Über vesikulären Transport erreichen dann diese Peptid:HLA Komplexe die Zellmembran und werden dort den T-Zellen präsentiert. Entscheidend für den gesamten Prozess ist hierbei dessen Komplexität im Kontext der Evolution. Eine hohe Diversität der präsentierten Peptide hat sich offensichtlich als evolutionärer Vorteil erwiesen, weswegen das HLA Protein System einen sehr starken Polymorphismus aufweist. Aktuell sind knapp 40,000 unterschiedliche HLA Allele beschrieben (5), welche sich in ihren Eigenschaften bezüglich der Peptidpräsentation teils relevant unterscheiden. Dies erweitert dadurch nochmals die Möglichkeiten des Immunsystems möglichst vielen unterschiedliche Zielstrukturen den T-Zellen zu präsentieren.

Einer der größten biologischen, aber auch therapeutischen Vorteile dieses Prozesses ist die Tatsache, dass dieser Präsentationsmechanismus es erlaubt, auch intrazelluläre Proteine dem Repertoire möglicher Targets für Immuntherapien hinzuzufügen. Dies ist von besonderer Relevanz, da etwa nur ein Drittel des menschlichen Proteoms an der Zelloberfläche präsentiert wird (6) und die verbleibenden zwei Drittel deutlich schwierig pharmakologisch erreichbar sind. Um dieses große Repertoire an Zielmolekülen nutzbar zu machen, ist es aber unerlässlich, die exakte Aminosäuresequenz der Peptide zu identifizieren, da diese die Grundlage für alle nachfolgenden spezifischen T-Zell-Therapien darstellt. Aus diesem Grund sollen nun auch die Regeln für die Präsentation von Peptiden auf HLA Klasse I Komplexen noch etwas detaillierter beleuchtet werden.

Auf Grund ihrer hohen genetischen Homologie sind alle HLA Klasse I Allele, und hier insbesondere, die sogenannten klassischen A-, B-, und C-Allele, in der Lage, Peptide von einer Länge von 8-12 Aminosäuren zu präsentieren (7). Präferiert werden hierbei neun Aminosäuren, wobei sich auch HLA-Allele finden, welche überproportional häufig Peptide von 8 Aminosäuren Länge präsentieren wie z.B. HLA-B*08. Verantwortlich hierfür ist die sogenannte Bindungsfurche in Kombination mit Bindetaschen im HLA Komplex, welche durch ihre biochemischen Eigenschaften das Repertoire an Peptiden definiert, welches von einem bestimmten Allel gebunden werden kann (8). Wenige HLA-Allele, z.B. HLA-A*24:02, HLA-B*07:02 oder HLA-B*35:01 sind darüber hinaus in der Lage deutlich längere Peptide (bis zu 25 Aminosäuren Länge) zu komplexieren, wobei die Peptide dann N- oder C-terminal über die

gewöhnlichen Grenzen der Bindungsfurche hinausragen oder stark gebogene dreidimensionale Ausrichtungen einnehmen (9). Die Besonderheit der HLA-Komplexe liegt an deren spezifischen Bindemotiven, welche sich in erster Linie aus der Physik der Bindetaschen ergeben, welche ihrerseits Aminosäuren mit ähnlichen biochemischen oder biophysikalischen Eigenschaften wie Größe, Ladung oder Hydrophobizität präferieren. Diese Aminosäuren werden zusammen als Ankeraminosäuren bezeichnet. Die Bindetaschen treten hierbei meist an Position 2 des Peptids sowie an dessen C-Terminus auf. Zur Veranschaulichung führt Tabelle 1 einige HLA Allele mit deren bevorzugten Ankeraminosäuren auf.

Tabelle 1. Beispiele von Bindemotiven verschiedener HLA Allele		
HLA Allel	Präferierte Aminosäuren 1. Tasche	Präferierte Aminosäuren 2. Tasche
HLA-A*02:01	L, I, M	V, L, I, M
HLA-A*03:01	L, V, I, T	K, Y
HLA-B*07:02	P	L, M, V, I, F
HLA-B*40:01	E	L, M

(E=Glutaminsäure, F=Phenylalanin, I=Isoleucin, K=Lysin, L=Leucin, M=Methionin, P=Prolin, T=Threonin, V=Valin, Y=Tyrosin)

Nach der erfolgreichen Isolation von HLA Liganden sind diese Bindemotive hilfreich bei der Zuordnung welche Peptide auf welchen HLA Komplexen präsentiert werden. Das folgende Kapitel soll die einzelnen Schritte der Isolation von HLA Liganden nun näher beleuchten.

1.2 Immunozeptidomik als Goldstandard der Targetidentifikation

In Anbetracht des großen Erfolgs von T-Zell basierten Immuntherapien ist es erstaunlich, dass erst Mitte der 1980er erstmals gezeigt werden konnte, dass Peptide auf HLA Komplexen präsentiert und von T-Zellen erkannt werden (10). Anfang der 1990er Jahre wurden dann Techniken entwickelt, welche es erlaubten, die auf den HLA Komplexen präsentierten Peptide systematisch zu analysieren (11-12). Die Grundlage dieser Technik bildet die Immunpräzipitation von HLA Komplexen in Kombination mit der anschließenden Trennung von Peptiden und HLA Molekülen und schließlich die Identifizierung der Peptidsequenzen mittels Hochleistungsflüssigchromatographie gekoppelter Tandem-Massenspektrometrie (HPLC-MS/MS). Diese Technik wird heute unter dem Begriff der Immunozeptidomik zusammengefasst und ist die einzige verfügbare Technik, welche es zweifelsfrei erlaubt diejenigen Peptide zu definieren, welche auf der Zelloberfläche von Tumorzellen präsentiert werden. In den vergangenen Jahren wurden nicht nur die Techniken zur biochemischen Isolation von HLA Liganden kontinuierlich weiterentwickelt (13,14), sondern auch die

massenspektrometrischen Analyseverfahren (15,16) sowie die bioinformatische Auswertung (17,18). Insgesamt sind wir nun dadurch im Stande aus wenigen Millionen Tumorzellen Tausende von HLA Liganden zu isolieren (19) und in Bezug auf deren Eignung als tumorspezifische Immuntherapietargets zu untersuchen. Die einzelnen Schritte sollen nun im Detail erläutert werden.

Für den ersten Schritt der Immunpräzipitation ist es unumgänglich das zu untersuchende Zellmaterial (Zellen aus Zellkultur, Tumorproben, Organoide etc.) zu lysieren. Hierbei sollten für die Herstellung der Lysepuffer nicht-ionische Detergenzien verwendet werden, da ionische Moleküle im Massenspektrometer zu deutlichen Hintergrundsignalen führen, welche die Messungen beeinträchtigen. Neben dem nicht-ionischen Tensid *n*-Octyl- β -D-glucopyranosid (OPG) wird auch sehr häufig das zwitterionische Molekül 3-[[3-Cholamidopropyl)dimethylammonium]-1-propansulfonat (CHAPS) verwendet. Beide Substanzen sind nicht-denaturierend und eignen sich besonders für die Aufreinigung von membrangebundenen Proteinen wie den HLA Komplexen. Nach Inkubation der Zellen und anschließender Zentrifugation wird das resultierende Proteinlysate mit Antikörpern inkubiert, welche klassischer Weise entweder an einer Affinitätssäule oder unterschiedlichen Beads immobilisiert werden. Bei der Verwendung von Protein-A-Beads wird der gebundene Antikörper häufig chemisch mit Natriumtetraborat gecrosslinkt um eine spätere Ko-Elution des Antikörpers zu verhindern, was die weitere Aufreinigung der HLA Liganden erschwert und die Wiederverwendung der Beads ermöglicht (15). Eine andere Methode basiert analog den Beads auf der Verwendung von Sepharose. Diese spezielle Sepharose trägt jedoch Cyanobromid (CNBr) Seitenketten, welche mittels Säure aktiviert werden und somit einen nukleophilen Angriff von primären Aminogruppen ermöglichen. Diese werden meist von N-Termini von Proteinen bereitgestellt, welche dann kovalent an die Sepharose gekoppelt werden und somit ebenfalls nicht nach erfolgreicher Immunpräzipitation mit den HLA Komplexen eluiert werden. Die zur Herstellung der Affinitätschromatographie verwendeten Antikörper sind meistens (wie auch in den später diskutierten Publikationen) gegen humane Proteine wie z.B. die Klasse I Moleküle HLA-A,B,C (Klon W6-32) oder Klasse II Komplexe wie z.B. HLA-DR (Klon L243) gerichtet. Alternativ können jedoch auch Antikörper gegen mausspezifische MHC Komplexe (z.B. Klon Y-3 gegen H2-Kb) oder TZR-imitierende Antikörper zur Evaluation der Targetspezifität verwendet werden. Im direkten Vergleich dieser beiden Strategien zur Prävention der Elution der Antikörper hat sich ein kleiner Vorteil gegenüber der CNBr-Verlinkung gegenüber dem Natriumtetraborat basierten Verfahren gezeigt, was in einer ca. 20% höheren Ausbeute an unterschiedlichen HLA Liganden bei der CNBr-Methode widerspiegelt (13).

Diese mit Antikörper beladenen Säulen oder Beads sind dann in der Lage die HLA Komplexe aus den Proteinlysaten spezifisch herauszufiltern. Nach kurzem Waschen des Affinitätsmaterials kann dann eine Elution, z.B. mit Trifluoressigsäure erfolgen, welche am weitesten verbreitet ist. Diese führt nicht nur zum Herauslösen der HLA Komplexe, sondern denaturiert auch leicht die freigesetzten HLA Komplexe, so dass diese die nicht-kovalent gebundenen Peptide aus der Bindungsfurche freigeben. Es resultiert somit ein Gemisch aus Anteilen des HLA Komplexes (α -Kette sowie β 2-Mikroglobulin) und der bis dahin gebundene Peptide. Um diese nun voneinander zu trennen, haben sich drei Methoden etabliert. Die älteste und unkomplizierteste nutzt Zentrifugationskonzentratoren mit Membranen, welche Moleküle gemäß ihrer molekularen Masse selektionieren können. Werden hier Filter mit einer Selektionsgröße von 3 kDa verwendet, können die deutlichen schwereren und größeren Peptidketten (α -Kette sowie β 2-Mikroglobulin) von 44 kDa und 12 kDa den Filter nicht passieren, wohingegen die Peptide, welche meist zwischen 0,8 und 1,5 kDa liegen problemlos filtriert werden. Demgegenüber steht ein Verfahren, welches nicht auf dem unterschiedlichen Gewicht oder Größe, sondern auf der resultierenden Hydrophobizität der Moleküle basiert. Hierbei wird das Gemisch aus α -Kette, β 2-Mikroglobulin und Peptiden auf eine tC18 Säule geladen, welche vor allem mittels van-der-Waals-Wechselwirkungen diese an die vorhandenen Kohlenstoffmoleküle bindet. Nun können mittels definierter Konzentrationen eines unpolaren Lösungsmittels wie Acetonitril (meist ca. 30%) die Peptide selektiv eluiert werden, wohingegen die deutlich stärker mit der Säule wechselwirkende α -Kette und das β 2-Mikroglobulin an dieser verbleiben. Diese Methode hat sich als deutlich potenter gegenüber dem Filter erwiesen (13), wobei der genaue Mechanismus hierfür nicht abschließend geklärt werden kann. Es kann spekuliert werden, dass der Filter doch nicht so gut wie erwartet die Peptide passieren lässt. Eine andere Vermutung wäre, dass die Peptide teilweise nicht komplett aus den HLA Komplexen durch die Trifluoressigsäure herausgelöst werden und das Acetonitril diesen Prozess bei der Variante mit der tC18 Säule begünstigt. Man kann sich hierbei jedoch leicht vorstellen, dass Peptide gemäß ihrer unterschiedlichen Hydrophobizität besser oder schlechter von der tC18 Säule eluieren wenn eine konstante Konzentration an Acetonitril verwendet wird. Eine der Publikationen wird sich noch im Detail mit diesem Problem befassen. Um eine möglichst große Bandbreite an unterschiedlichen Acetonitrilkonzentrationen für die Elution verwenden zu können, hat insbesondere die Arbeitsgruppe um Anthony Purcell ein Verfahren entwickelt, bei welchem sie diesen Elutionsschritt mittels einer eigenen HPLC durchführen und die entstehenden Fraktionen als separate Proben weiterverwenden und im Massenspektrometer messen. Dies hat zu einer signifikanten Zunahme der Ausbeute an HLA Liganden geführt. Der zusätzliche HPLC Schritt sowie die über zehnfache Erhöhung der Messzeit am Massenspektrometer durch die Vergrößerung der

Probenzahl haben jedoch dazu geführt, dass diese Methode bisher nur punktuell verbreitet ist (14). Alle diese Methoden führen zu einer suffizienten Trennung von Peptiden und Komponenten des HLA Komplexes, welche die weitere Analyse ermöglicht. Dennoch bleibt dies wohl der wichtigste und teilweise stark unterschätzte Schritt der Isolation, da viele HLA Liganden an diesem Punkt verloren gehen oder insuffizient eluiert werden, was eine spätere Detektion im Massenspektrometer erschwert oder unmöglich macht.

Die isolierten Peptide können nun in eine Kombination aus HPLC und Tandemmassenspektrometer eingespeist werden. Da eine ausführliche Einführung in die Massenspektrometrie den Rahmen der Arbeit sprengen würde und nicht den Schwerpunkt meiner Arbeit darstellt, wird diese nicht im Detail dargestellt werden. Kurz zusammengefasst erlaubt die HPLC erneut eine Auftrennung aller zu analysierenden Peptide gemäß ihrer biochemischen Eigenschaften, allen voran gemäß ihrer Hydrophobizität. Kleine Peptidmengen, werden aus der HPLC kommend meist in einem Elektrospray ionisiert, welches durch die Konzentration von Ionen auf engem Raum entsteht. Der genaue Mechanismus ist nach wie vor nicht eindeutig geklärt, die wahrscheinlichste Erklärung ist jedoch, dass sogenannte Coulomb-Explosionen die Bildung des Elektrosprays initiieren. Die so entstandenen Ionen können nun vom Massenspektrometer angesammelt, detektiert, gefiltert und letztlich fragmentiert werden. Hierbei ist zum einen zu erwähnen, dass die Entwicklung der sogenannten Orbitrap Massenspektrometer die Analyse von HLA Liganden entscheidend vorgebracht hat (20). Im Vergleich zu früheren Time-of-flight Massenspektrometern, welche an Hand der unterschiedlichen Flugzeit das Masse-zu-Ladung-Verhältnis eines Moleküls errechneten, nutzen Orbitrap Massenspektrometer die Tatsache, dass Ionen, welche tangential um eine spindelförmige Elektrode oszillieren, mit einer Kreisfrequenz oszillieren, die zu deren Ladung-zu-Masse-Verhältnis proportional ist. Somit lässt sich das Ladung-zu-Masse-Verhältnis aus der Kreisfrequenz berechnen, was eine deutlich schnellere Messung der Peptide erlaubt. Essenziell für die Bestimmung der Aminosäuresequenz ist jedoch die zweistufige Messung der Peptide. Zuerst wird die Gesamt-Masse-zu-Ladung bestimmt und im Anschluss werden bestimmte oder alle Peptide meist durch die Kollision mit inerten Edelgasen fragmentiert. Die Fragmentierung der Peptide mit den stärksten Signalen in der ersten Messung wird dabei als „data dependent acquisition“ (DDA) und die Fragmentierung aller Peptide als „data independent acquisition“ (DIA) bezeichnet. Letztere rückt immer mehr in den Vordergrund, da verbesserte Analysealgorithmen die Auswertung dieser Daten erleichtern und damit auch Peptide mit niedriger Abundanz besser detektierbar machen (15). Die Analyse aller dieser Daten beruht jedoch auf der Tatsache, dass die durch Kollision entstehenden Fragmente, welche dann wiederum vom Massenspektrometer detektiert werden, unterschiedliche Masse-zu-Ladung-Verhältnisse aufweisen und dass jeder proteinogenen Aminosäure mit Ausnahme von Leucin

und Isoleucin ein individueller Wert zugeordnet werden kann. Dies ermöglicht dann ähnlich einem Sequenzierungsverfahren das schrittweise Aufschlüsseln der einzelnen Aminosäuren innerhalb einer Peptidsequenz. Dabei ist zu betonen, dass auch hier die automatisierten Algorithmen zur Bestimmung dieser Sequenzen erhebliche Fortschritte gemacht haben, wobei leider die wissenschaftliche Grundlage dafür bei den kommerziellen Programmen nicht offengelegt wird. Auch wenn open-source Algorithmen vorhanden sind und eine hinreichend gute Analyse erlauben, sind manche kommerzielle Programme diesen in vielen Aspekten weiterhin überlegen (17,18). Insbesondere die „de novo Sequenzierung“, einem Verfahren bei welchem der Zuordnung der Aminosäuresequenz keine Datenbank für die annotierbaren Sequenzen zu Grunde liegt, bleibt komplex und kann nur von wenigen Algorithmen zufriedenstellend gelöst werden (16).

Zusammenfassend lässt sich allerdings sagen, dass alle Schritte von der Isolation bis zur Analyse von HLA Liganden in den vergangenen Jahren eine deutliche Verbesserung erfahren haben und nur dadurch die Immunpeptidomik als weiteres Puzzleteil der „Multi-omics“ anerkannt werden kann auch wenn sie neben der Genomik und Proteomik noch einen untergeordneten Stellenwert in der allgemeinen Wahrnehmung einnimmt. Für die Identifikation von Zielstrukturen für T-Zell basierte Therapien bildet sie jedoch den unumstößlichen Goldstandard und ist die einzige Methode, welche die Präsentation von HLA Liganden beweisen kann. Welche Arten von tumorspezifischen Peptiden isoliert werden können soll nun der Inhalt des folgenden Abschnitts sein.

1.3 Untergruppen von tumorspezifischen Zielantigenen

Auf der Suche nach tumorspezifischen Targets für Immuntherapien kommt immer wieder die Frage auf, welche Gruppen von Antigenen sich als ideale Kandidaten erweisen. Hierbei steht vor allem die Tumorspezifität im Vordergrund, welche sich aus einer exklusiven Expression des Antigens in den Tumorzellen ableitet. Hieraus ergeben sich unterschiedliche Subgruppen von Antigenen, welche die Mehrzahl der adressierten Targets darstellt. Es muss jedoch betont werden, dass eine Tumorspezifität auch bei vorhandener Expression eines Genes in gesundem Gewebe auf dem Level der Immunpeptidomik vorhanden sein kann, da unterschiedlichste Aspekte der Antigenprozessierung in den verschiedenen Geweben die Präsentation der HLA Liganden entscheidend beeinflussen.

Dennoch ist die wohl am häufigsten untersuchte Gruppe die der Cancer-Germline Antigene (CGAs). Der Grund hierfür liegt in deren oft Tumorentitäten überspannenden aberranten Expression und hohen Expressionsfrequenz innerhalb einzelner Tumortypen wie z.B. am Beispiel von MAGE-A4 deutlich wird, ein CGA dessen Expression in einer Studie in einem Drittel aller Tumorproben von Ösophaguskarzinomen, Ovarialkarzinomen und Kopf-Hals-Tumoren nachgewiesen werden konnte (21). Es ist aber sehr wichtig zu betonen, dass per

Definition diese Gene zusätzlich neben den Tumoren beinahe ausnahmslos im Hoden und dem Ovar exprimiert werden. Außerdem konnten viele CGAs, welche als tumorspezifisch eingeordnet wurden, nach genauer Analyse sowohl auf dem Expressionslevel als auch als HLA Liganden in weiteren Organen wie dem Uterus oder Ösophagus nachgewiesen werden, wie das Beispiel des PRAME Proteins gut illustriert (22). Des Weiteren ist zu beachten, dass viele CGAs eine hohe Sequenzhomologie aufweisen, was in Verbindung mit unterschiedlichen Expressionsmustern der vermeintlich tumorspezifischen CGAs bereits fatale Nebenwirkungen zur Folge hatte: Eine Zielsequenz aus MAGE-A3, welche von einem TZR erkannt werden sollte, wurde in sehr ähnlicher Weise vom neuronal exprimierten MAGE-A12 präsentiert, was zu neurologischen Toxizitäten mit Todesfolge in frühen klinischen Studien geführt hat (23). Im Gegensatz dazu definieren viralen Antigene eine deutlich kleinere, aber sehr wichtige Gruppe an Antigenen, welche eine nochmals höhere Tumorspezifität aufweisen, da sie direkt in die Onkogenese der Tumoren involviert sind. So konnten zum Beispiel HLA Liganden aus dem E7 Protein des Humanen Papillomavirus wiederholt in Proben von Zervixkarzinomen nachgewiesen werden ohne dass bisher ein Nachweis in gesunden Gewebeproben gelang (24).

Die wohl interessanteste Gruppe für tumorspezifische Targets stellen die HLA Liganden aus „public neoepitopes“ dar. Dies sind HLA Liganden, welche aus mutierten Onkogenen stammen, welche für die Entstehung des Tumors unerlässlich sind (25, 26), wie z.B. KRAS-Mutationen im Pankreaskarzinom. Hierdurch erreichen diese HLA Liganden nicht nur eine sehr hohe Tumorspezifität per se, sondern es sollten auch alle Subklone des Tumors therapeutisch angebar sein, da diese alle von den entsprechenden Onkogenen abhängig sind. Da diese Untergruppe scheinbar ideale Targets zur Verfügung stellt, ist ihre systematische Erforschung von sehr großem Interesse. Es muss dennoch betont werden, dass die häufig angewandte Strategie der Vorhersage von public neoepitopes *in silico* und der nachfolgende Nachweis einer T-Zell Aktivierung durch diese Peptidsequenzen kein Beweis für die therapeutische Aktivität dieser Sequenzen darstellt, da nur der Nachweis deren Präsentation auf der Tumorzelloberfläche diese HLA Liganden als relevante Targets definiert. Zum Nachweis dieser Präsentation haben sich inzwischen Überexpressionssysteme etabliert, welche systematisch Kombinationen aus HLA Allelen und mutierten Onkogenen in einer Zelle überexprimieren und mittels Immunpeptidomik die Präsentation von mutierten HLA Liganden evaluieren (27). Der Grund hierfür ist, dass in vielen Zelllinien public Neoepitopes sehr schwer nachzuweisen sind, da sie oft nur in sehr geringer Anzahl präsentiert werden und somit die Sensitivität der Massenspektrometrie an ihre Grenzen stößt. Dies illustriert andererseits die Mechanismen der Immunsurveillance, da diese HLA Liganden bewusst von den Tumoren schlecht präsentiert werden, um eine Elimination durch das Immunsystem zu vermeiden. Dies wird unter anderem von einer Arbeit unterstützt, welche zeigen konnte, dass unter dem

immunologischen Selektionsdruck der Immuncheckpointblockade vor allem diejenigen HLA Allele von Tumoren deletiert werden, welche in der Lage sind diese mutierten Onkogene zu präsentieren (28). Dies relativiert teilweise die Eignung dieser Gruppe als ideale Targets, wobei die positiven Aspekte der Tumorspezifität und der breiten Anwendbarkeit über Tumorentitäten hinweg diesen Nachteil wahrscheinlich mehr als ausgleicht.

Zwei weitere Gruppen von potenziellen Zielstrukturen leiten sich in ähnlicher Weise von den biologischen Unterschieden von Tumoren und Normalgewebe ab. Einer liegt in den unterschiedlichen Phosphorylierungsmustern, welche über die Aktivierung von pathogenen Signalwegen zur Präsentation von phosphorylierten HLA Liganden führt, welche sonst womöglich nicht präsentiert werden würden. Mehrere Arbeiten haben mögliche tumoragnostische Targets in Form von phosphorylierten HLA Liganden identifiziert und konnten zugleich zeigen, dass die Immunogenität dieser Liganden essenziell von der Phosphorylierung abhängig ist (29-31). Das Problem bei der systematischen Targetidentifikation bei phosphorylierten HLA Liganden ist jedoch das Fehlen einer guten Kontrollgruppe in gesunden Geweben. Der bereits erwähnte HLA Ligand Atlas mit seiner systematischen Analyse des Immunopeptidoms gesunder Gewebe hat diese leider nicht auf post-translational modifizierte HLA Liganden ausgeweitet, so dass die Tumorspezifität dieser Targets leider deutlich schwerer zu beantworten ist. Ein ähnliches Problem trägt die Gruppe der sogenannten kryptischen HLA Liganden. Dies fasst in den meisten Definitionen diejenigen Peptide zusammen, welche durch unkonventionelle Transkription und Translation entstehen. Beispiele hierfür sind eine veränderte ribosomale Prozessierung der mRNA, d.h. alternative Reading Frames (32) oder die Transkription und Translation von sonst irrelevanten genomischen Regionen, wie z.B. von Long Terminal Repeats (LTRs) aus ehemals retroviralen genomischen Sequenzen, welche noch in humaner DNA kodiert sind und durch die Therapie mit epigenetisch wirksamen Substanzen wieder aktiviert werden können (33).

Die letzte Gruppe in dieser Aufzählung sind diejenigen HLA Liganden, welche ihre Spezifität dadurch erlangen, dass sie ausschließlich unter der Einwirkung von bestimmten Medikamenten in Tumorzellen präsentiert werden. Als Beispiel seien hier ALK- und RET-Inhibitoren genannt, für welche nicht nur gezeigt werden konnte, dass diese direkt das Wachstum von Tumorzellen hemmen, sondern auch das Immunpeptidom relevant derart verändern, dass bisher unbekannte HLA Liganden präsentiert werden und diese von T-Zellen erkannt werden können (34). Hierbei handelt es sich allerdings um ein Prinzip, welches sich stark verallgemeinern lässt, da die pharmakologische Manipulation von Tumorzellen durch die Veränderungen auf dem Level des Proteoms zu einer Änderung des Immunpeptidoms führen. Inwieweit Tumorspezifität durch diese Modulation des Immunpeptidoms erlangt werden kann, muss für viele Wirkstoffe jedoch noch abschließend geklärt werden.

Abschließend soll aber nochmals betont werden, dass es für beinahe alle diese HLA Liganden erst die Immunpeptidomik war, welche es ermöglichte deren Existenz zu beweisen und sie als relevante Targets der Immuntherapien zu definieren. Deshalb ist es für die im folgenden Kapitel vorgestellten therapeutischen Ansätze zwingend erforderlich, die Präsentation der Targets auf den Tumorzellen in relevanter Anzahl nachzuweisen.

1.4 Therapeutische Ansätze für T-Zell basierte Immuntherapien

Vor dem Hintergrund der technischen Verbesserungen in Bezug auf die Immunpeptidomik, d.h. der Isolation und Analyse von HLA Liganden, sind wir nun in der Lage immer mehr tumorspezifische Targets für T-Zell basierte Immuntherapien zu definieren. Hierbei war die Publikation des „HLA Ligand Atlas“ von großer Bedeutung, da dieser erstmalig systematisch eine Vielzahl an gesunden Gewebeproben einer immunpeptidomischen Analyse unterzog und damit erlaubt die Tumorspezifität von HLA Liganden enger einzugrenzen (22).

Zusätzlich zu den neuen Erkenntnissen im Bereich der Immunpeptidomik waren es aber Fortschritte in der Medikamentenentwicklung und insbesondere dem Bioengineering, welche nun drei unterschiedliche Therapieansätze erlauben, welche alle in klinischen und präklinischen Studien berücksichtigt werden (35). Einer der ältesten Ansätze besteht darin, eine Vakzinierung mittels Peptiden oder RNA durchzuführen, welche tumorspezifische HLA Liganden kodieren und somit zu einer Verstärkung der Immunantwort gegen Tumorzellen führen sollen. Da initiale Ansätze mit alleiniger Vakzinierung keine positiven klinischen Ergebnisse erbrachten (36), ist nun die Kombination mit Checkpoint-Inhibitoren zum Standard geworden, welche zu deutlich besseren klinischen Resultaten, z.B. auch im adjuvanten Setting der Therapie des Pankreaskarzinoms führten (37). Insgesamt ist es auch wahrscheinlich, dass Vakzinierungsstrategien zur Unterstützung der Immunsurveillance in der Adjuvanz erfolgversprechender erscheinen, da die immunsuppressiven Mechanismen der Tumoren noch nicht vollständig etabliert sind. Im Anschluss an die Vakzinierung erfolgt im Rahmen der Studien dann ein Immunmonitoring, welches reaktive T-Zell Klone gegen die HLA Liganden der Vakzinierung nachverfolgt und über deren Vergrößerung die Erfolgsaussichten der Therapie abzuschätzen versucht. Auch wenn dieses Vorgehen sich als Goldstandard etabliert hat, soll hier darauf hingewiesen werden, dass eine Evaluation der Präsentation der Targets essenziell wäre. Auf Grund der Kürze der Zeit für die Zusammenstellung einer individuellen Vakzine erscheint dies oft nicht möglich (37), obwohl es für die sinnvolle Interpretation der Ergebnisse hoch relevant wäre. Die Nutzung von HLA Liganden aus CGAs mit gesicherter Präsentation stellt hier eine gute Alternative dar, welche bis heute nicht in einem hinreichend guten Setting klinisch evaluiert wurde, da Immunpeptidom Daten sehr lange nicht als Standard in die Auswahlkriterien integriert wurden.

Die aktuell wohl am häufigsten genutzte Herangehensweise ist die Isolation von T-Zell-Rezeptoren gegen tumorspezifische HLA Liganden mit dem Ziel einer adoptiven T-Zell Therapie. Dies beinhaltet die genetische Modifikation von aus Patient:innen gewonnenen T-Zellen *ex vivo*, welche zur Expression eines tumorspezifischen TZR führt, und die anschließender Rückgabe der T-Zellen nach einer lymphodepletierenden Chemotherapie. Nach initialen Rückschlägen in frühen klinischen Studien (23,38) sind nun zuletzt vielversprechende Ergebnisse für HLA Liganden aus den Genen MAGE-A4 (39) und CTG1B (40) publiziert worden. Eine große technische Herausforderung stellt in diesen Studien das Screening der Patient:innen dar, da neben der Evaluation der korrekten HLA-Status auch die Expression der Targetantigens in den Tumorzellen mittels Biopsie bestätigt werden muss. Auch wenn diese beiden Komponenten die Voraussetzungen für eine Präsentation des HLA Liganden sind, lassen sich dennoch keine sicheren Schlüsse über die Präsentation ziehen. Eine Evaluation der Korrelation zwischen HLA Liganden Präsentation und klinischen Ansprechen ist demnach eine Frage, welche von höchster Relevanz ist, aber bis heute in den oben genannten Studien leider unbeantwortet bleibt.

Eine Strategie, welches dieses Problem umgeht und sich ebenfalls schon lange in klinischer Erprobung befindet, ist die Nutzung von tumor-infiltrierenden Lymphozyten (TILs). Ausgehend von der Annahme, dass den Tumor infiltrierende Immunzellen diesen effektiv bekämpfen, werden Lymphozyten aus diesen Tumoren expandiert, den Patient:innen wieder zurückgeführt und die Expansion dieser Zellen mit Interleukin-2 unterstützt. Diese Strategie hat zu einer deutlichen Verbesserung des progressionsfreien Überlebens bei der Behandlung des Melanoms geführt im Vergleich zur Immuncheckpointblockade (41). Trotz dieses Erfolges bleibt die Frage, ob diese Strategie gut auf andere Tumore übertragbar sein wird, da dies eine hohe Immunogenität des Tumors voraussetzt, da nur dadurch funktionelle TILs isoliert werden können. Eine adoptive T-Zell Therapie mit einem spezifischen TZR erscheint daher für andere Tumorentitäten erfolgversprechender.

Die wohl innovativste Strategie im Bereich der T-Zell basierten Immuntherapien ist der Einsatz von T-Zell-imitierenden „chimeric antigen receptor“ (CAR)-T-Zellen oder bispezifischen T-Zell-imitierenden Molekülen. Vor allem die zuerst genannte zelluläre Therapie vereint die Vorteile der spezifischen Expansion einer potenten CAR-T-Zell Therapie mit der Spezifität von T-Zell-Rezeptoren und deren unerreichten Repertoire an möglichen Zielstrukturen. Die Isolation eines T-Zell-imitierenden Agens ist jedoch aufwändig und wird meist dadurch erreicht, dass mittels hochdiverser Phagenbibliotheken (mindestens 100 Milliarden Klone) Proteine identifiziert werden, welche spezifisch Peptide in Kombination mit HLA Komplexen gleichsam einem TZR erkennen können. Obwohl die meisten dieser Medikamente sich noch in präklinischer Entwicklung befinden (42,43), gibt es auch schon frühe klinische Daten für den Einsatz von TZR-imitierenden CAR-T-Zellen (44). Der wohl größte Unterschied zwischen T-

Zellen mit endogenen oder transduzierten TZR und TZR-imitierenden CAR-T-Zellen ist die deutlich höhere Anzahl an HLA Liganden, welche für eine suffiziente Aktivierung von TZR-imitierenden CAR-T-Zellen nötig ist. Dies bedeutet im Umkehrschluss, dass relevante Targets dieser Therapie sich gut mittels Immunpeptidomik nachweisen lassen, da diese HLA Liganden im Bereich der üblichen Sensitivität der Massenspektrometrie liegen. Bezüglich der höheren Schwellenwertes der Aktivierung muss jedoch betont werden, dass inzwischen CAR-T-Zellen entwickelt wurden, welche auch von Targets mit niedriger Abundanz erfolgreich aktiviert werden (45). Dieses Konzept ließe sich problemlos auch auf TZR-imitierenden CAR-T-Zellen übertragen. Ein weiterer klarer Vorteil liegt in der Tatsache, dass die Erkennung von HLA Liganden unabhängig von der Immunogenität dieser Peptide erfolgt, da die Erkennung nicht auf thymischer Selektion, sondern auf reiner biochemischer Interaktion beruht. Dies erweitert das Repertoire an möglichen HLA Liganden als Zielstruktur auf beinahe jedes Protein des menschlichen Proteoms. Zusammenfassend lässt sich also sagen, dass T-Zell basierte Immuntherapien ein hohes Zukunftspotenzial haben und die Definition von neuen Targets mittels Immunopeptidomik ein wichtiger Schritt für den Erfolg dieser Therapien darstellt.

2 Eigene Arbeiten

2.1 Fragestellung

Vor dem Hintergrund des hohen Potenzials von TZR-basierten Therapien und der Notwendigkeit des Nachweises der Präsentation der angegangenen HLA Liganden mittels Massenspektrometrie, ergeben sich somit essenzielle Fragen für die Entwicklung von Medikamenten, welche Tumorzellen über HLA Liganden erkennen und eliminieren sollen:

- Erstens, welchen Stellenwert nimmt die Art und Weise der HLA Liganden Isolation ein und wie lässt sich diese weiter verbessern - insbesondere vor dem Hintergrund vieler unterschiedlicher Isolationsstrategien?
- Zweitens, wie lässt sich das Immunpeptidom pharmakologisch so verändern, dass Tumorzellen HLA Liganden effektiver präsentieren und hierdurch entweder neue Zielstrukturen oder bestehende Targets in größerer Anzahl präsentiert werden?
- Drittens, erlaubt die systematische Analyse des Immunpeptidoms die Identifikation eines tumorigen HLA Liganden, welcher therapeutisch von einer TZR-basierten Therapie genutzt werden kann?

Insgesamt beschäftigen sich demnach die folgenden Arbeiten mit der gesamten Pipeline von der Isolation von HLA Liganden über deren Modulation bis hin zur Entwicklung eines neuen Therapeutikums und gibt somit eine breite Übersicht, wie meine Forschungsarbeit die Entwicklung von spezifischen Immuntherapien gegen HLA Liganden beeinflusst und vorangebracht hat.

2.2. Optimierung und Standardisierung der HLA Liganden Isolation

2.2.1 Optimierung der HLA Liganden Isolation

Originalarbeit 1

Klatt MG, Mack KN, Bai Y, Aretz ZEH, Nathan LI, Mun SS, Dao T, Scheinberg DA. Solving an MHC allele-specific bias in the reported immunopeptidome. *JCI Insight*. 2020;5(19).

Diese Studie unterstreicht die Bedeutung der Identifizierung von HLA-Klasse-I-gebundenen Peptiden durch Immunpräzipitation und Massenspektrometrie. Diese Technik ist entscheidend für das Verständnis der T-Zell-Immunität und die Entwicklung von Immuntherapien. Umso wichtiger ist es, dass die Isolation der HLA Liganden effizient und vollständig erfolgt, da eine inkomplette Isolation zu Verzerrungen innerhalb der möglichen Targets für Immuntherapien führen.

In dieser Arbeit wurde festgestellt, dass etablierten Isolationstechniken einen bisher unbekanntem Bias für Peptide mit geringerer Hydrophobizität aufweisen. Da die Hydrophobizität von HLA Liganden mit ihrer Immunogenität korreliert, ist zudem die Identifizierung besonders hydrophober HLA Liganden für wirksame Immuntherapien entscheidend. Um diesen Bias zu überwinden, wurden in dieser Arbeit höhere Konzentrationen von Acetonitril (ACN) bei der Trennung von HLA Liganden und ihren Komplexen verwendet. Diese Anpassung erhöhte die Anzahl an identifizierten HLA Liganden um das Zwei- bis Dreifache und verbesserte den Nachweis von Peptiden aus CGAs um 50%. Hierbei ist zu betonen, dass die Effizienz der HLA Liganden Isolation zwischen den verschiedenen HLA Allelen variierte, was wahrscheinlich auf die Hydrophobizität der Ankeraminosäuren zurückzuführen ist. Somit profitieren manche HLA Allele und Patient stärker von der optimierten Isolation als andere.

Abschließend konnten wir nachweisen, dass eine höhere Hydrophobizität der isolierten HLA Liganden, die durch höhere ACN-Konzentrationen erreicht wird, Auswirkungen auf die T-Zell-Erkennung hat. Immunogene HLA Liganden weisen im Allgemeinen eine höhere Hydrophobizität an ihren TZR-Erkennungsstellen auf, was sich bei deren Erkennung durch TZRs als energetisch günstig erweisen kann. Die Verwendung höherer ACN-Konzentrationen verbesserte somit nicht nur die Anzahl identifizierter HLA Liganden, sondern erhöhte auch die Erkennung potenziell immunogener Epitope, insbesondere für das gut charakterisierte HLA-A*02 Allel.

Zusammenfassend lässt sich sagen, dass die Studie einen bedeutenden Fortschritt bei der Isolierung und Identifizierung von HLA-Klasse-I-gebundenen Peptiden darstellt, der den bisherigen Bias in bestehenden Methoden behebt und das Potenzial für eine effektivere Identifizierung von Targets für Immuntherapien erhöht.

Solving an MHC allele-specific bias in the reported immunopeptidome

Martin G. Klatt,¹ Kyeera N. Mack,^{1,2} Yang Bai,^{1,2} Zita E. H. Aretz,^{1,3} Levy I. Nathan,¹ Sung Soo Mun,¹ Tao Dao,¹ and David A. Scheinberg^{1,2}

¹Molecular Pharmacology Program, Sloan Kettering Institute, Memorial Sloan Kettering Cancer Center, New York, New York, USA. ²Pharmacology Department and ³Physiology Biophysics and Systems Biology Program, Weill Cornell Medicine, New York, New York, USA.

Identification of MHC class I-bound peptides by immunopurification of MHC complexes and subsequent analysis by mass spectrometry is crucial for understanding T cell immunology and immunotherapy. Investigation of the steps for the MHC ligand isolation process revealed biases in widely used isolation techniques toward peptides of lower hydrophobicity. As MHC ligand hydrophobicity correlates positively with immunogenicity, identification of more hydrophobic MHC ligands could potentially lead to more effective isolation of immunogenic peptides as targets for immunotherapies. We solved this problem by use of higher concentrations of acetonitrile for the separation of MHC ligands and their respective complexes. This increased overall MHC ligand identifications by 2-fold, increased detection of cancer germline antigen-derived peptides by 50%, and resulted in profound variations in isolation efficacy between different MHC alleles correlating with the hydrophobicity of their anchor residues. Overall, these insights enabled a more complete view of the immunopeptidome and overcame a systematic underrepresentation of these critical MHC ligands of high hydrophobicity.

Introduction

Defining the landscape of peptides presented on major histocompatibility complex (MHC) proteins provides better understanding of T cell immunity and supports the identification of immunotherapy targets (1–3). Several peptide isolation techniques have been standardized, but not benchmarked, resulting in various distinct experimental approaches (4–7). Though direct comparisons of these techniques remain sparse (8, 9), existing data point toward differences in the subsets of isolated MHC ligands depending on the type of protocol. Additionally, we hypothesized that anchor amino acid characteristics in distinct MHC alleles could influence isolation of the bound peptides in an allele-specific and method-dependent manner.

Therefore, we investigated several aspects of the isolation process to identify potential biases introduced by the biochemical characteristics of these approaches. Separation of the MHC ligand and complex appeared to be the dominant step yielding ligandome variations, which were usually skewed toward an underrepresentation of MHC ligands of higher hydrophobicity. Using hydrophobicity-dependent isolation via C18 cartridges in conjunction with increased concentrations of acetonitrile (ACN) enabled a more comprehensive collection of MHC ligands and their complexes; the number of unique peptide isolations was increased by about 2-fold with substantial enrichment for more hydrophobic peptides. Furthermore, the largest increases in identified MHC ligands were seen for MHC alleles with anchor site preferences for highly hydrophobic amino acids, e.g., HLA-A*02. Therefore, new methods might restore a previous imbalance within peptide isolation approaches and provide a more useful representation of the ligandome.

Finally, hydrophobicity of MHC ligands correlates positively with their immunogenicity (10). We corroborated these data through an HLA-A*02-specific reanalysis of a published data set, which led to the assumption that the number of potentially immunogenic epitopes might be elevated in our new MHC ligand subsets with higher hydrophobicity. This hypothesis was further supported by higher predictions of immunogenicity through the T cell recognition score by Calis et al. (11) when 9-mer HLA-A*02 ligands identified through different ACN elution conditions were investigated. Furthermore, our analysis identified 76 cancer germline antigen-derived (CGA-derived) peptides from 3 cell lines. Eleven of these HLA ligands have not been described before to our knowledge, including 2 binders from the well-studied immunogenic

Conflict of interest: DAS has ownership in, income from, or research funds from OncoPep; Pfizer; Sellas Life Sciences Group, Inc.; Sapience; Invance Biotherapeutics; Actinium Pharmaceuticals; Lantheus Holdings; ContraFect; Arvinas; Ensysce Biosciences; and Eureka Therapeutics.

Copyright: © 2020, Klatt et al. This is an open access article published under the terms of the Creative Commons Attribution 4.0 International License.

Submitted: June 12, 2020

Accepted: August 31, 2020

Published: September 8, 2020.

Reference information: *JCI Insight*.

2020;5(19):e141264.

<https://doi.org/10.1172/jci.insight.141264>.

insight.141264.

CGAs, cyclin A1 (12, 13), and MAGE-A12 (14, 15); the latter peptide was identified only in the group with the highest concentration of ACN.

Overall, this study discovered a bias in the known immunopeptidome that favors more hydrophilic and possibly less immunogenic peptides. Resolution of the problem by more stringent biochemical isolation conditions could have broad implications for the fields of immunology and immunotherapy because it has the potential to redefine and enlarge the repertoire of identified MHC ligands and to deepen the understanding of the immunopeptidome.

Results

Separation of MHC ligands and complexes is the most influential step for MHC ligand isolation and highly protocol dependent. As many MHC isolation strategies differ widely, we compared method variations using 50 million BV173 cells per condition. Alterations were made at (a) the level of cell lysis, (b) antibody coupling/column preparation, and (c) the separation of MHC ligand and complex (Supplemental Figure 1A; supplemental material available online with this article; <https://doi.org/10.1172/jci.insight.141264DS1>). No significant differences were seen between the use of the detergent 3-[(3-cholamidopropyl) dimethylammonio]-1-propanesulfonate (CHAPS) and the combination of octyl- β -D-glucopyranoside and sodium desoxycholate (OGP/SDC), although there was a trend for superior performance of CHAPS (Supplemental Figure 1B and Supplemental Table 1).

Similarly, no major changes in peptide yields were observed for antibodies either bound or cross-linked to protein A-Sepharose beads or for covalent coupling of antibodies to a cyanogen bromide-activated Sepharose 4B (Supplemental Figure 1C and Supplemental Table 1). A clear dose-dependent correlation was seen for the amount of antibody used ($R^2 = 0.994$), allowing an optimal recovery of unique MHC ligands when at least a total of 0.5 mg of W6/32 antibody was used (Supplemental Figure 1D and Supplemental Table 1). All subsequent experiments were therefore performed with 0.5 mg of W6/32 antibody.

However, in the third step, separation of ligand and complex, we identified profound differences compared with the standard conditions. We compared 3 kDa size-exclusion spin filters (which segregate MHC peptide and complex by centrifugal force and only allow passage of the much smaller ligands whereas subunits of the MHC complex are retained) with C18 cartridges. These C18 columns bind the eluted MHC complexes and peptides that were previously dissociated by the use of 1% trifluoroacetic acid (TFA) through hydrophobic interactions. By using polar reagents, such as a mixture of 30% ACN/0.1% TFA, MHC ligands are separated from the much more hydrophobic MHC complexes that remain bound to the C18 column. With C18 cartridge separation, we observed 2.5 times more unique MHC peptides compared with size-exclusion spin columns (Figure 1A). We assumed that the ACN elution was superior because of a more effective separation of more hydrophobic MHC ligands with stronger binding to the MHC binding groove. To test this hypothesis, we expanded this experimental approach by splitting immunopurified MHC complexes from AML14, JMN, or BV173 cells equally into 3 fractions; bound every fraction to separate C18 columns; and then eluted peptides with 30%, 40%, or 50% ACN. For all cell lines, the increased concentrations of ACN led to improved peptide recovery, with over 2-fold increases for AML14 and JMN and 30% for BV173 (Figure 1B). These data led to the hypothesis that these differences in recovery improvement may be related to the specific biochemical characteristics of the HLA alleles, which will be discussed later.

Hydrophobicity of eluted MHC ligands correlates with concentrations of ACN used for MHC ligand isolation. Because the use of higher concentrations of ACN led to a consistent increase in unique MHC ligand identifications, we next asked whether the chemical properties of the eluted ligands differed between isolation conditions. We used the grand average of hydropathicity index (GRAVY) (16) as a scale for hydrophobicity of a peptide, which is expected to increase when ligands are isolated with more polar reagents. Indeed, with higher concentrations of ACN, significant changes in the peptides' average hydrophobicity were observed in BV173 cells (Figure 1C). In contrast, no significant difference in hydrophobicity was seen with MHC ligands isolated by the most commonly used isolation techniques (size exclusion or C18 cartridges eluted with 30% ACN).

Similar trends for the relationship between ACN and hydrophobicity were observed in AML14, JMN, and BV173 cells. In AML14 cells the increment from 40% to 50% ACN led to significant differences whereas for JMN and BV173 in the highest ACN groups, GRAVY scores were not statistically significant (Figure 1D). Importantly, every isolation condition led to a different set of MHC ligands, related to the method of isolation (Figure 1, E and F; and Supplemental Table 2). However, higher concentrations of ACN always gained more newly isolated unique HLA ligands than they lost (Supplemental Figure 2).

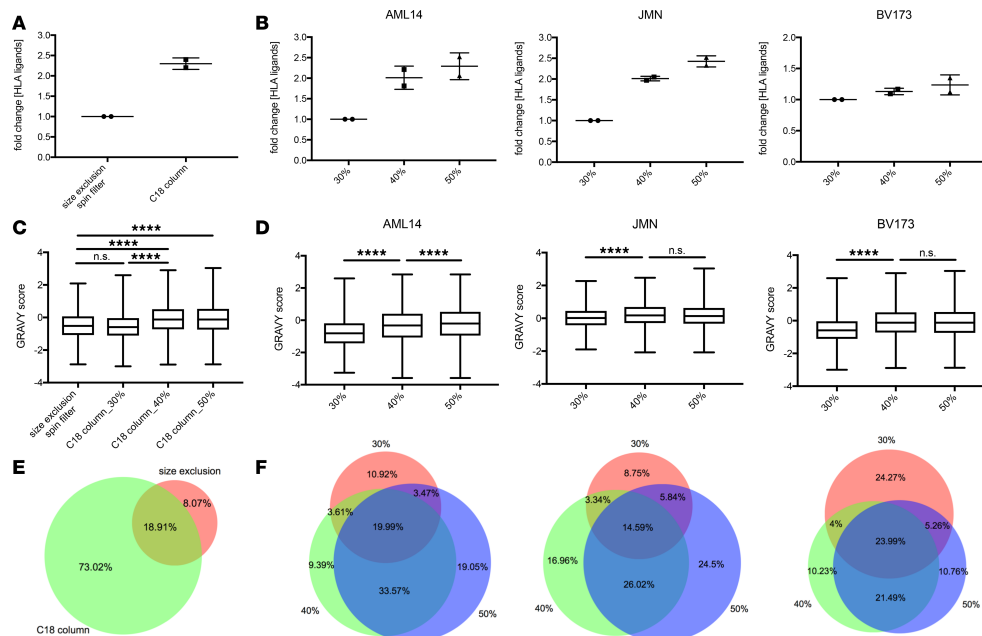


Figure 1. Characterization of MHC ligands eluted from C18 cartridges with various concentrations of ACN. (A) Comparison of size-exclusion spin filters and C18 cartridges with 30% ACN elution. (B) Relative changes for the yields of unique HLA ligands between different ACN elution conditions in AML14, JMN, and BV173 cells. (C) GRAVY scores for MHC-assigned peptides in BV173 cells. (D) GRAVY scores of different ACN elution conditions in AML14, JMN, and BV173 cells. Data sets were used from experiments shown in D. Data were normalized to samples with lowest yield of unique HLA ligand identifications. Key: 30% ACN in red, 40% ACN in green, and 50% ACN in blue. For A and B mean with SD is indicated. In C and D whiskers show range of GRAVY scores from min to max. Boxes show mean with SD. One-way ANOVA test was used for multiple comparisons. **** $P < 0.0001$.

Efficiency of MHC ligand isolation is MHC allele dependent. Because the hydrophobicity of anchor amino acids might influence the isolation process, we then asked whether the efficiency of ligand elution varied among MHC alleles. Such a result could further imply that the aforementioned bias in MHC ligand isolation could affect some MHC alleles and therefore some patient samples more than others. To test this hypothesis, we analyzed HLA assignments of ligands via netMHCpan 4.0 and normalized results to the 30% ACN specimens. While peptides increased with ACN concentrations for most alleles, HLA-A*30 showed a decrease by 25% in the total number of unique isolated MHC ligands with higher ACN (Figure 2A). The other MHC alleles demonstrated increases from 20% to over 400% in higher ACN conditions with high variation between individual alleles. Importantly, these profound differences in hydrophobicity and HLA allele-dependent increase in HLA ligands could not be achieved by the use of higher cell numbers, e.g., 200 million BV173 cells instead of 16.7 million, both eluted only with 30% ACN (Supplemental Figure 3 and Supplemental Table 2). The only MHC allele shared between the 3 studied cell lines, HLA-A*02:01, always showed at least a 2-fold increase in unique MHC ligand isolations. Because the most evident explanation for MHC allele dependency of this method would be a correlation with anchor amino acid characteristics, we calculated GRAVY scores for amino acids at positions 2 and 9 in all identified 9-mer MHC ligands for each allele, separately. Three major groups were identified that correlated with the average increase in MHC ligands per condition on the respective alleles: scores ranging from -1 to $+1$, scores from $+1$ to $+3$, and scores more than $+3$ (Figure 2B). For the first group with the most hydrophilic anchor residues (A*30:01, B*15:10, B*18:01, B*44:02), only small effects ($\pm 25\%$) were

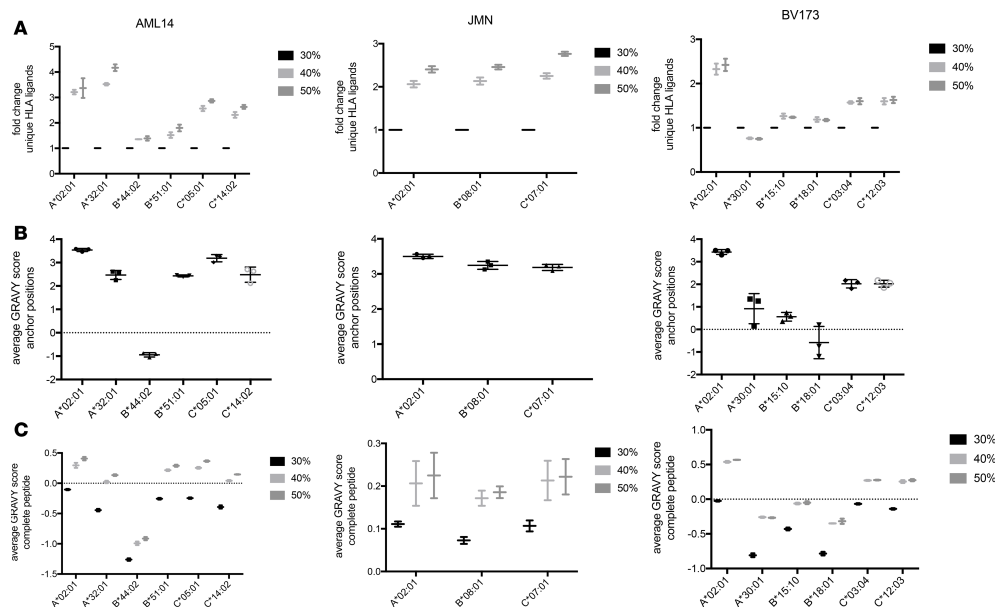


Figure 2. HLA allele-specific characterization of HLA ligands eluted from different ACN conditions. (A) Relative changes for the yields of unique HLA ligands between different ACN elution conditions and HLA alleles. HLA ligands were assigned to respective alleles by netMHCpan using a 2% rank cutoff. Results are normalized to the 30% ACN condition. (B) GRAVY scores for anchor amino acids (positions 2 and 9) in 9-mer HLA ligands. (C) GRAVY scores for complete 9-mer HLA ligands. In A and C whiskers indicate min to max. All experiments were performed in biological duplicates. In B mean with SD is indicated.

observed for alleles. The second subgroup (A*32:01, B*51:01, C*03:04, C*12:03, C*14:02) showed more varying effects, with increases between 50% (B*51:01) and 400% (A*32:01). More reliable trends were detected for the third group (A*02:01, B*08:01, C*05:01, C*07:01), with a constant 2- to 3-fold increase in unique MHC ligands between ACN subgroups.

To further determine the potential contribution of auxiliary anchors or other amino acid residues to the MHC allele-dependent isolation, we investigated the changes in the hydrophobicity of the complete peptide in an MHC allele- and ACN concentration-dependent manner. For all MHC alleles average hydrophobicity of eluted peptides went up with higher ACN concentrations, indicating that the effect was not solely attributable to anchor amino acid characteristics (Figure 2C).

High concentrations of ACN for MHC ligand isolation might support identification of immunogenic MHC ligands and improve detection of CGA-derived MHC ligands. Next, we asked whether the observed higher hydrophobicity of the isolated MHC ligand could have implications for T cell recognition. On average, immunogenic MHC ligands display higher hydrophobicity compared with nonimmunogenic MHC-binding peptides (10) at their TCR recognition site. Therefore, we reanalyzed the provided data set by Chowell et al. focusing on HLA-A*02 binders. For HLA-A*02-binding 9-mer peptides, the GRAVY score was significantly higher in the immunogenic peptide group compared with the nonimmunogenic control group (Figure 3A). Even stronger differences in the average GRAVY were observed if the score was calculated only at the TCR recognition site (positions 4 to 8) (Figure 3B and Supplemental Table 3) (17). Interestingly, similar differences in GRAVY were observed for our cell lines among the various ACN concentrations (Figure 3C), especially between 30% ACN and higher concentrations.

We then asked if prediction algorithms for T cell recognition of MHC ligands can detect differences between the subgroups of peptides eluted in different ACN conditions. We used the T cell recognition score defined by Calis et al. (11) and included all 9-mer HLA-A*02 ligands detected in our study, because

this algorithm is only validated for 9-mers and the most robust changes in the immunopeptidome were described for the HLA-A*02 allele. Strikingly, we observed significantly higher scores for the 40% and 50% ACN data sets compared with the 30% data set, further supporting our hypothesis that higher concentrations of ACN might support the isolation of more immunogenic HLA ligands (Figure 3D and Supplemental Table 3).

Finally, as another surrogate for immunogenicity of identified MHC ligands, we analyzed the detection of peptides from CGAs, as these antigens provide valuable targets for cancer immunotherapy (18, 19). We collected a list of 225 curated CGAs (Supplemental Table 3) (20) and matched these antigens to our data sets. For JMN, BV173, and AML14 cells, 8, 30, and 41 MHC ligands from CGAs were identified, respectively. Of importance, 88% (7/8), 27% (8/30), and 51% (21/41) of these subsets of peptides were exclusively found in the 40% and 50% ACN settings (Figure 3E). From a total of 76 CGA-derived detected peptides, 11 had not been described in the literature before. Moreover, 5 out of these 11 MHC ligands (45%) were only made detectable by use of 40% and 50% ACN in the elution conditions (Figure 3F), and 2 of the newly identified MHC ligands were derived from cyclin A1 (12, 13) and MAGE-A12 (14, 15), 2 antigens reported to be highly immunogenic. Though the MHC ligand from cyclin A1 could be detected in all 3 settings for the AML14 cell line, the MAGE-A12 peptide was identified only in a 50% ACN sample of JMN cells (Table 1).

Discussion

Though various MHC isolation protocols are consistently used in the field, direct comparisons of these methods are scarce. We compared parameters of MHC ligand isolation, such as cell lysis conditions or antibody column preparation, and did not observe significant differences. CHAPS, however, was the detergent with the most favorable characteristics as consistent with the literature (9). Whereas one recent study showed higher yields with size-exclusion filters compared with C18 columns (9), in our experiments C18 cartridges eluted with ACN yielded 2.5 times more unique MHC ligands as compared with size-exclusion spin filters. To further investigate the effect of ACN on MHC ligand elutions, we increased concentrations of ACN up to 50% and detected even better recovery of MHC ligands in 3 cell lines, with over 2-fold increases in unique identifications. To determine the changes of abundance for specific HLA ligands between different ACN elution conditions in correlation to their GRAVY score, future studies might use stable isotope labeling of HLA ligands (21), which would allow a more precise characterization of changes in the immunopeptidome when using higher ACN concentrations for isolation of HLA ligands.

One study that used concentrations of ACN higher than 30% (22) pooled elutions of different ACN concentrations but did not investigate them separately. To reduce the risk for coelution of MHC complexes with the peptides when higher ACN concentrations were used, we performed solid-phase extractions before the sample was injected into the mass spectrometer (23).

With more unique MHC ligands identified in the samples of higher ACN concentrations, we hypothesized that the major differences in unique peptide yields can be attributed to the more hydrophobic properties of isolated MHC ligands. In contrast, for size-exclusion filters and C18 cartridges eluted with 30% ACN, the most commonly used strategies for separation of peptides and MHC complexes (4–7), no significant differences related to the hydrophobicity of identified peptides were detected. This implies that large subsets of peptides might be missed with standard isolation protocols and that the MHC ligands isolated within these 2 subgroups might be biased toward lower hydrophobicity. This indicated that for the most complete data sets of MHC ligand isolations, various ACN elution concentrations should be employed; e.g., C18 cartridges can be eluted sequentially with 30%, 40%, and 50% ACN, and elution fractions can either be analyzed separately or pooled for a single MS analysis. This idea is further supported by recent data using HPLCs with ACN gradients for peptide MHC separation, resulting in higher yields compared with C18 cartridges (9). Based on the results shown here, we believe that this HPLC approach could further benefit from gradients up to 40% or 50% ACN. The upper limit of ACN might be cell line dependent as observed for the 3 lines used in this study.

Moreover, MHC allele-dependent differences in hydrophobicity of eluted ligands have been described before (24) and are in line with the respective hydrophobicity of their anchor amino acids. Consistent with these results, we observed a correlation between the hydrophobicity of anchor amino acids and the total increase in unique MHC ligands per allele when using more stringent elution conditions. Importantly, for HLA-A*02 a 2-fold increase was observed in every cell line even if the number of total ligands did not increase dramatically. In contrast, the use of higher cell numbers did not lead to an increase of mean hydrophobicity to a similar extent as seen with 40% ACN or to an HLA allele-specific increase of HLA ligands.

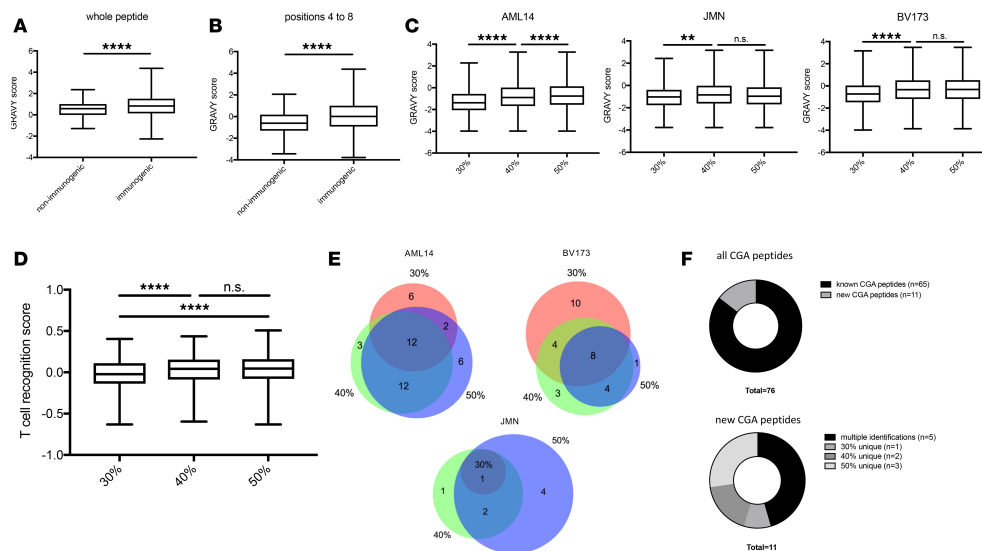


Figure 3. Correlation of hydrophobicity and immunogenicity. Epitopes eluted from CGAs. HLA-A*02 9-mer HLA ligands from Chowell et al. (10) were retrieved and GRAVY scores of immunogenic and nonimmunogenic peptides calculated for (A) the whole peptide and (B) amino acid positions 4 to 8. (C) GRAVY scores for positions 4 to 8 of 9-mer peptides identified in different ACN conditions. (D) T cell recognition score for 9-mer HLA-A*02 binder. (E) Venn diagrams for peptides derived from CGAs in different ACN elution conditions. Color key is the same as that for Figure 1. (F) Known and potentially novel peptides from CGAs. In A, B, C, and D, whiskers indicate min to max. Boxes show mean with SD. Experiments were performed in biological duplicates. One-way ANOVA test was used for multiple comparisons. ** $P < 0.01$; **** $P < 0.0001$.

Because HLA-A*02 is the best characterized HLA complex in the field, these analyses highlighted the importance of the findings and suggested that the number and characteristics of HLA-A*02 binders might have been systematically underestimated by the field.

Furthermore, the presence of hydrophobic amino acids at the TCR recognition site is thought to be a hallmark of TCR recognition because of improved binding kinetics, including a reduced desolvation penalty (10, 25). Because our improved strategy led to the identification of MHC ligands of higher hydrophobicity, we further investigated their characteristics at the TCR recognition site, which supported the trend seen before with more hydrophobic peptide segments between positions 4 and 8 of a 9-mer peptide in the 40% and 50% ACN elution samples. This might imply that our approach leads to more MHC ligands and to the discovery of peptides with greater chance of immunogenicity. Further support for this hypothesis was provided by immunogenicity predictions of HLA-A*02 restricted 9-mer HLA ligands from different elution conditions, which showed a highly significant difference (Figure 3D) in T cell recognition score, indicating higher potential for immunogenicity with increasing concentrations of ACN.

Another positive aspect of our method is the improved recovery of CGA-derived HLA ligands. On average, 50% more peptides from CGAs were detected in the 40% and 50% ACN samples compared with the 30% ACN samples.

In this study we discovered the importance of improving separation conditions for MHC ligands from their complexes for mass spectrometry analysis of the immunopeptidome. Our data suggest that current isolation protocols do not sufficiently separate peptides from MHC complexes after they have been dissociated by TFA, especially for MHC alleles with anchor amino acids of high hydrophobicity, e.g., HLA-A*02, which leads to a significant bias in the published immunopeptidome. Resolving the problem by the use of more polar conditions to separate MHC ligands and complexes not only will allow a more complete characterization of the immunopeptidome but also allows the possibility of identification of MHC ligands of higher immunogenicity due to the positive correlation of MHC ligand hydrophobicity and immunogenicity.

Table 1. Potentially previously undescribed epitopes of CGAs

Peptide sequence	HLA assignment (% rank)	Source protein	Sample
ASRDVFLK	A*30:01 (0.006)	KIF2C	BV173_40%
DARHNVSRV	B*51:01 (0.2259)	DCAF12	AML14_30%, AML14_40%, AML14_50%
EPFTKAEm	B*08:01 (0.378)	MAGE-A12	JMN_50%
IPHRPQAI	B*51:01 (0.0522)	CCNA1	AML14_30%, AML14_40%, AML14_50%
IVDsPEKL	C*05:01 (0.34)	NUF2	AML14_30%, AML14_50%
KESEHSNSF	B*44:02 (0.05)	TEX15	AML14_30%, AML14_40%, AML14_50%
KLRAESYNEW	A*32:01 (0.4128)	KDM5B	AML14_50%
RTKFFEDLILK	A*30:01 (1.178)	ATAD2	BV173_50%
SEGESKSV	B*44:02 (0.0098)	TEX15	AML14_30%, AML14_40%, AML14_50%
SEKEPGQQV	B*44:02 (0.0057)	RHOXF2	AML14_40%
YHDGIEKAA	B*15:10 (0.379)	NUF2	BV173_30%

For peptide sequences: m, oxidized methionine; s, phosphorylated serine.

Methods

Cell lines. AML14 cells were a gift from Ross Levine (Memorial Sloan Kettering Cancer Center, New York, New York, USA), and JMN cells were maintained at Sloan Kettering Institute. BV173 cells were provided by H.J. Stauss (University College London, London, United Kingdom). All cell lines were HLA typed by the Department of Cellular Immunology at Memorial Sloan Kettering Cancer Center. All cell lines were maintained in RPMI medium and supplemented with 10% FBS and 2 mM glutamine.

Immunopurification of HLA class I ligands. For immunopurification several variations of different protocols were employed (5–8). Suspension cells were harvested through direct resuspension, and adherent cell lines were harvested after incubating 15 minutes with CellStripper solution (Corning, catalog 25056CI). Harvested cells were pelleted and washed 3 times in ice-cold sterile PBS (Media Preparation Core, Memorial Sloan Kettering Cancer Center). For all comparisons of protocols, 50 million BV173 cells were used per experiment. In 1 experiment, 200 million BV173 cells were used with a 30% ACN isolation strategy. For experiments comparing different concentrations of ACN, 50 million cells were used as well, but TFA eluates were later split into 3 equal portions. Then, cells were lysed in 7.5 mL of either 1% CHAPS (MilliporeSigma, catalog C3023) or 0.25% SDC (MilliporeSigma, catalog 30970) in combination with 1% OGP (MilliporeSigma, catalog O8001), all dissolved in PBS, supplemented with protease inhibitors (cOmplete, Roche, catalog 11836145001). The combination strategy was used only once for a direct comparison with CHAPS. All other experiments were exclusively performed with CHAPS. Cell lysis was performed for 1 hour at 4°C, lysates were spun down for 1 hour with 20,000g at 4°C, and supernatant fluids were isolated.

Affinity columns were prepared according to the protocols mentioned above in 3 variants.

For variant 1, 40 mg of cyanogen bromide-activated-Sepharose 4B (MilliporeSigma, catalog C9142) was activated with 1 mM hydrochloric acid (MilliporeSigma, catalog 320331) for 30 minutes. Subsequently, 0.5 mg (and for the experiments considering amount of antibody usage, 0 µg, 50 µg, 200 µg, 500 µg, or 1000 µg) of W6/32 antibody (Bio X Cell, catalog BE0079) were coupled to Sepharose in the presence of binding buffer (150 mM sodium chloride, 50 mM sodium bicarbonate, pH 8.3; sodium chloride: MilliporeSigma, catalog S9888; sodium bicarbonate: MilliporeSigma, catalog S6014) for at least 2 hours at room temperature. Sepharose was blocked for 1 hour with glycine (MilliporeSigma, catalog 410225) and washed 3 times with PBS.

For variant 2, 100 µg of protein A-Sepharose beads (Thermo Fisher Scientific catalog 15918014) were incubated with 0.5 mg of W6/32 antibody in PBS overnight at 4°C and then washed 3 times.

For variant 3, 100 µg of protein A-Sepharose beads were incubated with 0.5 mg of W6/32 antibody in 0.2 M sodium borate buffer (MilliporeSigma, catalog B3545) overnight at 4°C, then cross-linked with 20 mM dimethyl pimelimidate (MilliporeSigma, catalog 80490), and finally washed 3 times in PBS.

Supernatants of cell lysates were run over the different types of columns through peristaltic pumps (Pharmacia Biotech, Model P-1) with 1 mL/min flow rate overnight in a cold room. Affinity columns

were washed with PBS for 30 minutes and water for 30 minutes, then run dry, and HLA complexes were subsequently eluted 5 times with 200 μ L 1% TFA (MilliporeSigma, catalog 02031). For experiments where different settings for MHC ligand and complex isolation were investigated, the TFA eluates were pooled and then split in as many portions as settings were investigated (mostly 3 portions for the 30%, 40%, and 50% ACN settings, a fourth portion if spin filters were examined).

For separation of HLA ligands from their HLA complexes, C18 columns (Sep-Pak C18 1 cc Vac Cartridge, 50 mg sorbent per cartridge, 37–55 μ m particle size, Waters, catalog WAT054955) were prewashed with 80% ACN (MilliporeSigma, catalog 34998) in 0.1% TFA and equilibrated with 2 washes of 0.1% TFA. Samples were loaded, washed again with 0.1% TFA, and eluted in 400 μ L of 30%, 40%, or 50% ACN in 0.1% TFA. For separation by size-exclusion filters 0.5 mL 3 kDa–cutoff filters were used (Millipore Sigma, catalog UFC5003). Before use spin filters and tubes were prewashed with 1% TFA overnight to reduce polyethylene glycol content. Samples were then loaded into the filters and spun at 14,000g for 40 minutes. Flow-throughs were used for further analysis. Sample volume was reduced by vacuum centrifugation for mass spectrometry analysis.

Solid-phase extractions. In-house C18 minicolumns were prepared as follows: for solid-phase extraction of 1 sample, 2 small disks of C18 material (1 mm in diameter) were punched out from CDS Empore C18 disks (Thermo Fisher Scientific, catalog 13-110-018) and transferred to the bottom of a 200 μ L Axygen pipette tip (Thermo Fisher Scientific, catalog 12639535). Columns were washed once with 100 μ L 80% ACN/0.1% TFA and equilibrated 3 times with 100 μ L 1% TFA. All fluids were run through the column by centrifugation in mini tabletop centrifuges, and eluates were collected in Eppendorf tubes. Then, dried samples were resuspended in 100 μ L 1% TFA and loaded onto the columns, washed twice with 100 μ L 1% TFA, run dry, and eluted with 50 μ L 80% ACN/0.1% TFA. Again, sample volume was reduced by vacuum centrifugation.

Liquid chromatography-tandem mass spectrometry analysis of HLA ligands. Samples were analyzed by high-resolution/high-accuracy liquid chromatography-tandem mass spectrometry (LC-MS/MS) (Lumos Fusion, Thermo Fisher Scientific). Peptides were separated using direct loading onto a packed-in-emitter C18 column (75 μ m ID/12 cm, 3 μ m particles, Nikkyo Technos Co., Ltd.). The gradient was delivered at 300 nL/min increasing linearly from 2% buffer B (0.1% formic acid in 80% ACN)/98% buffer A (0.1% formic acid) to 30% buffer B/70% buffer A, over 70 minutes. MS and MS/MS were operated at resolutions of 60,000 and 30,000, respectively. Only charge states 1, 2, and 3 were allowed. The isolation window was chosen as 1.6 thomsons, and collision energy was set at 30%. For MS/MS, maximum injection time was 100 ms with an automatic gain control of 50,000.

MS data processing. MS data were processed using Byonic software (version 2.7.84, Protein Metrics) through a custom-built computer server equipped with 4 Intel Xeon E5-4620 8-core CPUs operating at 2.2 GHz and 512 GB physical memory (Exxact Corporation). Mass accuracy for MS1 was set to 6 ppm and to 20 ppm for MS2. Digestion specificity was defined as unspecific, and only precursors with charges 1, 2, and 3 and up to 2 kDa were allowed. Protein FDR was disabled to allow complete assessment of potential peptide identifications. Oxidization of methionine; phosphorylation of serine, threonine, and tyrosine; as well as N-terminal acetylation were set as variable modifications for all samples. Samples were searched against UniProt Human Reviewed database (20,349 entries, <http://www.uniprot.org>, downloaded June 2017) with common contaminants added. Peptides were selected with a minimal log probability value of 2, indicating *P* values for peptide spectrum matches of less than 0.01 and duplicates removed.

Assignment of peptide sequences to HLA alleles. To assign peptides that passed the MS quality filters described above to their HLA complexes that they most likely bind to, we used the netMHCpan 4.0 algorithm (24) with default settings. No binding affinity predictions were enabled. Therefore, all peptides with affinity percentage ranks below 2 were considered binders.

Prediction of HLA ligand immunogenicity. T cell recognition score was calculated for 9-mer HLA-A*02 binders using the online platform via IEDB (<http://tools.iedb.org/immunogenicity/>) (11).

Statistics. All graphs except Venn diagrams were drawn with GraphPad Prism 7. For statistics built-in analyses from GraphPad Prism were used. One-way ANOVA tests with Tukey's multiple-comparisons test were used for comparing GRAVY scores in different isolation conditions. Venn diagrams were prepared using the BioVenn online platform (26). *P* values less than 0.05 were considered significant.

Author contributions

MGK, KNM, YB, ZEHA, LIN, and SSM performed and analyzed experiments. MGK and DAS designed experiments. MGK wrote the original draft of the manuscript. TD and DAS supervised the project. DAS provided funding and edited the manuscript. All authors reviewed and contributed to the manuscript.

Acknowledgments

This study was supported by Leukemia and Lymphoma Society; NIH P30CA 008748, R01 CA55349, P01 CA23766, and R35 CA241894; Solomon Foundation; and Tudor Funds. MGK is supported by the German Research Foundation (DFG) with the individual research grant KL 3118/1-1. We thank Alex Kentis for access to the Byonic software and the Proteomics Resource Center at Rockefeller University for the performance of all LC/MS-MS experiments.

Address correspondence to: David A. Scheinberg, Center for Experimental Therapeutics, 1275 York Avenue, Box 531, New York, New York 10065, USA. Email: scheinbd@mskcc.org.

- Bassani-Sternberg M, et al. Direct identification of clinically relevant neoepitopes presented on native human melanoma tissue by mass spectrometry. *Nat Commun*. 2016;7:13404.
- Schuster H, et al. A tissue-based draft map of the murine MHC class I immunopeptidome. *Sci Data*. 2018;5:180157.
- Lübke M, et al. Identification of HCMV-derived T cell epitopes in seropositive individuals through viral deletion models. *J Exp Med*. 2020;217(3):e20191164.
- Caron E, Kowalewski DJ, Chiek Koh C, Sturm T, Schuster H, Aebersold R. Analysis of major histocompatibility complex (MHC) immunopeptidomes using mass spectrometry. *Mol Cell Proteomics*. 2015;14(12):3105–3117.
- Ghosh M, et al. Guidance document: validation of a high-performance liquid chromatography-tandem mass spectrometry immunopeptidomics assay for the identification of HLA class I ligands suitable for pharmaceutical therapies. *Mol Cell Proteomics*. 2020;19(3):432–443.
- Marino F, Chong C, Michaux J, Bassani-Sternberg M. High-throughput, fast, and sensitive immunopeptidomics sample processing for mass spectrometry. *Methods Mol Biol*. 2019;1913:67–79.
- Purcell AW, Ramarathinam SH, Ternette N. Mass spectrometry-based identification of MHC-bound peptides for immunopeptidomics. *Nat Protoc*. 2019;14(6):1687–1707.
- Lanoix J, et al. Comparison of the MHC I immunopeptidome repertoire of B-cell lymphoblasts using two isolation methods. *Proteomics*. 2018;18(12):e1700251.
- Nicastri A, Liao H, Muller J, Purcell AW, Ternette A. The choice of HLA-associated peptide enrichment purification strategy affects peptide yields creates a bias in detected sequence repertoire. *Proteomics*. 2020;20(12):e1900401.
- Chowell D, et al. TCR contact residue hydrophobicity is a hallmark of immunogenic CD8+ T cell epitopes. *Proc Natl Acad Sci U S A*. 2015;112(14):E1754–E1762.
- Calis JJ, et al. Properties of MHC class I presented peptides that enhance immunogenicity. *PLoS Comput Biol*. 2013;9(10):e1003266.
- Ochsenreither S, et al. Cyclin-A1 represents a new immunogenic targetable antigen expressed in acute myeloid leukemia stem cells with characteristics of a cancer-testis antigen. *Blood*. 2012;119(23):5492–5501.
- Teck AT, et al. Cancer testis antigen Cyclin A1 harbors several HLA-A*02:01-restricted T cell epitopes, which are presented and recognized in vivo. *Cancer Immunol Immunother*. 2020;69(7):1217–1227.
- Chinnasamy N, et al. A TCR targeting the HLA-A*0201-restricted epitope of MAGE-A3 recognizes multiple epitopes of the MAGE-A antigen superfamily in several types of cancer. *J Immunol*. 2011;186(2):685–696.
- Zhu S, et al. Characterization of T-cell receptors directed against HLA-A*01-restricted and C*07-restricted epitopes of MAGE-A3 and MAGE-A12. *J Immunother*. 2012;35(9):680–688.
- Kyte J, Doolittle RF. A simple method for displaying the hydropathic character of a protein. *J Mol Biol*. 1982;157(1):105–132.
- Calis JJ, de Boer RJ, Keşmir C. Degenerate T-cell recognition of peptides on MHC molecules creates large holes in the T-cell repertoire. *PLoS Comput Biol*. 2012;8(3):e1002412.
- Amir AL, et al. PRAME-specific Allo-HLA-restricted T cells with potent antitumor reactivity useful for therapeutic T-cell receptor gene transfer. *Clin Cancer Res*. 2011;17(17):5615–5625.
- Nowicki TS, et al. A pilot trial of the combination of transgenic NY-ESO-1-reactive adoptive cellular therapy with dendritic cell vaccination with or without ipilimumab. *Clin Cancer Res*. 2019;25(7):2096–2108.
- Almeida LG, et al. CTdatabase: a knowledge-base of high-throughput and curated data on cancer-testis antigens. *Nucleic Acids Res*. 2009;37(Database issue):D816–D819.
- Lemmel C, et al. Differential quantitative analysis of MHC ligands by mass spectrometry using stable isotope labeling. *Nat Biotechnol*. 2004;22(4):450–454.
- Singh NK, Riley TP, Baker SCB, Borrman T, Weng Z, Baker BM. Emerging concepts in TCR specificity: rationalizing and (maybe) predicting outcomes. *J Immunol*. 2017;199(7):2203–2213.
- Abelin JG, et al. Mass spectrometry profiling of HLA-associated peptidomes in mono-allelic cells enables more accurate epitope prediction. *Immunity*. 2017;46(2):315–326.
- Risticvic S, Lord H, Görecki T, Arthur CL, Pawliszyn J. Protocol for solid-phase microextraction method development. *Nat Protoc*. 2010;5(1):122–139.
- Hassan C, et al. The human leukocyte antigen-presented ligandome of B lymphocytes. *Mol Cell Proteomics*. 2013;12(7):1829–1843.

25. Jurtz V, Paul S, Andreatta M, Marcatili P, Peters B, Nielsen M. NetMHCpan-4.0: improved peptide-MHC class I interaction predictions integrating eluted ligand and peptide binding affinity data. *J Immunol.* 2017;199(9):3360–3368.
26. Hulsen T, de Vlieg J, Alkema W. BioVenn - a web application for the comparison and visualization of biological lists using area-proportional Venn diagrams. *BMC Genomics.* 2008;9:488.

2.2.2 Standardisierung der HLA Liganden Isolation

Originalarbeit 2

Klatt MG, Aretz ZEH, Curcio M, Gejman RS, Jones HF, Scheinberg DA. An input-controlled model system for identification of MHC bound peptides enabling laboratory comparisons of immunopeptidome experiments. *J Proteomics*. 2020;228:103921.

Diese Studie hatte sich zum Ziel gesetzt, eine Standardisierung zu entwickeln, um die sehr heterogene Landschaft der unterschiedlichen Strategien zur HLA Liganden Isolation vergleichbarer zu machen. Die Charakterisierung von HLA gebundenen Peptiden mittels Massenspektrometrie ist komplex, und es fehlt an standardisierten Protokollen, was Vergleiche zwischen den verschiedenen Isolationsmethoden unterschiedlicher Arbeitsgruppen schwierig macht. Insbesondere die Standardisierung der Menge der eingesetzten HLA Liganden kann dazu beitragen, Unterschiede in der Isolationstechnik zu egalisieren und somit eine bessere Vergleichbarkeit herzustellen.

Hierzu wurde ein Modellsystem entwickelt, welches aus drei Zelllinien besteht, die genau definierte Peptid:HLA (pHLA) Komplexe präsentieren. Zwei dieser Zelllinien wurden gentechnisch so verändert, dass sie nur einen einzelnen pHLA exprimieren, und die dritte war eine Standardzelllinie, die mehrere unterschiedliche pHLAs präsentiert, was dem physiologischen Setting entspricht.

TZR-imitierende Antikörper, welche spezifisch nur den zu isolierenden pHLA Komplex binden, ermöglichten zudem die genaue Messung der Anzahl an pHLA pro Zelle mittels Radioimmunoassays und Durchflusszytometrie. Diese Quantifizierung war entscheidend für die Festlegung des numerischen Inputs an pHLA-Molekülen pro Experiment und somit die Basis der Standardisierung.

Die nachfolgende Isolation der HLA Liganden und die massenspektrometrische Analyse zeigte eine robuste Korrelation mit dem pHLA-Input, verdeutlichte aber auch die Auswirkungen der Diversität des Immunopeptidoms auf den Nachweis spezifischer HLA Liganden durch die Verminderung des signal-to-noise Verhältnis. Dennoch ermöglicht diese Methode standardisierte Vergleiche von immunpeptidomischen Experimenten sowohl innerhalb als auch zwischen verschiedenen Labors. Sie eignet sich besonders für HLA-A*02-positive Zelllinien und könnte in Zukunft auf andere HLA-Allele ausgeweitet werden.

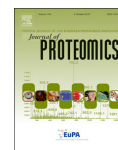
Zusammenfassend lässt sich sagen, dass diese Studie ein Modellsystem etabliert, welches den Input von HLA-gebundenen Peptiden für die Immunpeptidom Analyse standardisiert und damit vergleichbare immunpeptidomische Experimente in verschiedenen Forschungseinrichtungen erleichtert.



ELSEVIER

Contents lists available at ScienceDirect

Journal of Proteomics

journal homepage: www.elsevier.com/locate/jprot

An input-controlled model system for identification of MHC bound peptides enabling laboratory comparisons of immunopeptidome experiments

Martin G. Klatt^a, Zita E.H. Aretz^{a,b}, Michael Curcio^a, Ron S. Gejman^{a,c}, Heather F. Jones^{a,d}, David A. Scheinberg^{a,d,*}

^a Molecular Pharmacology Program, Sloan Kettering Institute, Memorial Sloan Kettering Cancer Center, New York 10065, USA

^b Physiology Biophysics and Systems Biology Program, Weill Cornell Medicine, New York 10065, USA

^c Tri-Institutional MD-PhD Program, Sloan Kettering Institute, Weill Cornell Medicine and Rockefeller University, New York 10065, USA

^d Pharmacology Department, Weill Cornell Medicine, New York 10065, USA

ABSTRACT

Characterization of MHC-bound peptides by mass spectrometry (MS) is an essential technique for immunologic studies. Many efforts have been made to quantify the number of MHC-presented ligands by MS and to define the limits of detection of a specific MHC ligand. However, these experiments are often complex and comparisons across different laboratories are challenging. Therefore, we compared and orthogonally validated quantitation of peptide:MHC complexes by radio-immunoassay and flow cytometry using TCR mimic antibodies in three model systems to establish a method to control the experimental input of peptide:MHC complexes for MS analysis. Following isolation of MHC-bound peptides we identified and quantified an MHC ligand of interest with high correlation to the initial input. We found that the diversity of the presented ligandome, as well as the peptide sequence itself affected the detection of the target peptide. Furthermore, results were applicable from these model systems to unmodified cell lines with a tight correlation between HLA-A*02 complex input and the number of identified HLA-A*02 ligands. Overall, this framework provides an easily accessible experimental setup that offers the opportunity to control the peptide:MHC input and in this way compare immunopeptidome experiments not only within but also between laboratories, independent of their experimental approach.

Significance: Although immunopeptidomics is an essential tool for the characterization of MHC-bound peptides on the cell surface, there are no easily applicable established protocols available that allow comparison of immunopeptidome experiments across laboratories. Here, we demonstrate that controlling the peptide:MHC input for immunopurification and LC-MS/MS experiments by flow cytometry in pre-defined model systems allows the generation of qualitative and quantitative data that can easily be compared between investigators, independently of their methods for MHC ligand isolation for MS.

1. Introduction

Identification of peptides presented on major histocompatibility complex (pMHC) molecules by immunopurification and subsequent mass spectrometry (MS) is a crucial technique for understanding T cell immunity and design of immunotherapies [1,2]. Additionally, MS offers not only a qualitative, but also a quantitative approach to measure the amount of an HLA ligand of interest on the cell surface [3]. However, the isolation processes, as well as LC-MS/MS analyses of MHC-presented peptides, are complex procedures with numerous variables that can differ between laboratories. Furthermore, it has been reported that sample handling leads to losses of up to 97–99% of pMHCs during MHC ligand isolation [4], and therefore the isolation method is an important factor that can substantially bias experimental procedures. Therefore, there has been a call for “standardized protocols leading to comparable results between different laboratories” independently of their isolation method or the analytical approach used [5].

To address the problem of inter-laboratory comparability we

investigated the sensitivity and robustness of input-controlled MHC ligand isolations and subsequent untargeted MS to mimic standard MHC ligand identification experiments and to demonstrate that the investigated model systems can provide the basis for comparable inter-laboratory model experiments.

Briefly, our model consisted of three major steps, see Fig. 1: First, we used three cell line models expressing a pMHC of interest. Two of the cell lines are *transporter associated with peptide presentation* (TAP)-deficient which were genetically engineered with the PresentER genetic system [6] to express only a single pMHC (H2-Kb:SIINFEKL or HLA-A*02:RMFPNAPYL) on the cell surface of each cell; the third cell line was EL4-OVA, which presents the SIINFEKL epitope, among other peptides normally found on the cell. The amount of pMHC presented on the cell surface was determined with two orthogonal methods, radio-immunoassay and flow cytometry, the latter being the technique we envision to be used when inter-laboratory comparisons are performed, because of its widespread availability. We were able to quantitate the number of cell surface ligands precisely because we also had available

* Corresponding author at: Molecular Pharmacology Program, Sloan Kettering Institute, Memorial Sloan Kettering Cancer Center, New York 10065, USA.
E-mail address: scheinbd@mskcc.org (D.A. Scheinberg).

<https://doi.org/10.1016/j.jprot.2020.103921>

Received 1 May 2020; Received in revised form 6 July 2020; Accepted 20 July 2020

Available online 03 August 2020

1874-3919/ © 2020 Elsevier B.V. All rights reserved.

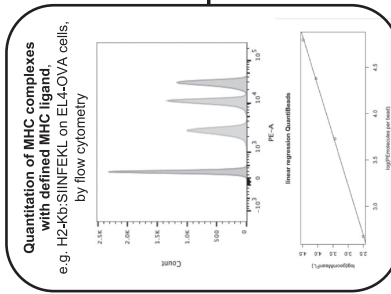
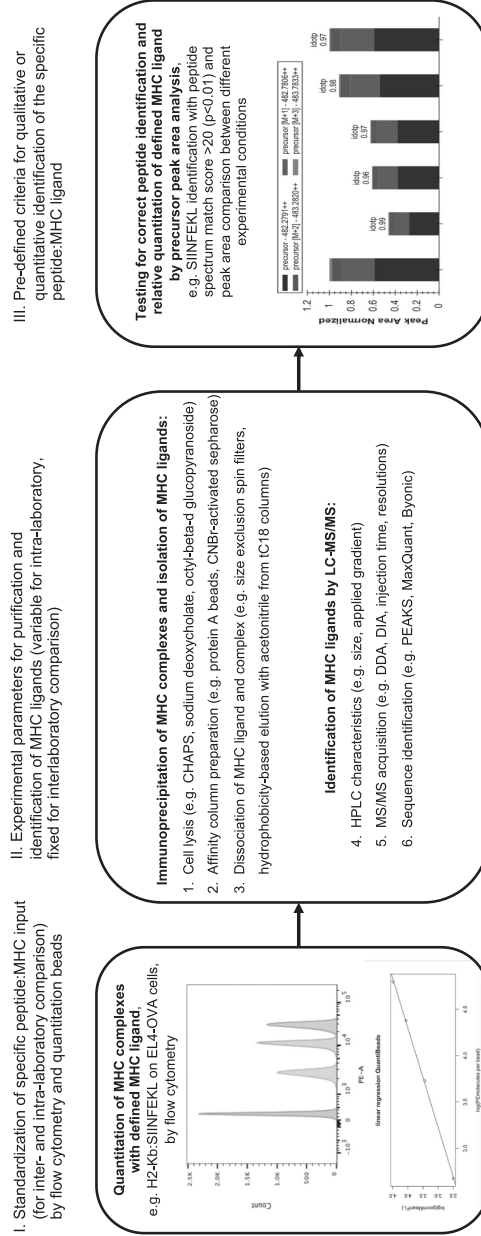


Fig. 1. Experimental workflow for input-controlled analysis of immunopeptidome experiments. (I) Flow cytometry-based quantitation is performed to determine the number of molecules of a specific pMHC per cell. In conjunction with transduction efficiency and total cell number it allows to define the pMHC input. (II) Exemplifying lists of different variables of MHC ligand isolation as well as LC-MS/MS analysis, which can or can not be altered in the experimental setting. (III) Analysis of MS data with different algorithms for qualitative and quantitative detection of the MHC ligand of interest. These results can be used for experimental comparisons.

TCR mimic monoclonal antibodies that bind to the pMHC epitope. The measurement of the exact numbers of pMHC on a single cell in combination with cell number and transduction efficiency (ranging between 16.6 and 94.6%) then allowed us to define the numerical input of pMHC molecules per experiment.

Second, immunopurification of pMHC, elution of MHC ligands, and MS analyses were performed using a merged protocol from two different publications [7,8]. However, for inter-laboratory comparisons, the parameters of this multistep procedure can be varied, and are not of interest for the final readout of the experiment.

In the last step, acquired untargeted MS data were analyzed with whole proteome databases to mimic standard MHC ligand isolation experiments. Precursor intensities were used for relative quantitation and to determine the detection threshold for the model MHC ligands. Of note, only MS1 data were used to define the limit of detection, MS2 spectra were used to validate that the respective precursor signal actually corresponds to the target sequence and to identify other MHC ligands present in the sample. Finally, these quantitative, input-controlled results, which include the detection limit as well as the *p*-values for peptide spectrum matches (PSMs), can then be used for intra-laboratory comparisons if identical processing software and parameters are utilized.

As it is crucial for our approach to ensure a reliable technique for the standardized pMHC input we characterized and compared two orthogonal assays in three model systems. Radio-immunoassay and flow cytometry with commercially available quantitation beads were utilized to determine the copy number of pMHC complexes on the cell surface of two TAP-deficient cell lines (RMA-S and T2) that were transduced with PresentER construct expressing H2-Kb:SIINFEKL or A*02:RMFPNAPYL, respectively. Additionally, EL4-OVA cells were analyzed as they also present H2-Kb:SIINFEKL on the cell surface; as this cell line is not TAP-deficient, many other MHC ligands are displayed simultaneously, as might be expected in a typical immunopeptidome experiment. For quantitation of H2-Kb:SIINFEKL, the antibody 25-D1.16 was used; for A*02:RMFPNAPYL, we used the TCR mimic antibody ESK1[9]. All cell lines were repeatedly tested by radioimmunoassay and flow cytometry-based quantitation for the total amount of MHC class I complexes displaying the ligand of interest (H2-Kb or HLA-A*02) and the copy number of the specific pMHC (Fig. 2A.) The observed much higher number of MHC molecules on T2 cells versus RMA-S cells can be explained by the bigger cell size of T2 cells compared to RMA-S cells as both cell lines are TAP-deficient. EL4 cells on the other hand express more MHC molecules on the cell surface compared to RMA-S cells as EL4 cells are TAP-sufficient. Moreover, for the two presentER transduced cell lines the ratio of target peptide:MHC to total MHC was much higher for SIINFEKL compared to RMFPNAPYL. This difference might occur as the presentER system cannot perfectly mimic the physiological peptide:MHC loading which might result in these differences or through different levels of TAP-deficiency in these two cell lines.

Although the radioimmunoassay systematically detected 3-fold higher copy numbers of whole MHC and specific pMHC, the two quantification methods were highly correlated ($R^2 = 0.994$) (Fig. 2B.) This difference in absolute numbers of cell surface molecules read by these two methods is likely because the number of fluorescent moieties on each antibody might not be exactly 1, and is not disclosed by the manufacturer, whereas the specific activity of the radioimmunoassay can be calculated to determine the exact number of CPM per antibody molecule units. Another explanation for the discrepancy between the two methods might be that for flow cytometry Fc receptor blocking reagents were used, whereas for the RIA no such reagents were used which could result in more unspecific Fc receptor mediated binding.

However, as flow cytometry is more broadly available to most laboratories, we chose this method as the standard quantitation assay to determine the input of pMHC in our MS experiments.

Immunopurification experiments were performed for all three

model systems after copy numbers of specific MHC ligands and transduction efficiency were determined by flow cytometry to define the initial amounts of pMHCs that were used in every experiment. All experiments were carried out in technical duplicates or triplicates. For the identification of the target MHC ligands we used the Byonic software [10] searching against the complete human or mouse proteome (plus ovalbumin) and for calculating the precursor intensities skyline software [11] was utilized. Importantly, for all model systems the MHC ligand of interest could be detected with *p*-values for peptide spectrum matches (PSM) < 0.01 and precursor intensity by peak area always correlated well with the pMHC input. For the RMFPNAPYL peptide immunoprecipitated from the PresentER T2 cells, 4.8 fmol of pMHC input were sufficient for detection whereas for the MHC ligand SIINFEKL, that was also displayed and isolated from the PresentER system, 10 amol of pMHC was the limit of detection when only detection of the precursor was considered. Of note, for samples with 100 and 10 amol H2-Kb:SIINFEKL input target sequence identification via MS2 spectra through Byonic was only feasible with *p*-values for PSM of < 0.05 and 0.83 respectively, see Fig. 2C, D and Table 1. Consistent with the reports of T-cell epitopes associated with impaired peptide processing (TEIPPs) [12] we detected a small set of peptides presented by H2-Kb and H2-Db complexes in RMA-S cells and by HLA-A*02 molecules in T2 cells which showed the known characteristics of TEIPPs such as above average peptide length and suboptimal affinity to MHC complexes (Suppl. Table 1).

In contrast to RMA-S cells, for high confidence detection of the SIINFEKL peptide in the EL4-OVA setting, a much higher input of 727 fmol was needed, see Fig. 2E and Table 1. This required increase in input of over 700-fold is most likely to be the consequence of higher background in the EL4-OVA model system that continues to present cytoplasmic peptides, compared to the TAP-deficient RMA-S cells. To illustrate this possibility, we identified all MHC binders that were detected with *p*-values < 0.01 and that were assigned to either H2-Kb, H2-Kb or HLA-A*02 alleles by netMHCpan 4.0 [13] algorithm with a standard 2% rank cutoff for MHC binders. On EL4-OVA cells, over 150 times more background MHC ligands were identified compared to RMA-S PresentER SIINFEKL cells. These background MHC ligands could lower the sensitivity for detection of any particular pMHC either during the immunopurification or the LC-MS/MS analysis steps (Suppl. Table 1). As the correlation between peptide:MHC complex input measured by flow cytometry and identification of MHC ligands seemed robust, we also asked if these results could be transferred to unmodified HLA-A*02 positive cell lines used in classic immunopeptidome experiments. We quantified the HLA-A*02 surface levels from 6 different cell lines using the BB7.2 antibody by flow cytometry and subsequently performed immunoprecipitation and MS analysis on 10 million cells per cell line so that the input of HLA complexes was only affected by the different HLA-A*02 surface levels. Strikingly, there was as very strong correlation ($R^2 = 0.993$) between HLA-A*02 complexes per cell and the number of identified unique HLA-A*02 ligands (Fig. 2F and G, Suppl. Table 1) Additionally, a calculation of the average number of HLA-A*02 complexes per peptide necessary for detection in the 6 different cell lines showed that for 5 out of the 6 cell lines, molecule concentrations ranged between 1.8 and 5.1 fmol, which represents the thresholds seen in our presentER model system very well. This theoretical number is then thought to benchmark the complete immunopeptidome isolation process including all variables in one specific laboratory and will allow interlaboratory comparison

Defining easy to implement model systems and approaches that allow comparison of immunopeptidomic experiments between laboratories is a problem that has not been addressed by the field in a satisfactory manner. Using identical cell numbers or cell pellets shared between laboratories can still be biased by shipment or numerous other factors as well as variable expression and presentation of MHC ligands. In this study, we demonstrated that using cell lines that are engineered to display an MHC ligand of choice either exclusively or in combination

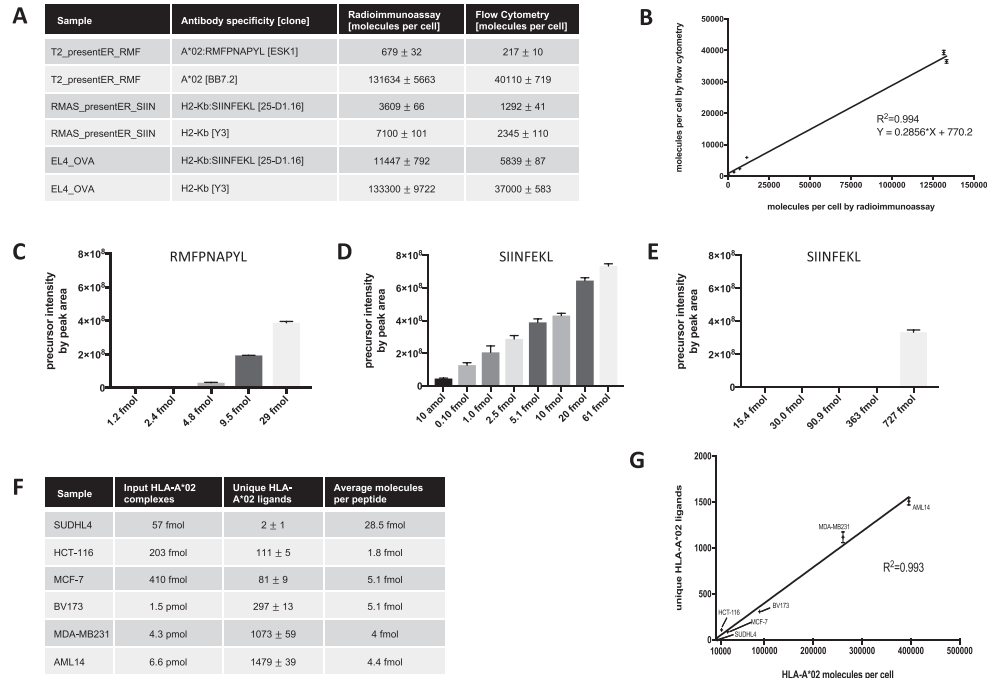


Fig. 2. Comparison and orthogonal validation of flow cytometry-based quantitation of pMHC and radioimmunoassay. (A) Copy numbers of specific pMHC and total MHC determined by radioimmunoassay and flow cytometry-based quantitation. (B) Visualization and linear regression of the results in (A). All data points are the mean of technical triplicates and all quantitations have been performed at least twice with similar results. (C-E) Relative quantitation of input-controlled immunopeptidomics experiments. (C-E) Relative quantitation by precursor intensity measured by peak area with skyline software for.

T2-PresentER:RMFPANPYL (C), RMA-S-PresentER:SIINFEKL (D) and EL4-OVA cells (E). Quantitation was calculated by skyline software and time window for quantitation was 30 s before and after the detection of the target sequence in MS2 spectra.

Correlation of HLA-A*02 complex input and number of identified HLA-A*02 binding peptides in unmodified cancer cell lines. (F) Sample and input characteristics (G) Correlation of HLA-A*02 complex input and identified A*02 assigned HLA ligands. Error bars in 2B and 2G as well as deviations in 2A and 2F indicate SD.

Table 1

Overview of experimental input by cell number and molecules, p-values for MHC ligand identification and number of other identified MHC ligands.

RMA-S PresentER SIINFEKL				EL4-OVA				T2 PresentER RMFPNAPYL			
# of cells [cells]	input [pMHC]	p-value for PSM [target]	diversity [MHC ligands]	# of cells [cells]	input [pMHC]	p-value for PSM [target]	diversity [MHC ligands]	# of cells [cells]	input [pMHC]	p-value for PSM [target]	diversity [MHC ligands]
180 M	61 fmol	< 0.01	11	80 M	727 fmol	< 0.01	318	85 M	29 fmol	< 0.01	9
60 M	20 fmol	< 0.01	2	40 M	363 fmol	n.d.	255	28 M	9.5 fmol	< 0.01	6
30 M	10 fmol	< 0.01	6	10 M	90.9 fmol	n.d.	117	14 M	4.8 fmol	< 0.01	3
15 M	5.1 fmol	< 0.01	6	3.3 M	30.0 fmol	n.d.	32	7 M	2.4 fmol	n.d.	2
7.5 M	2.5 fmol	< 0.01	3	1.7 M	15.4 fmol	n.d.	22	3.5 M	1.2 fmol	n.d.	0
3 M	1.0 fmol	< 0.01	2								
0.3 M	0.10 fmol	< 0.05	2								
0.03 M	10 amol	0.83	2								

Transduction efficiencies for MS experiments: RMA-S:SIINFEKL = 16.6%, EL4-OVA = 93.7%, T2:RMFPNAPYL = 94.6%. n.d. = not detected.

with other MHC ligands can form the basis to solve this problem. Flow cytometry-based quantitation of the target MHC ligand, e.g. with the H2Kb:SIINFEKL specific antibody 25-D1.16 has been shown through orthogonal validation by radioimmunoassay to be a reliable method to provide a measurement of exact input of pMHCs which allows an intra-

and interlaboratory standardization of immunopeptidomic experiments. Immunopurification and analysis of the isolated MHC ligands by LC-MS/MS demonstrated a robust correlation with the pMHC input, but also illustrated the strong effect of the diversity of the immunopeptidome for the detection of a defined MHC ligand. In EL4 cells,

the detection of the MHC ligand SIINFEKL required over 700 times higher input of peptide:MHC complexes than in the PresentER system, in which presentation of cytoplasmic peptides is reduced. These differences might have been overcome by performing a targeted MS experiment; in order to mimic more realistic experimental procedures, we assumed in all experiments to be agnostic of the peptide sequence of interest. However, in a single peptide MHC displaying system, detection of the SIINFEKL and the RMFPNAPYL peptide was feasible with *p*-values for PSM < 0.01 with an input of 1 and 5 fmol of pMHC, respectively. If higher *p*-values were accepted SIINFEKL would be identified with only 10 amol of pMHC input. Immunopeptidomic experiments are usually performed in systems with hundreds to thousands of different pMHCs displayed and therefore a single epitope model does not reflect the complexity of a biological sample. On the contrary, having background-free model systems might allow better optimization of the isolation protocol as there are fewer confounding variables. However, when we applied the idea to control the input of an immunopeptidome experiment by flow cytometry to 6 HLA-A*02 positive cell lines we observed a tight correlation between the amounts of HLA-A*02 complexes per cell and the numbers of identified A*02 HLA ligands. Furthermore, the theoretical amount of HLA complex input sufficient for HLA ligand detection was around 5 fmol in 5 out of 6 samples which overlaps well with the thresholds of detection seen in the PresentER model systems. Calculation of this theoretical parameter can then be used to characterize the complete immunopeptidome isolation and identification setup from cell lysis to peptide identification in a certain laboratory and can furthermore be compared to other laboratories independent of their isolation methods or mass spectrometry instruments used.

Therefore, reporting the amount of input material by flow cytometry quantification of surface MHC may help to make experiments comparable within and between laboratories.

Altogether, studies of both the PresentER and EL4-OVA system provided a highly controlled model to either optimize protocols within laboratories or to compare performance of isolation techniques between different laboratories independently of all variables in the immunopurification and peptide analysis workflow. The method also provides an even more broadly applicable system for HLA-A*02 positive cell lines and could be further expanded to other common HLA alleles in the future; in the case of A*02, the input of total A*02 complexes can be easily determined and the number of identified HLA-A*02 binders thus allows average estimation of a laboratory- or method-specific threshold of detection for comparison between laboratories.

2. Materials and methods

2.1. Cell lines

T2, MCF-7, MDA-MB231 and EL4-OVA cell lines were purchased from American Type Culture Collection (ATCC). T2 cells were maintained in IMDM media, MCF-7 and MDA-MB231 in DMEM media and EL4-OVA cells in RPMI media adjusted to contain 1.5 g/l sodium bicarbonate, 4.5 g/l glucose, 10 mM HEPES and 1.0 mM sodium pyruvate and supplemented with 0.05 mM 2-mercaptoethanol and 0.4 mg/ml G418. RMA-S cells were a generous gift from the Schietinger Lab at MSKCC. BV173 was provided by H. J. Stauss (University College London, London, United Kingdom), AML14 was a gift from Ross Levine, SUDHL4 was provided by Ana Younes and all the aforementioned cells were maintained in RPMI media. All media were supplemented with 10% FBS and 2 mM glutamine.

2.2. Cloning the PresentER cassette and different PresentER constructs

All cloning was performed as described previously [6]. The PresentER cassette as well as the SIINFEKL and RMFPNAPYL minigenes can be found at Addgene (Cat. #102942 and #102944).

2.3. Production of retrovirus and transduction

HEK293T Phoenix amphoteric cells were transfected with polyethylenimine (PEI) and PresentER plasmid (15 µg DNA: 45 µg PEI) in 10 cm TC plates. Virus was harvested every 12 h, pooled, concentrated with Clontech Retro-X and frozen. T2 cells were spinoculated with virus in non-TC treated 6-well plates at 32 °C x 2,000 × g for 2 h with 4 µg/ml of polybrene. RMA-S cells were spinoculated with virus in non-TC treated 6-well plates at 32 °C x 1,000 × g for 2 h with 4 µg/ml of polybrene. The volume of viral supernatant that led to 1/3 maximal transduction efficiency was established for each batch of virus produced by transduction with serial dilutions of viral supernatant. Transduced cells were selected with 1 µg/ml (T2) or 4 µg/ml (RMA-S) of puromycin for 2–3 days and transduction efficiency determined by GFP levels.

2.4. Antibodies and labeling reagents

ESK1 monoclonal antibody specific for HLA-A*02:RMFPNAPYL was purified by Eureka Therapeutics and used for either radioimmunoassay or flow cytometry. H2-Kb:SIINFEKL specific antibody 25-D1.16 and H2-Kb specific Y3 were purchased from BioXcell (Cat. #BE0207 and #BE0172) and used for either radioimmunoassay or flow cytometry. The BB7.2 clone was purified at the MSKCC antibody core facility. For flow cytometry ESK1 and 25-D1.16 were labeled with Innova Biosciences Lightning Link kits (Cat. #703–0010) according to manufacturer's protocols to results in an equimolar ratio of antibody and fluorophore. For H2-Kb and HLA-A*02 quantitation Y3-PE and BB7.2-PE antibodies were purchased from BioLegend (Cat. #141603 and #343305).

2.5. Quantitation of surface molecules by flow cytometry

For flow cytometry-based quantitation experiments BD Quantibrite-PE kits were used (BDBiosciences, Cat. #340495) according to the manufacturer's protocol. Flow cytometry was performed with a standard protocol and a dilution of the above mentioned antibodies at 1:100 for 30 min on ice. Flow cytometry data were collected on a Fortessa (BD Biosciences) and analyzed with FlowJo V9.9.

2.6. Radioimmunoassay

ESK1, 25-D1.16, BB7.2 and Y-3 was labeled with ¹²⁵I (PerkinElmer) using the chloramine-T method. Antibody (100 µg) was reacted with 1 mCi ¹²⁵I and 20 µg chloramine-T, quenched with 200 µg Na-metabisulfite, then separated from free ¹²⁵I using a 10DG column and equilibrated with 2% bovine serum albumin in PBS. Specific activities of products were in the range of 4–8 mCi/mg. PresentER or EL4-OVA cells (only cells with transduction efficiencies > 95% were used) and respective wildtype variants (T2, RMA-S and EL4) were harvested. Cells were washed once with PBS and re-suspended in 2% human serum in PBS at 10⁷ cells/ml on ice. Cells (10⁶ per tube, in duplicate) were incubated with ¹²⁵I-labeled antibody (1 µg/ml) for 45 min on ice, then washed extensively with 1% bovine serum albumin in PBS on ice. Bound radioactivity was measured by a gamma counter, specific binding was determined, and the number of bound antibodies per cell was calculated from specific activity. For final copy numbers unspecific background binding of T2, RMA-S or EL4 cells was subtracted.

2.7. Immunopurification of HLA class I ligands

For immunopurification affinity columns were prepared as follows: 40 mg of Cyanogen bromide-activated-Sepharose® 4B (Sigma-Aldrich, Cat# C9142) was activated with 1 mM hydrochloric acid (Sigma-Aldrich, Cat# 320331) for 30 min. Subsequently, 0.5 mg of W6/32 antibody (BioXCell, Cat #BE0079) and for mouse cell lines 0.5 mg M1/42.3.9.8 antibody (BioXCell, Cat #BE0077) was coupled to sepharose in

presence of binding buffer (150 mM sodium chloride, 50 mM sodium bicarbonate, pH 8.3; sodium chloride: Sigma-Aldrich, Cat# S9888, sodium bicarbonate: Sigma-Aldrich, Cat#S6014) for at least 2 h at room temperature. Sepharose was blocked for 1 h with glycine (Sigma-Aldrich, Cat# 410225). Columns were equilibrated with PBS for 10 min. Suspension cells were harvested directly, adherent cell lines after incubating 15 min with CellStripper solution (Corning™, Cat# 25056CI) and washed three times in ice-cold sterile PBS (Media preparation facility MSKCC). For presentER and EL4-OVA cells number of cells used is indicated in Table 1, for all other experiments 10^7 cells were used. Afterwards, cells were lysed in 7.5 ml 1% CHAPS (Sigma-Aldrich, Cat# C3023) in PBS, supplemented with protease inhibitors (cComplete, Cat# 11836145001) for 1 h at 4 °C. Lysate was spun down for 1 h with 20,000 g at 4 °C. Supernatant was run over column through peristaltic pumps with 1 ml/min flow rate overnight in cold room. Affinity columns were washed with PBS for 30 min, water for 30 min, then run dry, and HLA complexes subsequently eluted five times with 200 µl 1% trifluoroacetic acid (TFA, Sigma/Aldrich, Cat# 02031). For separation of HLA ligands from their HLA complexes tC18 columns (Sep-Pak tC18 1 cc Vac Cartridge, 50 mg Sorbent per Cartridge, 37–55 µm Particle Size, Waters, Cat# WAT036820) were prewashed with 80% acetonitrile (ACN, Sigma-Aldrich, Cat# 34998) in 0.1% TFA and equilibrated with two washes of 0.1% TFA. Samples were loaded, washed again with 0.1% TFA and eluted in 400 µl 30% ACN in 0.1%TFA. Sample volume was reduced by vacuum centrifugation for mass spectrometry analysis.

2.8. LC-MS/MS analysis of HLA ligands

Samples were analyzed by high resolution/high accuracy LC-MS/MS (Lumos Fusion, Thermo Fisher). Peptides were desalted and concentrated prior to being separated using direct loading onto a packed-in-emitter C18 column (75µm ID/12 cm, 3 µm particles, Nikkyo Technos Co., Ltd. Japan). The gradient was delivered at 300 nl/min increasing linear from 2% Buffer B (0.1% formic acid in 80% acetonitrile) / 98% Buffer A (0.1% formic acid) to 30% Buffer B / 70% Buffer A, over 70 min. MS and MS/MS were operated at resolutions of 60,000 and 30,000, respectively. Only charge states 1, 2 and 3 were allowed. 1.6 Th was chosen as isolation window and collision energy was set at 30%. For MS/MS, maximum injection time was 100 ms with an AGC of 50,000.

2.9. Mass spectrometry data processing

Mass spectrometry data was processed using Byonic software (version 2.7.84, Protein Metrics, Palo Alto, CA) through a custom-built computer server equipped with 4 Intel Xeon E5-4620 8-core CPUs operating at 2.2 GHz, and 512 GB physical memory (Exxact Corporation, Fremont, CA). Mass accuracy for MS1 was set to 6 ppm and to 20 ppm for MS2, respectively. Digestion specificity was defined as unspecific and only precursors with charges 1, 2 and 3 and up to 2 kDa were allowed. Protein FDR was disabled to allow complete assessment of potential peptide identifications. Oxidization of methionine was set as variable modifications for all samples. T2 samples were searched against UniProt Human Reviewed Database (20,349 entries, <http://www.uniprot.org>, downloaded June 2017) and RMA-S cells as well as EL4-OVA cells were searched against UniProt Mouse Reviewed Database (17,033 entries, <http://www.uniprot.org>, downloaded August 2019) supplemented with the ovalbumin protein sequence. All databases included target decoys derived from the reversed sequences of all included proteins. Peptides were selected with a minimal log prob. value of 2 corresponding to *p*-values from PSMs < 0.01. We added false positive hits that were identified after selection for peptides of 8–12 amino acids in length and assigned to HLA-A*02 complexes via netMHCpan (Suppl. Table 1). For AML14 false positive peptide identifications without HLA assignment were also included in the Suppl.

Table 1). The calculated FDR based on these false and true positive identifications was < 1% for all analyzed samples reassuring our selection for the logprob filter value of 2. For relative quantitation skyline software (version 3.1, MacCoss Lab Software) was used. Masses of precursors of peptide target sequences were searched in all relevant.raw files and peak areas of all replicates compared. We enabled matching mass and retention times of target precursors to other samples to ensure highest sensitivity and detection in all relevant samples independently of selection for MS2 fragmentation. For quantitation only time windows 30 s before and after the identification of the correct MHC ligand sequence were considered.

2.10. Assignment of peptide sequences to HLA alleles

To assign peptides which passed the above-mentioned MS quality filters to their HLA complexes which they most likely bind to we used the netMHCpan 4.0 algorithm [13] with default settings. No binding affinity predictions were enabled. Therefore, all peptides with affinity %ranks below 2 were considered binder.

2.11. Software

All graphs were drawn with Graphpad Prism 7.

Author contributions

M.G.K., Z.A., M.C., H.F.J and R.S.G. performed and analyzed experiments. M.G.K. and D.A.S. designed experiments. M.G.K., Z.A. wrote the original draft of the manuscript. D.A.S. provided funding, edited the manuscript, and supervised the project. All authors reviewed and contributed to the manuscript.

Funding

This study was supported by Leukemia and Lymphoma Society, NHP30CA 008748, NIH R01 CA55349, P01 CA23766, R35 CA241894, Solomon Foundation, and Tudor Funds. M.G.K. is supported by the German Research Foundation (DFG) with the individual research grant KL 3118/1-1. RSG is supported by NCIF30 CA200327 and NIGMST32GM07739. HFJ is supported by NIHT32 CA062948. The content of this study is solely the responsibility of the authors and does not necessarily represent official views of the German Research Foundation.

Declaration of Competing Interest

D.A. Scheinberg has potential conflicts of interest, defined by Elsevier Publishing Group by ownership in, income from, or research funds from: Pfizer, Sella Life Sciences, Iovance, Eureka Therapeutics, and Bristol Myers Squibb. DAS, MGK and RSG are inventors of technology owned by MSK that has been filed for patent protection.

Acknowledgements

We thank Alex Kentis for access to the Byonic Software and the Proteome Resource Center at Rockefeller University for the performance of all LC-MS/MS experiments.

Appendix A. Supplementary data

Supplementary data to this article can be found online at <https://doi.org/10.1016/j.jprot.2020.103921>.

References

- [1] M. Bassani-Sternberg, G. Coukos, Mass spectrometry-based antigen discovery for cancer immunotherapy, *Curr. Opin. Immunol.* 41 (2016) 9–17.
- [2] N. Hillen, S. Stevanovic, Contribution of mass spectrometry-based proteomics to immunology, *Exp. Rev. Proteomics* 3 (6) (2006) 653–664.
- [3] C.T. Tan, N.P. Croft, N.L. Dudek, N.A. Williamson, A.W. Purcell, Direct quantitation of MHC-bound peptide epitopes by selected reaction monitoring, *Proteomics* 11 (11) (2011) 2336–2340.
- [4] C. Hassan, M.G. Kester, G. Oudgenoeg, A.H. de Ru, G.M. Janssen, J.W. Drijfhout, R.M. Spaapen, C.R. Jimenez, M.H. Heemskerk, J.H. Falkenburg, P.A. van Veelen, Accurate quantitation of MHC-bound peptides by application of isotopically labeled peptide MHC complexes, *J. Proteome* 109 (2014) 240–244.
- [5] E. Caron, D.J. Kowalewski, C. Chiek Koh, T. Sturm, H. Schuster, R. Aebersold, Analysis of major histocompatibility complex (MHC) Immunopeptidomes using mass spectrometry, *Mol. Cell. Proteomics* 14 (12) (2015) 3105–3117.
- [6] R.S. Gejman, H.F. Jones, M.G. Klatt, A.Y. Chang, C.Y. Oh, S.S. Chandran, T. Korontsvit, V. Zakhaleva, T. Dao, C.A. Klebanoff, D.A. Scheinberg, Identification of the targets of T cell receptor therapeutic agents and cells by use of a high throughput genetic platform, *Cancer Immunol. Res.* 8 (5) (2020) 672–684.
- [7] A. Nelde, D.J. Kowalewski, S. Stevanovic, Purification and identification of naturally presented MHC class I and II ligands, *Methods Mol. Biol.* (2019) (1988) 123–136.
- [8] M. Bassani-Sternberg, E. Braunlein, R. Klar, T. Engleitner, P. Sinitcyn, S. Audehm, M. Straub, J. Weber, J. Slotta-Huspenina, K. Specht, M.E. Martignoni, A. Werner, R. Hein, H.B. D.C. Peschel, R. Rad, J. Cox, M. Mann, A.M. Krackhardt, Direct identification of clinically relevant neoepitopes presented on native human melanoma tissue by mass spectrometry, *Nat. Commun.* 7 (2016) 13404.
- [9] T. Dao, S. Yan, N. Veomett, D. Pankov, L. Zhou, T. Korontsvit, A. Scott, J. Whitten, P. Maslak, E. Casey, T. Tan, H. Liu, V. Zakhaleva, M. Careio, E. Doubrovina, R.J. O'Reilly, C. Liu, D.A. Scheinberg, Targeting the intracellular WTI oncogene product with a therapeutic human antibody, *Sci. Transl. Med.* 5 (176) (2013) 176ra33.
- [10] M. Bern, Y.J. Kil, C. Becker, Byonic: advanced peptide and protein identification software, *Curr Protoc Bioinformatics Chapter 13* (2012) (Unit13 20).
- [11] B. MacLean, D.M. Tomazela, N. Shulman, M. Chambers, G.L. Finney, B. Frewen, R. Kern, D.L. Tabb, D.C. Liebler, M.J. MacCoss, Skyline: an open source document editor for creating and analyzing targeted proteomics experiments, *Bioinformatics* 26 (7) (2010) 966–968.
- [12] U.J. Seidel, C.C. Oliveira, M.H. Lampen, T. Hall, A novel category of antigens enabling CTL immunity to tumor escape variants: Cinderella antigens, *Cancer Immunol. Immunother.* 61 (1) (2012) 119–125.
- [13] V. Jurtz, S. Paul, M. Andreatta, P. Marcatili, B. Peters, M. Nielsen, NetMHCpan-4.0: improved peptide-MHC class I interaction predictions integrating eluted ligand and peptide binding affinity data, *J. Immunol.* 199 (9) (2017) 3360–3368.

2.3. Pharmakologische Modulation des Immunpeptidoms

2.3.1 Epigenetische Modulatoren

Originalarbeit 3

Bourne CM, Mun SS, Dao T, Aretz ZEH, Molvi Z, Gejman RS, Daman A, Takata K, Steidl C, **Klatt MG***, Scheinberg DA*. Unmasking the suppressed immunopeptidome of EZH2-mutated diffuse large B-cell lymphomas through combination drug treatment. *Blood Adv.* 2022;6(14):4107-4121. *geteilte Letztautorenschaft

Ein sehr häufiger Mechanismus der Immunevasion ist der Verlust oder die Downregulation der HLA Expression und somit der über das Immunpeptidom präsentierten Peptide. Besonders häufig wird dieser Mechanismus in Lymphomen beobachtet und Ziel dieser Arbeit war es, das durch die Downregulation unterdrückte Immunpeptidom pharmakologisch wiederherzustellen und die Tumoren somit einer Immunantwort erneut zugänglich zu machen. Diffus großzellige B-Zell-Lymphome (DLBCLs) stellen für die Fragestellung eine besonders geeignete Entität dar, da sie neben der Downregulation von HLA auch oft EZH2-Mutationen aufweisen, von welchen nachgewiesen wurde, dass deren Inhibition zu einer Heraufregulation der HLA Expression führt. Diesen Mechanismus konnten wir replizieren und erweiterten ihn auf Kombinationstherapien mit Decitabin und Tazemetostat sowie Interferon (IFN)- γ . Hierbei wirken Decitabin als DNA demethylierende Substanz und Tazemetostat als spezifischer EZH2-Inhibitor. Insbesondere die Kombination der beiden Medikamente verbesserte in dieser Arbeit nachweislich die IFN- γ abhängige HLA Hochregulierung in EZH2-mutierten DLBCL-Zelllinien. Diese Hochregulierung wurde für die Zelloberflächenexpression von HLA Klasse I und II beobachtet, wobei Decitabin im Vergleich zu Tazemetostat eine etwas stärkere Hochregulierung als Einzelsubstanz zeigte.

Darüber hinaus modulierten diese Medikamente einzelne HLA-Allele unabhängig voneinander und verstärkten die Transkription der Antigenpräsentationsmaschinerie in DLBCLs. Dies deutet darauf hin, dass diese Wirkstoffe das Repertoire des Immunpeptidoms signifikant beeinflussen und zu einer Wiederherstellung des sonst maximal supprimierten HLA Ligandoms führt. Das wiederhergestellte Repertoire des Immunpeptidoms war in der Anzahl der präsentierten HLA Liganden sogar wieder mit dem von gesunden B-Zellen vergleichbar. Aus qualitativer Sicht ist aber zu betonen, dass innerhalb dieser neuen Immunopeptidoms viele HLA Liganden identifiziert wurden, welche sich aus lymphomtypischen Antigenen ableiteten und zu großen Teilen auch nicht auf gesunden Geweben nachweisbar waren.

Insgesamt zeigt diese Studie das Potenzial von Kombinationstherapien mit epigenetischen Modulatoren in DLBCLs, da diese Immunpeptidom nicht nur quantitativ deutlich heraufregulieren, sondern auch qualitativ zur Präsentation von HLA Liganden führt, welche als tumorspezifische Targets in zukünftigen Studien genutzt werden können.

Unmasking the suppressed immunopeptidome of EZH2-mutated diffuse large B-cell lymphomas through combination drug treatment

Christopher M. Bourne,¹ Sung Soo Mun,² Tao Dao,² Zita E. H. Aretz,³ Zaki Molvi,³ Ron S. Gejman,^{2,4} Andrew Daman,⁵ Katsuyoshi Takata,^{6,7} Christian Steidl,^{6,7} Martin G. Klatt,^{2,*} and David A. Scheinberg^{2,8,*}

¹Immunology and Microbial Pathogenesis Program, Weill Cornell Medicine, New York, NY; ²Molecular Pharmacology Program, Memorial Sloan Kettering Cancer Center, New York, NY; ³Physiology Biophysics and Systems Biology Program, Weill Cornell Medicine, New York, NY; ⁴Tri-Institutional MD-PhD Program, Sloan Kettering Institute, Weill Cornell Medicine and Rockefeller University, New York, NY; ⁵Laboratory of Epigenetics and Immunity, Department of Pathology and Laboratory Medicine, Weill Cornell Medicine, New York, NY; ⁶Centre for Lymphoid Cancer, British Columbia Cancer, Vancouver, BC, Canada; ⁷Department of Pathology and Laboratory Medicine, University of British Columbia, Vancouver, BC, Canada; and ⁸Pharmacology Department, Weill Cornell Medicine, New York, NY

Key Points

- Combination therapy of IFN- γ with epigenetic regulators leads to large increases in the immunopeptidome of DLBCL.
- HLA ligands from proteins RGS13 and E2F8 may provide DLBCL-specific targets for immunotherapy.

Exploring the repertoire of peptides presented on major histocompatibility complexes (MHCs) helps identify targets for immunotherapy in many hematologic malignancies. However, there is a paucity of such data for diffuse large B-cell lymphomas (DLBCLs), which might be explained by the profound downregulation of MHC expression in many DLBCLs, and in particular in the enhancer of zeste homolog 2 (*EZH2*)-mutated subgroup. Epigenetic drug treatment, especially in the context of interferon- γ (IFN- γ), restored MHC expression in DLBCL. In DLBCL, peptides presented on MHCs were identified via mass spectrometry after treatment with tazemetostat or decitabine alone or in combination with IFN- γ . Such treatment synergistically increased the expression of MHC class I surface proteins up to 50-fold and the expression of class II surface proteins up to threefold. Peptides presented on MHCs increased to a similar extent for both class I and class II MHCs. Overall, these treatments restored the diversity of the immunopeptidome to levels described in healthy B cells for 2 of 3 cell lines and allowed the systematic search for new targets for immunotherapy. Consequently, we identified multiple MHC ligands from the regulator of G protein signaling 13 (*RGS13*) and E2F transcription factor 8 (*E2F8*) on different MHC alleles, none of which have been described in healthy tissues and therefore represent tumor-specific MHC ligands that are unmasked only after drug treatment. Overall, our results show that *EZH2* inhibition in combination with decitabine and IFN- γ can expand the repertoire of MHC ligands presented on DLBCLs by revealing suppressed epitopes, thus allowing the systematic analysis and identification of new potential immunotherapy targets.

Introduction

Diffuse large B-cell lymphoma (DLBCL) is the most common lymphoma type in the western hemisphere. About 60% of patients with DLBCL can be cured by using standard chemoimmunotherapy—rituximab plus cyclophosphamide, doxorubicin, vincristine, and prednisone (R-CHOP)—but successful treatment

Submitted 3 September 2021; accepted 29 April 2022; republished online on *Blood Advances* First Edition 13 May 2022; final version published online 15 July 2022. DOI 10.1182/bloodadvances.2021006089.

*M.G.K. and D.A.S. contributed equally to this study. Immunopeptidomics data are available upon request by sending an e-mail to David A. Scheinberg at scheinbd@mskcc.org.

The full-text version of this article contains a data supplement.

© 2022 by The American Society of Hematology. Licensed under Creative Commons Attribution-NonCommercial-NoDerivatives 4.0 International (CC BY-NC-ND 4.0), permitting only noncommercial, nonderivative use with attribution. All other rights reserved.

remains challenging in patients who have relapsed DLBCL.¹ Because the R-CHOP regimen can cause considerable toxicity, which is poorly tolerated by older patients,² therapeutic agents that minimize adverse effects while still demonstrating antitumor efficacy are attractive. Immunotherapy has seen remarkable antitumor efficacy and on-tumor specificity,³⁻⁶ and the identification of neoepitopes that are specific to cancer cells can maximize on-tumor efficacy while minimizing off-target effects on healthy tissue.⁷⁻⁹ Currently, there are a number of cell surface targets for antibody therapies.¹⁰ Identification of suitable targets for T-cell immunotherapy relies on immunoprecipitation of major histocompatibility complexes (MHCs) and subsequent analysis of the bound peptides via mass spectrometry (MS), which has been performed on both solid and liquid cancers.¹¹⁻¹⁶

The immunopeptidome of DLBCL has not been well characterized to date; only 1 other study has examined the immunopeptidome of DLBCL at steady state.¹⁷ The lack of systematic descriptions of the immunopeptidome of DLBCL may be a result of the inability of DLBCL cells to downregulate antigen presentation and evade immune recognition, which masks neo-epitopes and the complete immunopeptidome.¹⁸ Downregulation of antigen presentation is also implicated in immune checkpoint blockade escape.¹⁴ To overcome this downregulation, chemotherapies that upregulate antigen presentation are being explored in combination with immune checkpoint blockade in numerous cancer types.¹⁹⁻²⁵ One mechanism for downregulation of HLA expression and antigen presentation is transcriptional silencing by repressive epigenetic marks.²⁶⁻²⁸ Epigenetic modifiers and immunotherapy are also being explored as rational combination therapeutics for their efficacy at relatively nontoxic doses and their ability to selectively reprogram cancer cells.^{24,29,30}

Promoter DNA methylation silences transcription of the downstream gene. Cancer cells dysregulate DNA methylation to silence antitumor genes. Decitabine, a DNA demethylating agent, covalently binds to the DNA methyltransferases to block deposition of DNA methylation. Because cancers silence antigen presentation using DNA methylation, DNA demethylating agents are actively being explored in preclinical models and in the clinic alongside checkpoint blockade inhibitors and other immunotherapies.³¹⁻³³ Given that DNA methylation correlates with other repressive epigenetic modifications, they may need to be targeted to overcome coordinated silencing pathways.

The oncogenic functions of EZH2 are being uncovered.^{34,35} Activating mutations in the catalytic pocket of EZH2 such as those at tyrosine 641 (Y641) cause excessive deposition of H3 lysine 27 trimethylation (H3K27me3), which is associated with repressed transcription.²⁸ These mutations are common in DLBCL and are linked to tumor progression.^{34,36} Agents that block EZH2 function, such as tazemetostat, bind the S-adenosyl methionine pocket causing competitive inhibition.^{28,37,38} Similar to DNA methylation, the EZH2 function in silencing antitumor immune responses has also been implicated by recent evidence.^{24,25,30} In line with these findings, EZH2 can directly recruit DNA methyltransferases to polycomb repressive complex 2 (PRC2) target genes to further stabilize gene silencing.³⁹ In DLBCL, more than half the de novo DNA methylation events overlap with PRC2 target genes, many of which are involved in the interferon- γ (IFN- γ) pathway.⁴⁰ Although manipulation of a single epigenetic mark can reprogram transcription, epigenetic programs are highly coordinated⁴¹ and therefore, targeting multiple

epigenetic silencing pathways could more effectively activate expression of antitumor genes than treatment with a single agent. Understanding how combinatorial epigenetic treatment impacts potential responses to immunotherapy could have an immediate high clinical impact.

Here, we explored the therapeutic potential of combining EZH2 inhibition that uses tazemetostat with DNA demethylation through decitabine in the presence of IFN- γ . Both EZH2 inhibitors and DNA demethylating agents positively regulated antigen presentation in EZH2-mutated DLBCL cell lines and demonstrated combinatorial effects on transcriptional activation of antigen presentation from both class I and II MHCs. The induced large increase in MHC surface expression of suppressed epitopes, especially in combination with IFN- γ , enabled the comprehensive MS analysis of the normally heavily suppressed immunopeptidome of these DLBCLs. The drugs induced 10-fold to more than 200-fold increases in total numbers of identified peptides presented by MHC class I molecules, tracking with strong upregulation of MHC expression. For HLA class II molecules, a twofold to threefold upregulation of the HLA complex level also translated into a more diverse ligandome. However, no clear tumor-specific immunotherapy targets could be identified from this subtype of HLA ligands. Still, our data demonstrated the feasibility of identifying immunotherapy targets in DLBCLs by using MS. Among the many newly presented HLA ligands, several highly cancer-specific HLA ligands were identified that can serve as potential targets for immunotherapy design and combination therapies in DLBCL.

Materials and methods

Cell culture and sources

Cells were maintained in RPMI 1640 with penicillin and streptomycin supplemented with 10% heat-inactivated fetal bovine serum (FBS) and 5 mM L-glutamine. All cells were maintained at 37°C in 5% CO₂. SUDHL-4 (A*02:01, B*15:01, C*03:04, DRB1*15:01), DB (A*02:01, B*18:01, C*05:01, DRB1*03:01), WSU-DLCL2, and Karpas 422 cells were from the Christian Steidl Laboratory (British Columbia Cancer Research Centre). SUDHL-6 (A*02:01, A*23:01, B*15:01, B*49:01, C*03:03, C*07:01, DRB1*01:01, DRB1*04:01), RI-1 (EZH2 WT), U9-293 (EZH2-WT), and SUDHL-10 were provided by Anas Younes, MD (Memorial Sloan Kettering Cancer Center). HLA typing was performed by the American Red Cross. Human cells were obtained after written informed consent from donors on protocols approved by the Memorial Hospital Institutional Review Board.

Drug treatments

Decitabine (Sellekchem, Cat. No. S1200) in dimethyl sulfoxide (DMSO), tazemetostat (Sellekchem, Cat. No. S7128) in DMSO, and IFN- γ (R&D Systems, 285-IF-100/CF) in 1% FBS were administered *in vitro* using the same treatment schedule: cells were treated with noted concentrations (decitabine 125-2000 nmol/mL, tazemetostat 312.5-5000 nmol/mL, IFN- γ 1-100 ng/mL) of each drug for 48 hours. Media was refreshed and new drug was added for an additional 48 hours. Untreated cells were given vehicle DMSO and media and were cultured for the duration of the drug treatment.

Flow cytometry

Cells were treated as indicated in the respective figures. Cells were harvested, washed with phosphate-buffered saline (PBS), and labeled in staining buffer (2% FBS and 0.1% sodium azide in PBS) for 30 minutes with a 1:400 dilution of fluorescein isothiocyanate (FITC) mouse anti-human HLA-A2 (clone BB7, BioLegend) and allophycocyanin (APC) anti-human HLA-A, -B, or -C (clone W6/32, BioLegend). Cells were washed after incubation with staining buffer and were analyzed by using a Fortessa flow cytometer (BD Biosciences) or a Guava flow cytometer (Millipore). Live cells were gated for analyses.

Western blot

Cells were treated as indicated in the respective figures. Total cell lysate was extracted with NP-40 buffer and were quantified by using a detergent compatible (DC) protein assay (Bio-Rad). Then, 15 to 30 μg of protein was loaded and run on 4% to 12% sodium dodecyl sulfate polyacrylamide gel electrophoresis gels. After a 1-hour block with 5% milk at room temperature, immunoblotting was performed by using rabbit anti-H3K27me3 (Cell Signalling, Cat. No. 9733). Antibodies were probed at the manufacturer's recommended dilution overnight at 4°C before a secondary antibody, goat anti-rabbit horseradish peroxidase conjugate (Jackson ImmunoResearch, Cat. No. 111-035-144), was used for imaging. Blots were stripped with Restore Western Blot Stripping Buffer (Thermo Fisher Scientific, Cat. No. 21063), re-blocked with 5% milk, and re-probed with mouse anti-H3 (active motif, AB_2650522), followed by goat anti-mouse horseradish peroxidase conjugate (Jackson ImmunoResearch, Cat. No. 115-035-146) as a loading control.

Quantitative reverse-transcriptase polymerase chain reaction

Untreated vehicle control and drug-treated cells were harvested and washed once with PBS. Cells were lysed in RLT buffer with β -mercaptoethanol, and RNA was extracted using Qiagen RNEasy Kit (QIAGEN, Cat. No. 74134). Extracted RNA was then converted to complementary DNA (cDNA) by using the one-step qSCRIPT cDNA solution. Then 5 ng of isolated cDNA per sample was mixed with 1 \times target primer and 1 \times endogenous control primer in Perfecta master mix (Quantabio, Cat. No. 95118). Reactions were performed in a thermocycler. Primers used in this study are Hs00388675_m1; human TAP1, Hs00241060_m1; TAP2, Hs00984230_m1; human B2M, Hs01058806_g1; human HLA-A, Hs00818803_g1; human HLA-B, Hs00740298_g1; and human HLA-C (Thermo Fisher Scientific).

Immunopurification of HLA ligands

HLA class I ligands (HLA-A, -B, and -C) and HLA class II ligands (HLA-DR) were isolated as described previously from all harvested cells.⁴² In brief, 40 mg of cyanogen bromide-activated-Sepharose 4B (Sigma-Aldrich, Cat. No. C9142) was activated with 1 mmol/L hydrochloric acid (Sigma-Aldrich, Cat. No. 320331) for 30 minutes. Subsequently, 0.5 mg of W6/32 antibody (Bio X Cell, BE0079; RRID: AB_1107730) or L243 antibody (Bio X Cell, BE0306; RRID: AB_2736986) was coupled to Sepharose in the presence of binding buffer (150 mmol/L sodium chloride [Sigma-Aldrich, Cat. No. S9888], 50 mmol/L sodium bicarbonate [pH 8.3; Sigma Aldrich, Cat. No. S6014] for at least 2 hours at room

temperature. Sepharose was blocked for 1 hour with glycine (Sigma-Aldrich, Cat. No. 410225). Columns were washed twice with PBS and equilibrated for 10 minutes. DB, SUDHL-4, and SUDHL-6 cells were treated with the indicated drugs. Cells (5×10^6 to 1.5×10^7) were harvested and washed 3 times in ice-cold sterile PBS (Media Preparation Facility, Memorial Sloan Kettering Cancer Center). Afterward, cells were lysed in 1 mL 1% CHAPS (Sigma-Aldrich, Cat. No. C3023) in PBS, supplemented with 1 tablet of protease inhibitors (Complete™ Protease Inhibitor Cocktail, Sigma-Aldrich Cat. No. 11836145001) for 1 hour at 4°C. This lysate was spun down for 1 hour at 20000g at 4°C. Supernatant was run over the affinity column through peristaltic pumps at 1 mL/minute overnight at 4°C. Affinity columns were washed with PBS for 15 minutes and run dry; subsequently, HLA complexes were eluted 5 times with 200 mL 1% trifluoroacetic acid (TFA; Sigma/Aldrich, Cat. No. 02031). To separate HLA ligands from their HLA complexes, tC18 columns (Sep-Pak tC18 1 cc VacCartridge, 100 mg sorbent per cartridge, 37-55 mm particle size, Waters, Cat. No. WAT036820) were prewashed with 80% acetonitrile (ACN; Sigma-Aldrich, Cat. No. 34998) in 0.1% TFA and were equilibrated with 2 washes of 0.1% TFA. Samples were loaded, washed again with 0.1% TFA, and eluted in 400 mL 30% ACN in 0.1% TFA followed by 400 mL 40% ACN in 0.1% TFA and then in 400 mL 50% ACN in 0.1% TFA. Sample volume was reduced by vacuum centrifugation for MS analysis.

LC-MS/MS analysis of HLA ligands

Samples were analyzed by using high-resolution/high-accuracy liquid chromatography-tandem MS (LC-MS/MS; Lumos Fusion, Thermo Fisher Scientific). Peptides were desalted using ZipTips (MilliporeSigma; Cat. No. ZTC18S008) according to the manufacturer's instructions and concentrated by using vacuum centrifugation before being separated using direct loading onto a packed in-emitter C18 column (75 μm inside diameter \times 12 cm, 3 μm particles; Nikkyo Technos). The gradient was delivered at 300 nL/minute increasing linear from 2% buffer B (0.1% formic acid in 80% acetonitrile)/98% buffer A (0.1% formic acid) to 30% buffer B/70% buffer A over 70 minutes. MS and MS/MS were operated at 60 000 and 30 000 resolution, respectively. Only charge states 1, 2, and 3 were allowed. The isolation window of 1.6 Th (mass/charge) was chosen, and the collision energy was set at 30%. For MS/MS, the maximum injection time was 100 ms with an automatic gain control of 50 000.

MS data processing

MS data were processed using Byonic software⁴³ version 2.7.84 (Protein Metrics) through a custom-built computer server equipped with 4 Intel Xeon E5-4620 8-core central processing units operating at 2.2 GHz and with 512 GB of physical memory (Exact). Mass accuracy was set to 6 ppm for MS1 and to 20 ppm for MS2 spectra. Digestion specificity was defined as unspecific, and only precursors with charges of 1, 2, or 3 and size of up to 2 kDa were allowed. Protein false discovery rate was disabled to allow complete assessment of potential peptide identifications. Oxidation of methionine, N-terminal acetylation, and phosphorylation of serine, threonine, and tyrosine were set as variable modifications for all samples. All samples were searched against the UniProt Human Reviewed Database (20349 entries; <http://www.uniprot.org>; downloaded June 2017). To detect mutated HLA ligands, mutated proteins according

to the collection of mutations from the Catalogue of Somatic Mutations in Cancer (COSMIC) database were included in our aforementioned database.⁴⁴ Peptides were selected with a minimal "log prob" value of 2 (as defined by the byonic software) corresponding to a *P* value <.01 for peptide spectrum match in the given database and were HLA assigned by netMHCpan 4.0⁴⁵ based on a 2% rank cutoff as set as default by netMHCpan. For HLA class II ligands, no binding predictions were performed.

Statistical methods

Experiments in shown in Figures 1–4 and supplemental Figures 3, 4, and 9 were analyzed using analysis of variance (ANOVA) followed by a post hoc Tukey's test to determine the significance of individual groups. IFN- γ dose-response experiments in Figure 4 and supplemental Figure 5 were analyzed by using a Student *t* test between control and treated conditions. Graphs and plots were made using R programming and Graphpad Prism.

Results

Decitabine and tazemetostat improved IFN- γ -responsive HLA upregulation in EZH2-mutated DLBCL cell lines

To understand how decitabine, a potent DNA demethylating agent, and tazemetostat, a highly specific EZH2 inhibitor, might have an impact on antigen presentation, we first measured HLA I cell surface expression in EZH2-mutated DLBCL cell lines via flow cytometry. We selected cell lines to be HLA-A*02:01-positive because that represents the most common HLA haplotype in the Western Hemisphere and therefore is of broad interest. A complete overview of the cell lines used in our study, their HLA types, and the assays we performed can be found in supplemental Table 1. Tazemetostat decreases global H3K27me3 with 96 hours of drug treatment (supplemental Figure 1). The concentrations of each drug were determined by dose-response curves on the SUDHL-4 cell lines by using concentrations that lead to upregulation of HLA without excessive loss in viability (supplemental Figure 2). Both DB and SUDHL-6 treated DLBCL cell lines variably upregulated HLA I and HLA-A*02 cell surface expression when treated with 1 μ M tazemetostat, 125 nM decitabine, or a combination of both (Figure 1A-D). Interestingly, decitabine led to a more robust upregulation of HLA as monotherapy compared with tazemetostat. Nonetheless, the combination of both decitabine and tazemetostat lead to the highest and most significant upregulation of HLA-A, -B, and -C in both cell lines. Trends toward increased HLA I expression were also observed for the EZH2-mutant DLBCL cell lines WSU-DLCL2, SUDHL-4, SUDHL-10, but not Karpas 422 (supplemental Figure 3). One potential explanation for the variable responsiveness might be the baseline HLA class I expression as determined by expression data from the Cancer Cell Line Encyclopedia (CCLE).⁴⁶ Here, we observed an inverse correlation between the HLA-A, -B, and -C expression and the strength of HLA upregulation. For example, the differential expression between DB and Karpas 422 cells was more than 170-fold, indicating strong repression by DB cells. Therefore, DB cells have the potential to upregulate HLA whereas the potential of further upregulation in Karpas 422 cells is limited (supplemental Table 2). Furthermore, when DLBCL cell lines were treated with IFN- γ in addition to the aforementioned

treatment schema, there was a cooperative increase in total HLA I expression, which reached more than 50-fold upregulation for DB cells, fivefold upregulation for SUDHL-6 cells, and more than 50-fold upregulation for DB cells when HLA-A*02 alone was assessed (Figure 1E-H). Similarly, modest trends in increased HLA expression were seen in WSU-DLCL2, SUDHL-4, and SUDHL-10, but not Karpas 422 (supplemental Figure 4).

To determine whether tazemetostat synergizes with decitabine in HLA I upregulation, we performed a matrix titration of decitabine in the presence of tazemetostat and 100 ng/mL IFN- γ and tested for HLA-A*02. Indeed, any concentration of tazemetostat shifted the expression of HLA-A*02 at each decitabine concentration tested (supplemental Figure 5A,C). Similarly, a shift in expression was seen by a tazemetostat titration in the presence of different concentrations of decitabine (supplemental Figure 5B-C). In addition, tazemetostat alone showed a dose-dependent increase in HLA expression in SUDHL-4 and DB cells in the presence or absence of IFN- γ (supplemental Figure 6). To demonstrate that decitabine and tazemetostat can increase IFN- γ responsiveness, we performed 10-fold dilutions of IFN- γ in the presence of 125 nM decitabine and 1 μ M tazemetostat. DB and SUDHL-6 cells showed significantly higher responses to IFN- γ , again reaching 50-fold upregulation for DB cells and increases up to sixfold for SUDHL-6 cells when treated with epigenetic modifiers (supplemental Figure 5D-E). We tested whether EZH2 wild-type (wt) DLBCL cell lines also upregulate HLA after treatment with tazemetostat. Tazemetostat strongly upregulated HLA-A, -B, and -C on the EZH2-mutated cell line SUDHL-4, but had little to no upregulation of HLA on the EZH2 wt cell lines RI-1 and U9-293 (supplemental Figure 7A,C,E). Interestingly, decitabine had a sizable effect on HLA upregulation regardless of EZH2 mutation status. Taken together, these results demonstrated that decitabine and tazemetostat upregulate HLA in EZH2-mutant DLBCL, whereas decitabine can upregulate HLA in a broader subset of DLBCLs.

Decitabine and tazemetostat modulated individual HLA alleles independently and upregulated the transcription of antigen presentation machinery in DLBCL

Given the general upregulation of HLA after treatment with tazemetostat or decitabine, we further evaluated the impact of these drugs on transcription of each HLA allele individually as well as their impact on other components of the antigen presentation machinery by using quantitative reverse-transcriptase polymerase chain reaction (qRT-PCR). SUDHL-6 cells showed a progressive increase in transcription of each allele, which was most prominent in the triple treatment group. In addition, confirming results from previous reports, IFN- γ upregulated HLA-B transcription more profoundly than HLA-A and HLA-C (Figure 2A-C).⁴⁷ DB cells similarly showed a progressive increase in expression of HLA-A and HLA-B loci when treated in combination with IFN- γ , decitabine, and tazemetostat (Figure 2D,E). Decitabine had a stronger impact on HLA upregulation compared with tazemetostat. Remarkably, HLA-B expression was increased 500-fold with IFN- γ treatment, which could be improved to about 1500-fold with combination decitabine, 1000-fold with combination tazemetostat, and 2200-fold in the triple treatment group across 2 independent biological replicates. For the DB cell line, HLA-C levels were undetectable. SUDHL-4 cells also showed significant

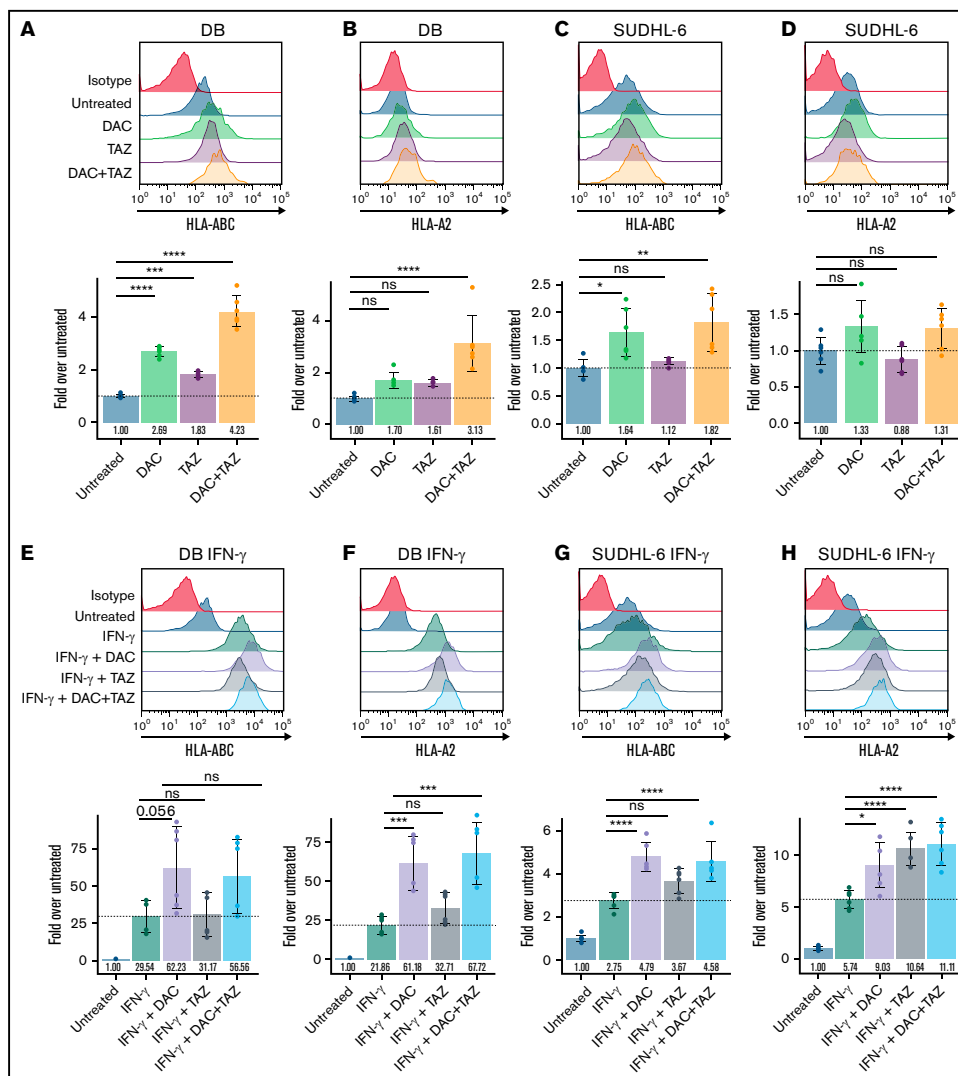


Figure 1. Decitabine (DAC) and tazemetostat (TAZ) upregulated HLA protein in DLBCL cell lines. (A-D) Cells were treated with indicated 125 nM decitabine or 1 μ M tazemetostat. DB and SUDHL-6 cells were assayed for HLA-A, -B, and -C or HLA-A-02 expression by flow cytometry. (E-H) Cells were treated as in panels A-D along with 100 ng/mL IFN- γ . Analysis of variance (ANOVA) was performed using either untreated (panels A-D) or IFN- γ alone (panels E-H) as control, followed by a post hoc Tukey's test for individual experimental groups. Mean \pm standard deviation (SD) is shown for 3 technical replicates per 2 biological replicates. ns, not significant. * $P < .05$; ** $P < .01$; *** $P < .001$; **** $P < .0001$.

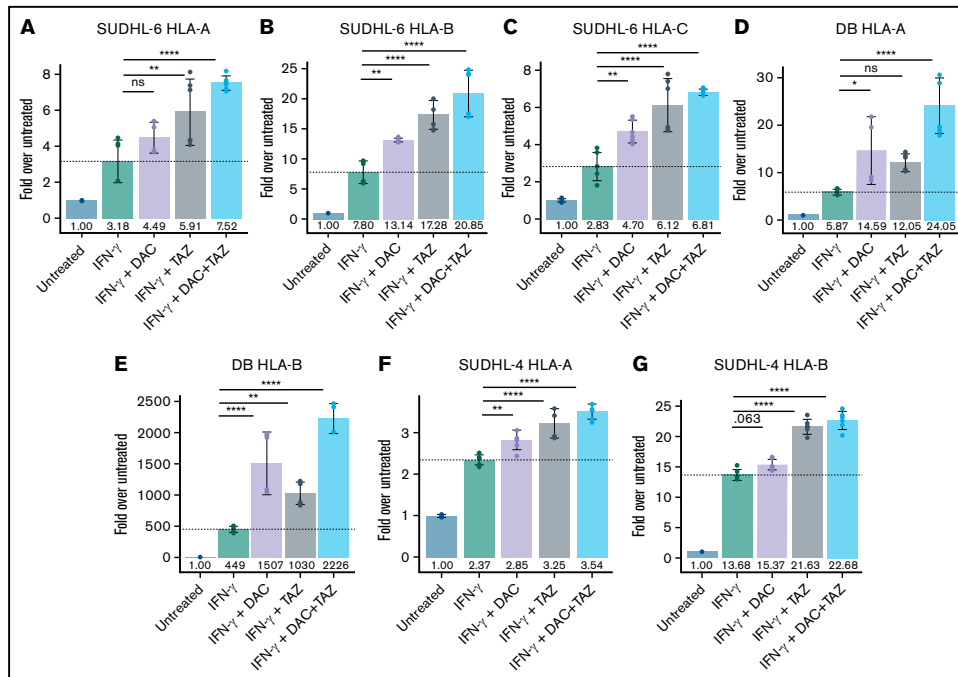


Figure 2. Decitabine and tazemetostat activated transcription of HLA alleles on DLBCL cell lines. (A-G) SUDHL-6, DB, and SUDHL-4 cells were treated with indicated drugs (decitabine, 100 nM; tazemetostat, 1 μ M; IFN- γ , 10 ng/mL). Graph of fold-change in transcript to untreated for each indicated gene (panels A, D, F) HLA-A, (panels B, E, G) HLA-B, and (panel C) HLA-C. ANOVA was performed using IFN- γ alone as control, followed by a post hoc Tukey's test for individual experimental groups. Mean \pm SD is shown for 3 technical replicates per 2 biological replicates. * P < .05; ** P < .01; **** P < .0001.

upregulation of HLA-A and HLA-B in combination epigenetic treatment (Figure 2F,G). As with DB cells, SUDHL-4 cells showed no expression of HLA-C transcript in multiple repetitions of the experiments. Although these results were surprising, they are in line with the very low expression levels of these cell lines reported in the CCLE.⁴⁶ Here, SUDHL-4 is among the 6.5% of cell lines with the lowest HLA-C expression, and DB cells are among the bottom 2%. In contrast, SUDHL-6 cells have reported transcript per million values close to the median of HLA-C expression compared with all other cell lines in the CCLE.

Given large upregulations of the different HLA I alleles during drug treatment, we assessed upregulation of antigen presentation machinery β 2-microglobulin (β 2M) and transporter associated with antigen processing (TAP) 1 and 2. Although less striking than HLA expression, β 2M, TAP1, and TAP2 were significantly increased in SUDHL-6, and β 2M and TAP1 were significantly upregulated in DB cells across 2 independent biological replicates when cells treated with IFN- γ were also treated with decitabine or tazemetostat (Figure 3). Similar but less profound upregulation of antigen presentation was also seen in SUDHL-4 cells (supplemental Figure 8). Yet overall, EZH2 and DNA

methylation inhibition upregulated transcripts involved in antigen processing and presenting at very high levels.

Decitabine upregulates HLA class II expression in DLBCL

To complete the analysis of proteins primarily involved in antigen presentation, we turned to HLA class II molecules because they are also highly expressed on DLBCLs in line with their B-cell origin. The overall limited expression of HLA class II molecules throughout the body also makes class II-presented peptides suitable immunotherapy targets. Therefore, we assessed the impact of decitabine and tazemetostat on expression of HLA class II molecules. Tazemetostat had no significant effect on HLA-DR or HLA-DQ expression. However, decitabine treatment trended toward upregulation of HLA-DR and HLA-DQ, whereas the combination led to significant upregulation in SUDHL-6 and SUDHL-10 and a similar trend in WSU-DLCL2 cells (supplemental Figure 9). Class II upregulation was further enhanced by the addition of IFN- γ to the cells treated with decitabine and tazemetostat, leading to significant upregulation by decitabine in all 3 cell lines (Figure 4A-C). To determine whether decitabine and tazemetostat lowered the threshold for

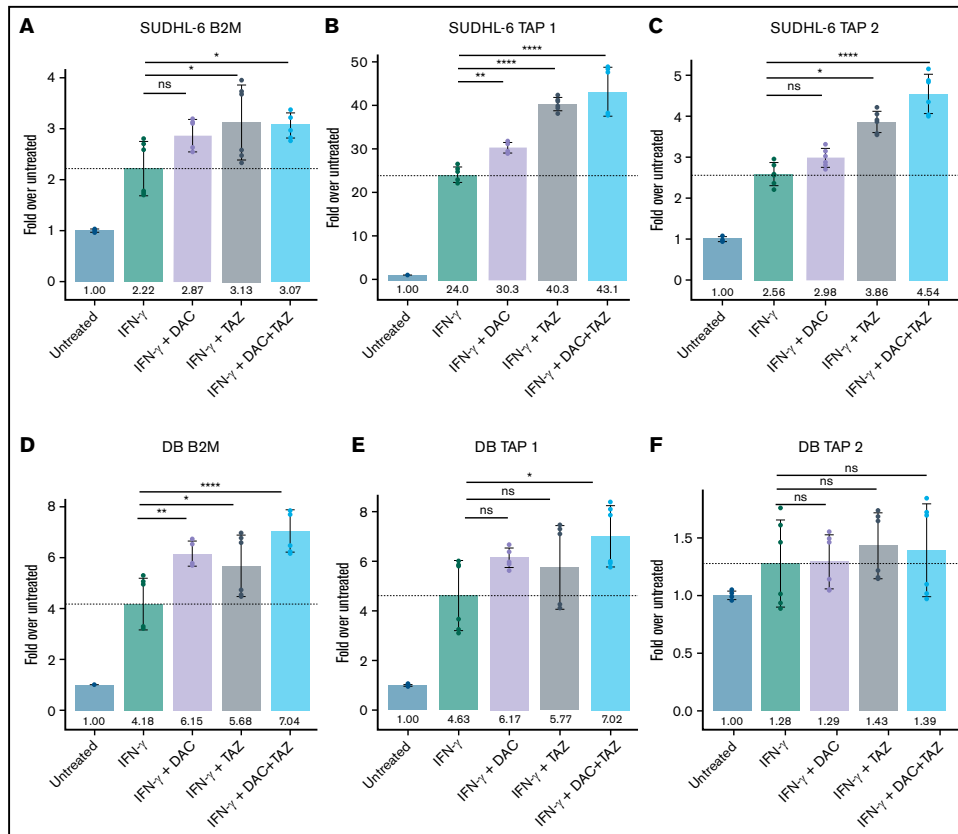


Figure 3. Decitabine and tazemetostat activated transcription of antigen-presentation genes in DLBCL cell lines. (A-F) SUDHL-6 and DB cells were treated with indicated drugs (decitabine, 100 nM; tazemetostat, 1 μ M; IFN- γ , 10 ng/mL). Graph of fold-change in transcript to untreated for each indicated gene (panels A, D) B2M, (panels B, E) *Tap1*, (panels C, F) *Tap2*. Mean \pm SD is shown for 3 technical replicates per 2 biological replicates. * $P < .05$; ** $P < .01$; **** $P < .0001$.

IFN- γ -mediated HLA class II upregulation, we titrated IFN- γ in the presence of 125 nM decitabine and 1 μ M tazemetostat. As seen with HLA class I expression, HLA-DR and HLA-DQ were significantly upregulated by decitabine and tazemetostat across each IFN- γ concentration (Figure 4D-E).

Epigenetic drug treatment in combination with IFN- γ allowed systematic analysis of the DLBCL immunopeptidome and identified disease-specific HLA ligands

Given the extensive increases in HLA class I and class II expression, antigen presentation machinery, and individual ligand presentation, which followed treatment with epigenetic modifiers in combination with IFN- γ , we wanted to systematically investigate the changes

and potential emergence of new peptides that are presented on the cell surface. By using immunoprecipitation with HLA-A, -B, -C, and -DR-specific antibodies, separation of the bound peptides, and subsequent MS, we identified increases in the numbers of unique HLA ligands similar to the fold changes seen in qRT-PCR and by flow cytometry for HLA levels in both HLA class I and HLA class II molecules. Strikingly, this method, which usually robustly identifies thousands of different HLA ligands in a single sample, detected few (between 7 and 19) unique peptides in the 3 untreated cell lines (SUDHL-4, DB, and SUDHL-6 for HLA-A, -B, and -C molecules), which resembles the profound downregulation of HLA levels in these cell lines. In contrast, when cell lines were treated with IFN- γ and the previously used schema of decitabine and tazemetostat, SUDHL-6 cells presented more than 400 unique HLA ligands, SUDHL-4 cells presented more than 1500 unique HLA ligands, and

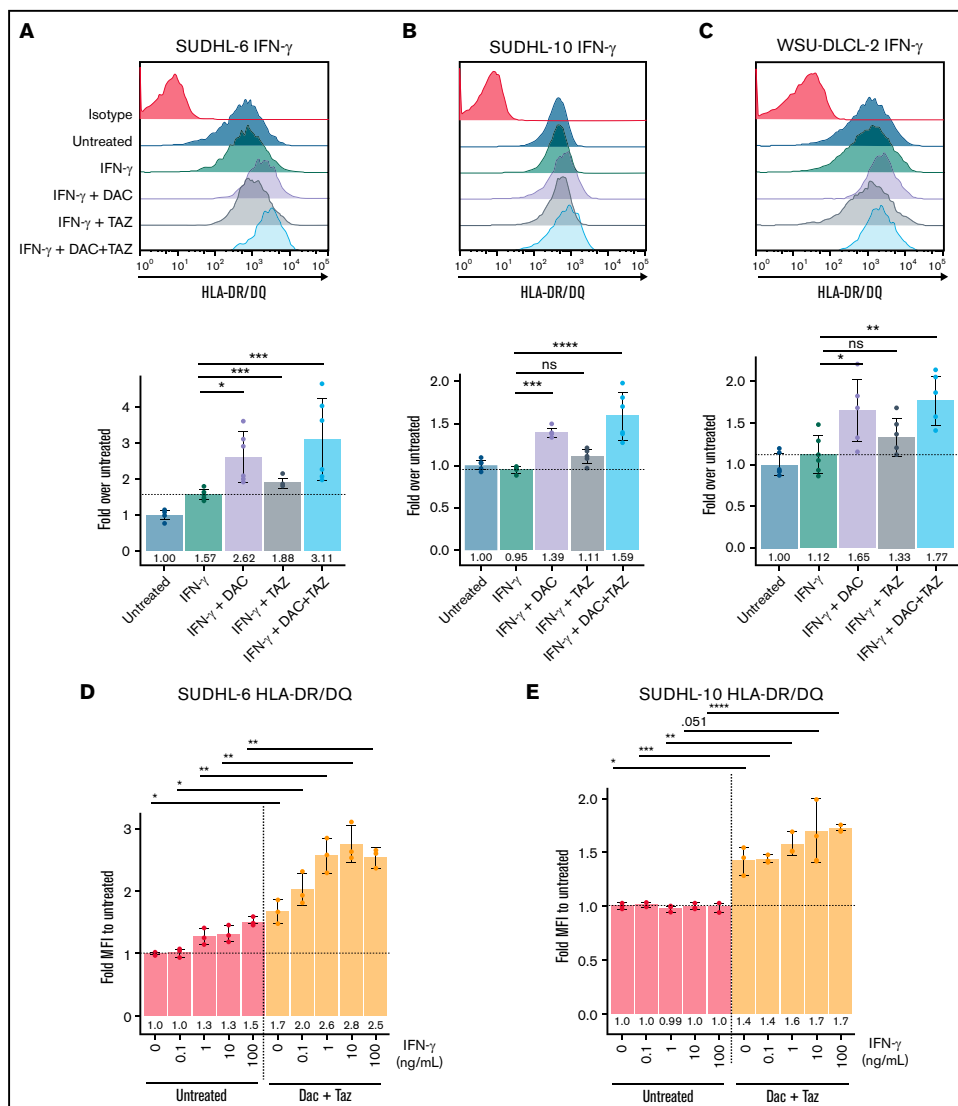


Figure 4. Decitabine upregulated HLA class II molecules in DLBCL cell lines. (A-C) Cells were treated with 125 nM decitabine or 1 μ M tazemetostat along with 100 ng/mL IFN- γ for SUDHL-6, SUDHL-10, and WSU-DLCL-2 cell lines and were assayed for expression of HLA-DR/DQ. Mean \pm SD is shown for 3 technical replicates per 2 biological replicates. (D-E) Serial dilutions of IFN- γ were performed in the presence or absence of decitabine and tazemetostat for SUDHL-6 and SUDHL-10 cell lines. Mean \pm SD is shown for 3 individual replicates. * $P < .05$; ** $P < .01$; *** $P < .001$; **** $P < .0001$.

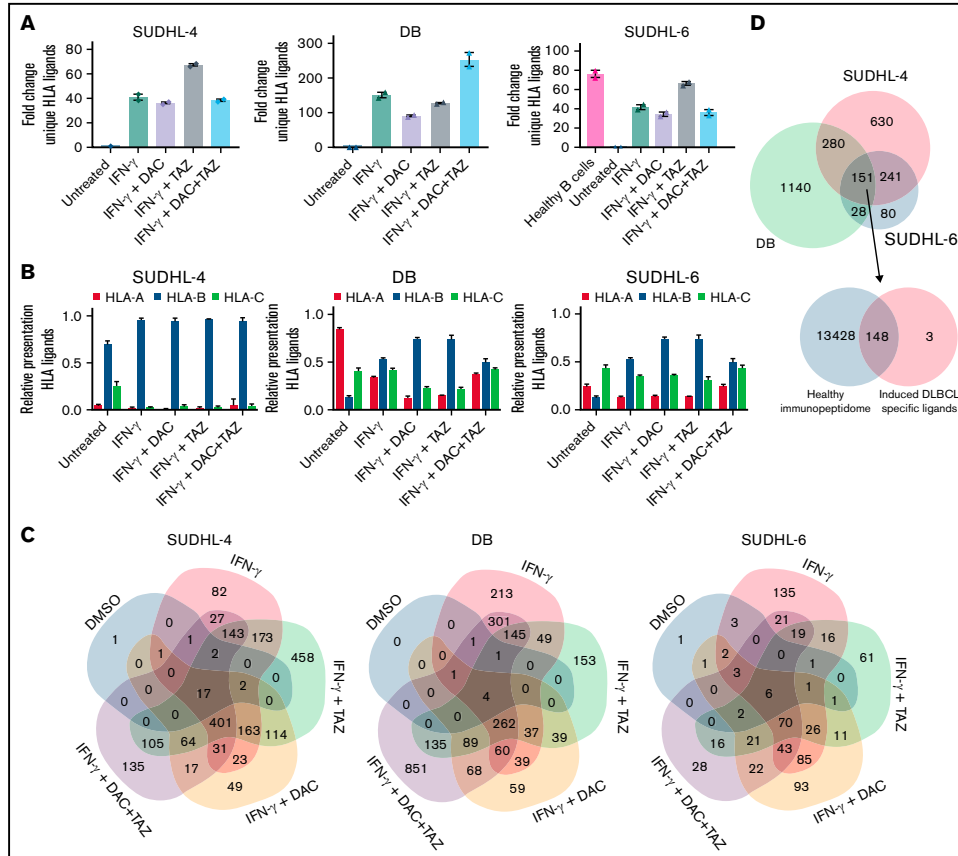


Figure 5. Epigenetic drug treatment in the presence of IFN- γ unmasked the immunopeptidome of DLBCL cell lines. (A) Cells were treated with 125 nM decitabine, 1 μ M tazemetostat or the combination of both in the presence of 100 ng/mL IFN- γ . Fold change of unique identifications of HLA ligands relative to untreated cells is depicted. Error bars indicate mean plus range. Experiments were performed in duplicates. (B) Relative distribution of HLA alleles after assignment to their respective alleles through NetMHCpan 4.0. (C) Overlap analysis of all peptides by cell line and respective treatment condition. (D) Overlap of source proteins for HLA ligands shared between the SUDHL-4, DB, and SUDHL-6 cell lines (top). Overlap of 151 source proteins from overlap at the top were matched with 13 428 source proteins of the HLA class I ligandome from healthy donors as published by Marcu et al.⁵⁰

DB cells presented more than 2000 unique HLA ligands when using the most effective treatment condition (supplemental Table 3). This number of ligands is similar to number of peptides identified on healthy B cells if similar numbers of cells had been used (supplemental Figure 10A-C). Thus, this corresponds to an upregulation of HLA ligand presentation in the range of 10-fold to 20-fold for SUDHL-6 cells, 40-fold to 70-fold for SUDHL-4 cells, and 100-fold to 250-fold for DB cells (Figure 5A). Although the combination of tazemetostat and IFN- γ induced the strongest changes in SUDHL-4 and SUDHL-6 cells, no clear drug combination induced the most

unique peptides. In all 3 cell lines, the addition of tazemetostat or tazemetostat in combination with decitabine showed additive effects over the IFN- γ treatment alone. Still, the IFN- γ treatment led to the largest upregulation, which was further enhanced by treatment with epigenetic drugs.

Next, we determined the allelic distribution of these newly presented HLA ligands. We used NetMHCpan 4.0 to assign each peptide to 1 of the expressed HLA alleles and then examined the fraction of peptides presented on each allele. First, all cell lines demonstrated

the known preferences for peptide presentation on HLA-B alleles after treatment with IFN- γ .⁴⁷⁻⁴⁹ Interestingly, all epigenetic monotherapies (tazemetostat or decitabine) enhanced this effect. However, the combination of both modifiers led to distribution patterns identical to treatment with IFN- γ alone (Figure 5B). In contrast to the undetectable HLA-C expression in DB and SUDHL-4 cells, we detected ligands predicted to bind HLA-C complexes. One explanation is that strong enrichment for the HLA complexes allows for successful detection of HLA-C ligand. Another likely explanation is false assignment of HLA ligands from the HLA-A*02 allele to the HLA-C allele. Because this discrepancy cannot be resolved by our current methods, we will continue to report these peptides as binders for both HLA alleles.

Furthermore, the overlapping HLA class I ligands between the 5 treatment conditions in each cell line demonstrated that for each single treatment condition, a relevant proportion of peptides that was unique to this treatment group was detectable (Figure 5C; a detailed overview of the peptides in each subgroup is provided in supplemental Table 4). This fraction could be as little as 8% (82 of 1022 peptides) (eg, in the SUDHL-4 cells treated with IFN- γ), but these fractions could be as high as 29% to 30%, as seen for the subgroups treated with IFN- γ and tazemetostat in SUDHL-4 (458 of 1555 peptides) and SUDHL-6 (130 of 431 peptides). The triple-treated condition in DB cells displayed HLA ligands of which 44% (851 of 1918 peptides) were unique to that treatment condition. No consistent pattern could be observed regarding which epigenetic treatment led to the strongest improvement, although it was evident that these drugs could lead to substantial changes in the immunopeptidome resulting in the presentation of many HLA class I ligands not previously displayed.

We investigated the origin of peptides that arose after different treatment conditions. First, to analyze whether the presented peptides correlated with the phenotype of a DLBCL, we specifically looked for HLA ligands derived from proteins that serve as histologic markers for the diagnosis of DLBCL or that are associated with relevant pathobiology of the disease (BCL-2, BCL-6, MYC, MYD88, CD79A/B, CREBBP, PAX5, and EZH2). HLA ligands could be identified for 4 of these 8 proteins. For bcl-6 and CD79A/B, multiple HLA ligands on different HLA alleles were detectable after drug treatment, whereas for the CREBBP and PAX-5 proteins, only 1 HLA ligand per protein was found (Table 1, "HLA ligands from proteins used as DLBCL markers").

More importantly, to identify potential immunotherapy targets, we looked for HLA ligands that met the following criteria: the peptides need to be derived from proteins that were identified in all 3 cell lines and from proteins that have not been reported in the immunopeptidome of healthy donors. Therefore, we overlapped the source proteins from which the HLA ligands were derived from all 3 cell lines and identified 151 proteins shared between all 3 lines, which corresponds to 5.9% of all reported proteins in our data set (supplemental Figure 11A). At this point, we focused only on the protein, but not the HLA ligand to account for the different HLA alleles present in these cell lines. We then took these 151 proteins and matched them against 13 576 proteins, which were recently reported by Marcu et al⁵⁰ to be the source of HLA ligands in healthy tissues. From this analysis, only 3 proteins were identified to be unique to the DLBCL group (Figure 5D). One protein, an HLA allele subtype, could also be annotated to proteins included in the 13 576

proteins after further analysis and therefore was determined to be a false positive. The remaining 2 proteins, regulator of G protein signaling 13 (RGS13) and E2F transcription factor 8 (E2F8), were highly tumor specific, because no HLA class I ligands from these proteins have been reported on healthy tissues. RGS13-derived peptides were identified in other malignant samples, and E2F8-derived HLA ligands were exclusively found in transformed B cells, according to the Immune Epitope Database (IEDB).⁵¹ Moreover, the identified HLA ligands from RGS13 and E2F8 in these cell lines were detectable in many different treatment replicates; in the case of ATKYGPVY (B*15) and PQAPSGPSY (B*15), the epitope was shared between the SUDHL-4 and SUDHL-6 cell lines, which renders these HLA ligands promising targets for immunotherapy. The high expression levels of RGS13 and E2F8 in DLBCL, which according to the CCLE did not correlate with the HLA-A, -B, or -C expression (supplemental Figure 12; supplemental Table 2), highlights the feasibility of these target proteins for immunotherapy. In addition, these targets are tumor specific. No HLA ligands from these 2 proteins were reported on any healthy tissues. In search of other tumor-specific HLA ligands, we also investigated the presentation of mutated HLA ligands. By using mutation data from the Catalogue Of Somatic Mutations In Cancer (COSMIC) database, we re-analyzed our data sets but did not detect any mutated HLA ligands in all treatment conditions and cell lines (data not shown).⁴⁴

To complement our analysis, we also performed a similar analysis for the overlap between the 3 cell lines on the HLA ligand level rather than the protein level. Because the HLA types of these cell lines vary, it is not surprising that only a very limited fraction of 4 peptides could be identified as being shared among the 3 cell lines (supplemental Figure 11B), and after matching these shared ligands to the healthy ligandome by Marcu et al,⁵⁰ no tumor-specific shared HLA ligands were identified. Although many tumor-specific HLA ligands could be identified on a per cell line basis, we favor our approach on the protein level because it led to the discovery of proteins clearly associated with DLBCL and high tumor specificity independent of HLA restriction. A potential solution to the problem of the low number of shared HLA ligands would be the definition of tumor-specific HLA ligands per cell line. In fact, this analysis defined 451 tumor-specific HLA ligands for SUDHL-4, 938 for DB, and 90 for SUDHL-6 cells.

We also investigated HLA class II ligands as potential immunotherapy targets. Similar to HLA class I complex levels, the upregulation of HLA class II complex levels on the cell surface corresponded with a more diverse immunopeptidome. Still, because increases were moderate compared with those of HLA class I complex levels, the number of potential immunotherapy targets was also lower. Overall, HLA class II ligands were identified in the DMSO-treated samples—20 for DB, 173 for SUDHL-4, and 280 for SUDHL-6. The unique HLA ligands were upregulated to 65 for DB, 390 for SUDHL-4, and 975 for SUDHL-6 cells under triple drug therapy. For HLA class II ligands, the effect of tazemetostat was very limited, and the most substantial increases were observed after treatment with decitabine combined with IFN- γ (supplemental Figure 11C). By following the analysis strategy for HLA class I peptides, we also defined treatment-associated HLA class II ligands (supplemental Figure 11D; supplemental Table 4) and matched the HLA ligands presented in all cell lines with the immunopeptidome of healthy cells as published by Marcu et al.⁵⁰ Although many HLA class II peptides were primarily defined as tumor specific, a detailed analysis

Table 1. HLA ligands identified from DLBCL markers and disease-specific HLA ligands

	SUDHL-4				DB				SUDHL-6				
	IFN- γ	IFN- γ / decitabine tazemetostat	IFN- γ / decitabine/ tazemetostat	Untreated	IFN- γ	IFN- γ / decitabine	IFN- γ / tazemetostat	IFN- γ / decitabine/ tazemetostat	IFN- γ	IFN- γ / decitabine	IFN- γ / tazemetostat	IFN- γ / decitabine/ tazemetostat	IFN- γ / decitabine/ tazemetostat
HLA ligands from proteins used as DLBCL markers													
BCL6	LIHTGEKPY (B*15), LIHTGEKPY (B*18), SOSFOHAEM (B*19), TVHTGEKPY (B*15)	RHSGEKPY (B*15), RHSGEKPY (B*18), SOSFOHAEM (B*15), AITNTKVCY (B*19), TVHTGEKPY (B*15), LIHTGEKPY (B*15), AITNTKVCY (B*15)	RHSGEKPY (B*15), RHSGEKPY (B*18), SOSFOHAEM (B*15), TVHTGEKPY (B*19), LIHTGEKPY (B*15), AITNTKVCY (B*15)										
CREBBP		AOAPAQSQF (B*15)											
CD79A/B	RVOEGNESY (B*15)	RVOEGNESY (B*15)	RVOEGNESY (B*15)	LLSAEPYPA (A*02), DEYEDENLY (B*18), LLSAEPYPA (B*15)	DEYEDENLY (B*18), LLSAEPYPA (B*15)	DEYEDENLY (B*18), LLSAEPYPA (B*15)	DEYEDENLY (B*18), LLSAEPYPA (B*15), LLSAEPYPA (A*02), TELPMMGF (B*18), TELPMMGF (B*18)	RVOEGNESY (B*15)	RVOEGNESY (B*15)	RVOEGNESY (B*15)	RVOEGNESY (B*15)	RVOEGNESY (B*15)	RVOEGNESY (B*15)
PAX5	YSHROYSSY (B*18)		YSHROYSSY (B*18)										
HLA ligands not present in healthy cells													
RGS13	ATKYGPIVY (B*15)	ATKYGPIVY (B*15)	ATKYGPIVY (B*15)										
E2F8	POAFSGFSY (B*15)	POAFSGFSY (B*15)	POAFSGFSY (B*15)	QEFDFIKSY (B*18)	QEFDFIKSY (B*18)	QEFDFIKSY (B*18)	QEFDFIKSY (B*18), QEFDFIKSY (B*18)	POAFSGFSY (B*15)	POAFSGFSY (B*15)	POAFSGFSY (B*15)	POAFSGFSY (B*15)	POAFSGFSY (B*15)	ATKYGPIVY (B*15)

Downloaded from <http://ashpub.onlinelibrary.com/doi/pdf/10.1182/jclinonc.2022.04.1071> by guest on 27 November 2023

demonstrated that all HLA class II peptides which were initially categorized as tumor specific had length variants of these peptides presented on healthy cells. This finding suggests that, in fact, no truly tumor-specific HLA ligands that are shared between all 3 cell lines were identified for the HLA class II peptides. However, on an individual cell line level, 229 HLA-DR peptides can be defined as tumor-specific for SUDHL-4, 50 for DB, and 448 for SUDHL-6 cells.

Overall, we demonstrated that the diversity of the immunopeptidome followed the trends for upregulation of surface levels for HLA class I ligands, although this trend did not always align perfectly with the relative levels of HLA upregulation (supplemental Figure 13A-C). For HLA class II peptides, the upregulation on the ligandome level followed the HLA upregulation almost perfectly (supplemental Figure 13D). The observed HLA ligandome per cell line was not a direct function of gene expression. This can be illustrated by comparing the complete transcriptome per cell line (supplemental Figure 14A) in contrast to the transcriptome of genes contributing to the HLA ligandome, which follows a normal distribution (supplemental Figure 14B).

Discussion

The immunopeptidome of many hematologic malignancies has been described in detail and provides a valuable source for possible targets of T-cell immunotherapy.^{11-13,52} In contrast, little data regarding the immunopeptidome are available for DLBCL, most likely because of a strong HLA downregulation, which has been reported especially for the EZH2-mutated subgroup.²⁴ Identifying possible targets in DLBCL is important because immunotherapies are often powerful therapies with relatively low toxicity.

Here, we demonstrated how EZH2 inhibitors and DNA demethylation in the presence of IFN- γ can overcome the immune evasion mechanisms of DLBCL, leading to the robust unmasking of novel, potentially targetable HLA ligands. First, these drug combinations led to substantial increases of HLA class I surface expression with increases up to 50-fold by flow cytometry, which were mediated to a large extent by IFN- γ , but which were clearly enhanced by the addition of tazemetostat or decitabine or the combination of both drugs. For HLA class II molecules, these effects were less profound, but they were constant between the cell lines leading to up to three-fold upregulation in the combination treatment group, although the strongest effects were mediated by decitabine. The therapeutic combination of DNA demethylating agents with selective EZH2 inhibitors is supported by evidence of direct, physical links between EZH2 and DNA methyltransferases. EZH2 recruits DNA methyltransferases to PRC2 gene loci for further stabilization of the repressive epigenetic program.³⁹ Therefore, genes that are initially silenced by overactive EZH2 function in DLBCL may be resistant to upregulation by EZH2 inhibitors if DNA methylation is redundantly silencing the locus. Indeed, more than half the de novo DNA methylation events between healthy B cells and B-cell lymphoma are at PRC2 target sites.⁴⁰

Moreover, when we investigated the allele-specific HLA upregulation, we discovered that HLA-C alleles were not detectable in DB and SUDHL-4 cells, which is consistent with published low HLA-C expression in the CCLE. The impression that these cell lines still present many HLA-C ligands comes from ambiguities in the HLA

ligand assignments through NetMHCpan because HLA-A*02 ligands also often score well for HLA-C alleles, although they do not score as well as for HLA-A*02. Still, because this problem cannot be solved systematically, we assigned the peptides to both alleles as potential binders.

Considering the allelic diversity, these cell lines were already homozygous for all 3 HLA class I alleles. This additional loss of HLA-C further reduces the number of HLA alleles that were able to present a diverse immunopeptidome to 2 alleles. Moreover, when we quantitatively examined the peptides presented by these cell lines, few HLA ligands were assigned to HLA-A*02 in SUDHL-4, rendering this cell line functionally nearly mono-allelic, which illustrates again the profound immunosuppressive mechanisms in DLBCL and another strategy for immune evasion in lymphoma. Of note, we also observed an inverse correlation of induction of HLA ligands and baseline HLA level expression, suggesting that especially highly suppressed DLBCL cell lines are the cells most susceptible to the triple treatment strategy which then overcomes their evasion mechanism.

Finally, the drug-induced unmasking of HLA ligands in the cell lines we investigated allowed us to conduct a systematic analysis of HLA ligands present in HLA-low DLBCL, which led to the detection of HLA I ligands from RGS13 and E2F8, which had not been observed in healthy tissues. Interestingly, ATKYGPVVY from RGS13 has not been described in any other sample of cancer cells, demonstrating that truly novel HLA ligands can arise after these drug treatments. Because 2 of the HLA ligands from HLA-B*15 (ATKYGPVVY from RGS13 and PQAPSGPSY from E2F8) were found on both cell lines expressing this allele (SUDHL-4 and SUDHL-6), we also demonstrated the feasibility of identifying tumor-specific shared antigens.

A limitation of this study is the lack of a thorough investigation of the immunogenicity of these or any other induced HLA ligands. Such studies need to be performed in the future to identify potential candidate peptides for immunotherapies. Nevertheless, we are convinced that HLA ligands derived from RGS13 and E2F8 could be interesting targets for T-cell receptor (TCR) mimic-based immunotherapies that can recognize their target independent of T-cell reactivity because these proteins are strongly and broadly expressed among DLBCLs (according to the CCLE). No reports of HLA ligands derived from these proteins were found in the immunopeptidome of healthy tissues for any HLA allele investigated. These findings underline the high tumor specificity of these targets for future immunotherapeutic development.

For HLA class II ligands, we could not define shared, clearly tumor-specific immunotherapy targets. However, because many HLA ligands were detected that clearly are not detected in healthy tissues, extensive characterization of these numerous peptides could identify a target that could synergize with HLA class I-presented peptides in a therapeutic approach. Furthermore, it must be noted that for all HLA class I and class II peptides, a limitation of this study could be the toxicity mediated by the triple treatment and the use of slightly different drug concentrations and time courses used to mitigate toxicity, which could have led to biases in the analysis of the HLA ligandome.

Overall, we are convinced that these treatment strategies can help us better understand the immune evasive mechanisms of DLBCLs and can also provide novel immunotherapy targets for a disease

which is so far lacking a highly tumor-specific target for T cell-based immunotherapy.

Acknowledgments

The authors thank Alex Kentsis for access to the Bionic Software, Henrik Molina from the Proteome Resource Center at The Rockefeller University for the performing all LC-MS/MS experiments, and Steven Josefowicz for guidance during this project.

This work was supported by the Leukemia and Lymphoma Society, grants from the National Institutes of Health, National Cancer Institute (P30 CA008748, R01 CA55349, P01 CA23766, and R35 CA241894), and Tudor Funds. Z.M. received funding from the Steven A. Greenberg Lymphoma Research award and Alex's Lemonade Stand Foundation. M.G.K. received funding from an individual research grant by the German Research Foundation (DFG) (KL3118/1-1) and is a member of the BIH (Berlin Institute of Health) clinician scientist program.

Authorship

Contribution: C.M.B., S.S.M., Z.E.H.A., Z.M., and M.G.K. performed experiments and analyzed the data; C.M.B., M.G.K., K.T., A.D.,

R.S.G., and D.A.S. designed the experiments; C.M.B. and M.G.K. wrote the original draft of the manuscript; T.D., C.S., M.G.K., and D.A.S. supervised the project; and D.A.S. provided funding and edited the manuscript; and all authors reviewed and contributed to the manuscript.

Conflict-of-interest disclosure: C.S. has performed consultancy for AbbVie and Bayer, and has received research funding from Trilium Therapeutics Inc and Epizyme. T.D. served as a consultant for Eureka Therapeutics. M.G.K. serves as a consultant for Ardigen. D.A.S. has ownership in, income from, or research funds from Pfizer, SELLAS Life Sciences, Iovance Biotherapeutics, Eureka Therapeutics, Colmune, Oncopep, and Repertoire Immune Medicines. The remaining authors declare no competing financial interests.

ORCID profiles: C.M.B., 0000-0001-9290-4223; S.S.M., 0000-0002-3735-6057; Z.E.H.A., 0000-0001-9851-8796; Z.M., 0000-0001-6728-4835; R.S.G., 0000-0001-5138-2772; A.D., 0000-0001-8144-0574.

Correspondence: David A. Scheinberg, Memorial Sloan Kettering Cancer Center, 1275 York Ave, Zuckerman 1960, New York, NY 10065; e-mail: scheinbd@mskcc.org.

References

1. Younes A. Promising novel agents for aggressive B-cell lymphoma. *Hematol Oncol Clin North Am.* 2016;30(6):1229-1237.
2. Feugier P, Van Hoof A, Sebban C, et al. Long-term results of the R-CHOP study in the treatment of elderly patients with diffuse large B-cell lymphoma: a study by the Groupe d'Etude des Lymphomes de l'Adulte. *J Clin Oncol.* 2005;23(18):4117-4126.
3. Sharpe AH, Pauken KE. The diverse functions of the PD1 inhibitory pathway. *Nat Rev Immunol.* 2018;18(3):153-167.
4. Ribas A, Wolchok JD. Cancer immunotherapy using checkpoint blockade. *Science.* 2018;359(6382):1350-1355.
5. Sadelain M. Chimeric antigen receptors: driving immunology towards synthetic biology. *Curr Opin Immunol.* 2016;41:68-76.
6. Rafiq S, Purdon TJ, Daniyan AF, et al. Optimized T-cell receptor-mimic chimeric antigen receptor T cells directed toward the intracellular Wilms tumor 1 antigen. *Leukemia.* 2017;31(8):1788-1797.
7. Schumacher TN, Schreiber RD. Neoantigens in cancer immunotherapy. *Science.* 2015;348(6230):69-74.
8. Chandran SS, Klebanoff CA. T cell receptor-based cancer immunotherapy: emerging efficacy and pathways of resistance. *Immunol Rev.* 2019; 290(1):127-147.
9. Khodadoust MS, Olsson N, Wagar LE, et al. Antigen presentation profiling reveals recognition of lymphoma immunoglobulin neoantigens. *Nature.* 2017;543(7647):723-727.
10. Carter P, Smith L, Ryan M. Identification and validation of cell surface antigens for antibody targeting in oncology. *Endocr Relat Cancer.* 2004;11 (4):659-687.
11. Berlin C, Kowalewski DJ, Schuster H, et al. Mapping the HLA ligandome landscape of acute myeloid leukemia: a targeted approach toward peptide-based immunotherapy. *Leukemia.* 2015;29(3):647-659.
12. Bilich T, Nelde A, Bauer J, et al. Mass spectrometry-based identification of a B-cell maturation antigen-derived T-cell epitope for antigen-specific immunotherapy of multiple myeloma. *Blood Cancer J.* 2020;10(2):24.
13. Bilich T, Nelde A, Bichmann L, et al. The HLA ligandome landscape of chronic myeloid leukemia delineates novel T-cell epitopes for immunotherapy. *Blood.* 2019;133(6):550-565.
14. Oh CY, Klatt MG, Bourne C, et al. ALK and RET inhibitors promote HLA class I antigen presentation and unmask new antigens within the tumor immunopeptidome. *Cancer Immunol Res.* 2019;7(12):1984-1997.
15. Chang AY, Gejman RS, Brea EJ, et al. Opportunities and challenges for TCR mimic antibodies in cancer therapy. *Expert Opin Biol Ther.* 2016;16 (8):979-987.
16. Brea EJ, Oh CY, Manchado E, et al. Kinase regulation of human MHC class I molecule expression on cancer cells. *Cancer Immunol Res.* 2016;4 (1):936-947.
17. Ruiz Cuevas MV, Hardy M-P, Holly J, et al. Most non-canonical proteins uniquely populate the proteome or immunopeptidome. *Cell Rep.* 2021;34 (10):108815.

18. Nijland M, Veenstra RN, Visser L, et al. HLA dependent immune escape mechanisms in B-cell lymphomas: implications for immune checkpoint inhibitor therapy? *Oncoimmunology*. 2017;6(4):e295202.
19. Gang AO, Frosig TM, Brimnes MK, et al. 5-Azacytidine treatment sensitizes tumor cells to T-cell mediated cytotoxicity and modulates NK cells in patients with myeloid malignancies. *Blood Cancer J*. 2014;4(3):e197.
20. Yu G, Wu Y, Wang W, et al. Low-dose decitabine enhances the effect of PD-1 blockade in colorectal cancer with microsatellite stability by re-modulating the tumor microenvironment. *Cell Mol Immunol*. 2019;16(4):401-409.
21. Klar AS, Gopinadh J, Kleber S, Wadle A, Renner C. Treatment with 5-aza-2'-deoxycytidine induces expression of NY-ESO-1 and facilitates cytotoxic T lymphocyte-mediated tumor cell killing. *PLoS One*. 2015;10(10):e0139221.
22. Almstedt M, Blagitko-Dorfs N, Duque-Afonso J, et al. The DNA demethylating agent 5-aza-2'-deoxycytidine induces expression of NY-ESO-1 and other cancer/testis antigens in myeloid leukemia cells. *Leuk Res*. 2010;34(7):899-905.
23. Mondello P, Tadros S, Teater M, et al. Selective inhibition of HDAC3 targets synthetic vulnerabilities and activates immune surveillance in lymphoma. *Cancer Discov*. 2020;10(3):440-459.
24. Ennishi D, Takata K, Béguelin W, et al. Molecular and genetic characterization of MHC deficiency identifies EZH2 as therapeutic target for enhancing immune recognition. *Cancer Discov*. 2019;9(4):546-563.
25. Béguelin W, Teater M, Meydan C, et al. Mutant EZH2 induces a pre-malignant lymphoma niche by reprogramming the immune response. *Cancer Cell*. 2020;37(5):655-673.e11.
26. Pera B, Tang T, Marullo R, et al. Combinatorial epigenetic therapy in diffuse large B cell lymphoma pre-clinical models and patients. *Clin Epigenetics*. 2016;8(1):79.
27. Kalac M, Scotto L, Marchi E, et al. HDAC inhibitors and decitabine are highly synergistic and associated with unique gene-expression and epigenetic profiles in models of DLBCL. *Blood*. 2011;118(20):5506-5516.
28. McCabe MT, Ott HM, Ganji G, et al. EZH2 inhibition as a therapeutic strategy for lymphoma with EZH2-activating mutations. *Nature*. 2012;492(7427):108-112.
29. Emran AA, Chatterjee A, Rodger EJ, et al. Targeting DNA methylation and EZH2 activity to overcome melanoma resistance to immunotherapy. *Trends Immunol*. 2019;40(4):328-344.
30. Burr ML, Sparbier CE, Chan KL, et al. An evolutionarily conserved function of polycomb silences the MHC class I antigen presentation pathway and enables immune evasion in cancer. *Cancer Cell*. 2019;36(4):385-401.e8.
31. Nervi C, De Marinis E, Codacci-Pisanelli G. Epigenetic treatment of solid tumours: a review of clinical trials. *Clin Epigenetics*. 2015;7(1):127.
32. Sutherland MK, Yu C, Anderson M, et al. 5-azacytidine enhances the anti-leukemic activity of lintuzumab (SGN-33) in preclinical models of acute myeloid leukemia. *MAbs*. 2010;2(4):440-448.
33. Ørskov AD, Treppendahl MB, Skovbo A, et al. Hypomethylation and up-regulation of PD-1 in T cells by azacytidine in MDS/AML patients: a rationale for combined targeting of PD-1 and DNA methylation. *Oncotarget*. 2015;6(11):9612-9626.
34. Morin RD, Johnson NA, Severson TM, et al. Somatic mutations altering EZH2 (Tyr641) in follicular and diffuse large B-cell lymphomas of germinal-center origin. *Nat Genet*. 2010;42(2):181-185.
35. Lavarone E, Barbieri CM, Pasini D. Dissecting the role of H3K27 acetylation and methylation in PRC2 mediated control of cellular identity. *Nat Commun*. 2019;10(1):1679.
36. Béguelin W, Popovic R, Teater M, et al. EZH2 is required for germinal center formation and somatic EZH2 mutations promote lymphoid transformation. *Cancer Cell*. 2013;23(5):677-692.
37. Italiano A, Soria J-C, Toulmonde M, et al. Tazemetostat, an EZH2 inhibitor, in relapsed or refractory B-cell non-Hodgkin lymphoma and advanced solid tumours: a first-in-human, open-label, phase 1 study. *Lancet Oncol*. 2018;19(5):649-659.
38. Brach D, Johnston-Blackwell D, Drew A, et al. EZH2 inhibition by tazemetostat results in altered dependency on B-cell activation signaling in DLBCL. *Mol Cancer Ther*. 2017;16(11):2586-2597.
39. Viré E, Brenner C, Deplus R, et al. The polycomb group protein EZH2 directly controls DNA methylation. *Nature*. 2006;439(7078):871-874.
40. Martín-Subero JI, Kreuz M, Bibikova M, et al; Molecular Mechanisms in Malignant Lymphomas Network Project of the Deutsche Krebshilfe. New insights into the biology and origin of mature aggressive B-cell lymphomas by combined epigenomic, genomic, and transcriptional profiling. *Blood*. 2009;113(11):2488-2497.
41. Laird PW. Principles and challenges of genomewide DNA methylation analysis. *Nat Rev Genet*. 2010;11(3):191-203.
42. Klatt MG, Mack KN, Bai Y, et al. Solving an MHC allele-specific bias in the reported immunopeptidome. *JCI Insight*. 2020;5(19):e141264.
43. Bern M, Kil YJ, Becker C. Byonic: advanced peptide and protein identification software. *Curr Protoc Bioinformatics*. 2012;40(13):13-14.
44. Tate JG, Bamford S, Jubb HC, et al. COSMIC: the Catalogue Of Somatic Mutations In Cancer. *Nucleic Acids Res*. 2019;47(D1):D941-D947.
45. Jurtz V, Paul S, Andreatta M, Marcatili P, Peters B, Nielsen M. NetMHCpan-4.0: improved peptide-MHC class I interaction predictions integrating eluted ligand and peptide binding affinity data. *J Immunol*. 2017;199(9):3360-3368.
46. Pacini C, Dempster JM, Boyle I, et al. Integrated cross-study datasets of genetic dependencies in cancer. *Nat Commun*. 2021;12(1):1661.
47. Javitt A, Barnea E, Kramer MP, et al. Pro-inflammatory cytokines alter the immunopeptidome landscape by modulation of HLA-B expression. *Front Immunol*. 2019;10:141.

Downloaded from <http://ashpublications.org/bloodadvances/article-pdf/6/7/441/171906934/advancesarticle.pdf> by guest on 27 November 2023

48. Girdlestone J, Milstein C. Differential expression and interferon response of HLA class I genes in thymocyte lines and response variants. *Eur J Immunol.* 1988;18(1):139-143.
49. Burrone OR, Kefford RF, Gilmore D, Milstein C. Stimulation of HLA-A,B,C by IFN-alpha. The derivation of Molt 4 variants and the differential expression of HLA-A,B,C subsets. *EMBO J.* 1985;4(11):2855-2860.
50. Marcu A, Bichmann L, Kuchenbecker L, et al. HLA Ligand Atlas: a benign reference of HLA-presented peptides to improve T-cell-based cancer immunotherapy. *J Immunother Cancer.* 2021;9(4):e002071.
51. Vita R, Mahajan S, Overton JA, et al. The Immune Epitope Database (IEDB): 2018 update. *Nucleic Acids Res.* 2019;47(D1):D339-D343.
52. Nelde A, Kowalewski DJ, Backert L, et al. HLA ligandome analysis of primary chronic lymphocytic leukemia (CLL) cells under lenalidomide treatment confirms the suitability of lenalidomide for combination with T-cell-based immunotherapy. *Onc Immunology.* 2018;7(4):e1316438.

Downloaded from <http://ashpublications.org/bloodadvances/article-pdf/6/14/4117/1906934/advances.a0210069.pdf> by guest on 27 November 2023

2.3.1 Modulation durch Tyrosinkinaseinhibitoren

Originalarbeit 4

Charles A, Bourne CM, Korontsvit T, Aretz ZEH, Mun SS, Dao T, **Klatt MG***, Scheinberg DA*. Low-dose CDK4/6 inhibitors induce presentation of pathway specific MHC ligands as potential targets for cancer immunotherapy. *Oncoimmunology*. 2021;10(1):1916243. *geteilte Letztautorenschaft

CDK4/6-Inhibitoren, wie Abemaciclib und Palbociclib, welche inzwischen einen festen Bestandteil der Therapie des Mammakarzinoms darstellen, sind nicht nur für ihre Wirkung auf den Zellzyklus bekannt, sondern auch für ihre Induktion einer T-Zell vermittelten Immunreaktion. Es wird angenommen, dass diese Wirkung auf spezifische Veränderungen der HLA Liganden zurückzuführen ist. In dieser Studie untersuchten wir daher die Wirkung von CDK4/6-Inhibitoren auf das Immunpeptidom von Brustkrebszelllinien. Unsere Analysen ergaben, dass Behandlung mit diesen Inhibitoren zu einer Hochregulierung der HLA Expression und zur Definition einer Vielzahl neuer HLA-Liganden in Brustkrebszelllinien führte, die insbesondere mit Peptiden angereichert waren, die von Proteinen stammen, die am G1/S-Übergang des Zellzyklus beteiligt sind, wie z.B. CDK4/6, Cyclin D1 und PSMC1.

Insbesondere konnte bereits eine niedrige dosierte Behandlung mit CDK4/6-Inhibitoren, welche womöglich nur geringe systemische Nebenwirkungen mit sich bringen sollte, die HLA-Expression an der Zelloberfläche von Brustkrebs-Zelllinien steigern. Dies wurde bei zwei Zelllinien, MCF7 und T47D, beobachtet, wenn sie mit Abemaciclib oder Palbociclib behandelt wurden.

Darüber hinaus ergab die massenspektrometrische Analyse, dass die Behandlung mit CDK4/6 Inhibitoren zu signifikanten Veränderungen im Immunpeptidom führte. Zum Beispiel stieg in der MCF7-Zelllinie die Zahl der identifizierten HLA-Liganden unter Palbociclib bzw. Abemaciclib um das 1,5- bzw. 1,9-fache. Weiterführende Netzwerkanalysen der Quellproteine aus welchen diese induzierten HLA-Liganden stammten, zeigten eine starke Anreicherung für Proteine aus dem CDK4/6-Komplex und der nachfolgenden Signalkaskade. Über weitere biochemische Experimente konnten wir nachweisen, dass die spezifische Inhibition des Signalweges zu einer vermehrten Ubiquitinierung und letztlich Präsentation der beteiligten Proteine führte und daher erhebliche spezifische Auswirkungen auf das Immunpeptidom hat. Außerdem konnten wir nachweisen, dass derart induzierte HLA Liganden in gesunden Spendern T-Zell Aktivierungen auslösen können, was den ursprünglichen Effekt der T-Zell vermittelten Immunität durch CDK4/6 Inhibitoren zumindest teilweise erklären könnte.

Insgesamt belegt diese Studie, dass niedrig dosierte CDK4/6-Inhibitoren die Präsentation spezifischer HLA Liganden induziert, welche als Target für T-Zell basierte Immuntherapien fungieren können.

Low-dose CDK4/6 inhibitors induce presentation of pathway specific MHC ligands as potential targets for cancer immunotherapy

Angel Charles^{a#}, Christopher M. Bourne^{b*#}, Tanya Korontsvit^a, Zita E. H. Aretz^c, Sung Soo Mun^a, Tao Dao^a, Martin G. Klatt^{a*}, and David A. Scheinberg^{a,d*}

^aMolecular Pharmacology Program, Sloan Kettering Institute, New York, USA; ^bImmunology and Microbial Pathogenesis Program, Weill Cornell Medicine, New York, USA; ^cPhysiology, Biophysics and Systems Biology, Weill Cornell Medicine, New York, USA; ^dPharmacology Program, Weill Cornell Medicine, New York, USA

ABSTRACT

Cyclin dependent kinase 4/6 inhibitors (CDK4/6i) lead to cell-cycle arrest but also trigger T cell-mediated immunity, which might be mediated by changes in human leukocyte antigen (HLA) ligands. We investigated the effects of CDK4/6i, abemaciclib and palbociclib, on the immunopeptidome at nontoxic levels in breast cancer cell lines by biochemical identification of HLA ligands followed by network analyses. This treatment led to upregulation of HLA and revealed hundreds of induced HLA ligands in breast cancer cell lines. These new ligands were significantly enriched for peptides derived from proteins involved in the "G1/S phase transition of cell cycle" including HLA ligands from CDK4/6, Cyclin D1 and the 26S regulatory proteasomal subunit 4 (PSMC1). Interestingly, peptides from proteins targeted by abemaciclib and palbociclib, were predicted to be the most likely to induce a T cell response. In strong contrast, peptides induced by solely one of the drugs had a lower T cell recognition score compared to the DMSO control suggesting that the observed effect is class dependent. This general hypothesis was exemplified by a peptide from PSMC1 which was among the HLA ligands with highest prediction scores and which elicited a T cell response in healthy donors. Overall, these data demonstrate that CDK4/6i treatment gives rise to drug-induced HLA ligands from G1/S phase transition, that have the highest chance for being recognized by T cells, thus providing evidence that inhibition of a distinct cellular process leads to increased presentation of the involved proteins that may be targeted by immunotherapeutic agents.

ARTICLE HISTORY

Received 2 December 2020
Revised 6 April 2021
Accepted 7 April 2021

KEYWORDS

CDK4/6; cell cycle; immunotherapy; HLA ligandome; mass spectrometry; breast cancer; antigen presentation; combination therapeutics; abemaciclib; palbociclib

Introduction



The development of targeted cancer therapies is an important and challenging part of cancer therapy, as traditional antineoplastic agents (e.g. chemotherapy, radiation) are nonspecific, and prone to off-target toxicities to healthy tissues and escape of cancer cells.^{1,2} Other successful therapies such as immune checkpoint blockade and adoptive T-cell therapy target cancer-associated antigens,^{3,4} but are generally nonspecific immune activators often associated with severe toxicities. Checkpoint blockade therapies rely on the ability of T-cells to recognize and kill cancer cells that express cognate HLA/peptide complexes presenting new antigens.^{5,6}

Mutated neoantigens as HLA ligands provide ideal cancer specificity, but are patient-specific.⁷ Therefore, more broadly expressed tumor-selective targets are needed to develop more widely applicable immunotherapies. T-cell receptor (TCR)-based therapies, including adoptive T cells and checkpoint blockade inhibitor antibodies, can target intracellular cancer-associated proteins if these are presented as peptides on the cell surface, thus making most proteins in the cell potential targets.^{8,9} This key feature of TCR surveillance can be exploited to target intracellular, oncogenic and tumor selective pathways.

Previous studies have shown that drugs interfering with oncogenic signaling pathways can lead to the presentation of


HLA ligands on cancer cells that are usually not displayed in healthy tissues,^{10,11} offering the potential for immunotherapeutic targeting. For example, inhibition of the mitogen-activated protein kinase (MAPK) pathway in MAPK-driven cancers leads to improved peptide/MHC target recognition and killing by T cells and TCR-mimic antibodies.¹⁰ Additionally, the inhibition of two tyrosine kinases, anaplastic lymphoma kinase (ALK), and rearranged during transfection (RET), in the cancers in which these pathways are oncogenic, promotes HLA class I antigen presentation, and induces expression of new peptides that are recognized by T cells.¹¹

Despite rapid advancements in the treatment of breast cancer, many patients still relapse and are not cured. T cell-based immunotherapy strategies for breast cancer have been largely unsuccessful.¹² Therefore, discovery of therapeutic strategies that would increase susceptibility of breast cancer to immunotherapies is an attractive goal. Cyclin dependent kinase 4/6 inhibitors (CDK4/6i), which prevent the transition from G1 to the S phase of the cell cycle, have been shown to increase the expression of HLA class I molecules in multiple breast cancer cell lines.^{13,14} CDK4/6i treatment has also been demonstrated to improve T cell infiltration into the tumor, and to work synergistically with immune checkpoint blockade (e.g. PD-L1) in mouse models.¹³

CONTACT David A. Scheinberg  scheinbd@mskcc.org  Molecular Pharmacology Program, Sloan Kettering Institute, 1275 York Avenue, New York, NY, USA, 10065

*These authors contributed equally to this work.

[#]Angel Charles and Christopher M. Bourne are co-first authors.

 Supplemental data for this article can be accessed on the [publisher's website](#)

© 2021 The Author(s). Published with license by Taylor & Francis Group, LLC.

This is an Open Access article distributed under the terms of the Creative Commons Attribution-NonCommercial License (<http://creativecommons.org/licenses/by-nc/4.0/>), which permits unrestricted non-commercial use, distribution, and reproduction in any medium, provided the original work is properly cited.

We hypothesized that CDK4/6 inhibitors could lead to presentation of new, drug-induced cancer-associated antigens that might be used for immunotherapeutic targeting and indeed, reports from single proteins of the CDK4/6 axis, such as cyclin D1 have been detected in melanoma after CDK4/6i treatment.¹⁵ Utilizing HLA-peptide immunoprecipitation in conjunction with mass spectrometry (MS), we identified the presentation of many new HLA ligands derived from proteins involved in G1/S phase of cell cycle transition, the phase in which cells are usually arrested when treated with CDK4/6i. Many of these drug-induced HLA ligands had not been identified in healthy tissues, which renders them appealing targets for immune checkpoint blockade, TCR-based therapies and TCRmimic antibodies.⁹ Additionally, we demonstrated reactivity of one of the induced HLA ligands with T cells from healthy donors. In summary, this concept illustrates drug-induced alteration of the immunopeptidome by CDK4/6i and also how disruption of G1/S phase transition of the mitotic cell cycle through small molecules can lead to increased presentation of proteins involved in that pathway. In this way, CDK4/6 inhibitors could potentially synergize with immunotherapeutic agents which target cell-cycle derived peptide-HLA complexes.

Results

Low-dose treatment with CDK4/6i increase HLA class I surface expression in breast cancer cells

MCF7 and T47D breast cancer cell lines were treated with either CDK4/6i abemaciclib or palbociclib to determine the lowest dose of CDK4/6i that would upregulate cell surface

HLA expression, as this effect has been reported in the literature.¹³ The MCF-7 cell line was chosen as positive control to repeat the published results. T47D cells were added as they also are known to be susceptible to CDK4/6i, but furthermore show higher HLA expression which made them a better candidate for an HLA ligand focused study. Drug concentrations of either abemaciclib or palbociclib ranging from 10 to 1,000 nM, were applied over 7 days on MCF7. Flow cytometric analysis showed 100 nM as the lowest dose in which cell surface HLA levels were significantly upregulated, with abemaciclib inducing higher expression for MCF7 (Supplementary Fig. S1A). 100 nM of each drug was also tested on T47D and both similarly upregulated HLA, so palbociclib was chosen for further study to demonstrate the effects of another CDK4/6i on a different breast cancer cell line (Supplementary Fig. S1B). Importantly, 100 nM of either drug was about 100-fold lower than the respective IC50 values (about 10uM) for the cytostatic effect mediated by these drugs (Supplementary Fig. S1B, S1C), and 2–3 fold lower than plasma concentrations in patients treated with these drugs.¹⁶ Therefore, observed effects were unlikely to be associated with the cytostasis of these cells. By bright field microscopy and flow cytometry, the 100 nM dose of Abemaciclib resulted in an increase in MCF7 cell size when compared to DMSO treatment (Figure 1a, Supplementary Fig. S1D); at the same time point, T47D cells also showed an increase in overall cell size, taking on a more spherical morphology and increase in granularity when compared to DMSO treated cells (Figure 1b, Supplementary Fig. S1E).

A 7 day time-course experiment with low-dose (100 nM) abemaciclib treatment resulted in a doubling of HLA-A*02 and pan-HLA class I surface expression per cell (Figure 1a, left and

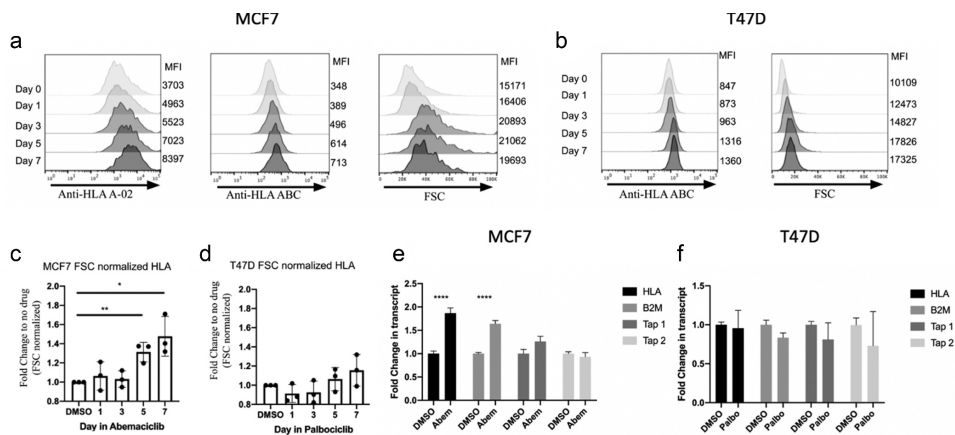


Figure 1. CDK4/6 inhibitors increase HLA surface expression. (a) MCF7 breast cancer cells were treated with 100 nM abemaciclib for the amount of time indicated on the Y axis. Flow cytometry for HLA-A02 levels (left), pan HLA levels (middle), and forward scatter (right) are displayed against corresponding mean fluorescence intensity (MFI) in x axis and the level is annotated on the right side. (b) T47D breast cancer cells were treated with 100 nM palbociclib for indicated times using flow cytometry as in panel A. (c) Normalized fold change in MFI from panel A of three biological replicates. HLA expression was normalized to forward scatter (FSC) to account for cell size changes and expressed as fold change to DMSO. (d) Normalized fold change in MFI from panel A of three biological replicates. HLA expression was normalized to forward scatter (FSC) to account for cell size changes and expressed as fold change to DMSO. (e-f) qRT-PCR for key proteins involved in antigen presentation transcripts noted on insert legend was performed on (e) MCF7 cells and (f) T47D cells, 7 days after treatment with a single dose of 100 nM abemaciclib or palbociclib on day 1. Error bars indicate SD, *P < .05, ** P < .01, *** P < .001, **** P < .0001. All experiments were performed in technical replicates.

middle), as well as moderate increases in cell size in MCF7 breast cancer cells (Figure 1a, right). Similar effects were observed after treatment with 100 nM palbociclib in T47D cells (Figure 1b). However, when total pan-HLA class I surface expression was recalculated and normalized for the increase in cell size, the treatment showed a statistically significant 50% increase in pan-HLA class I surface expression density in MCF7 cells treated with abemaciclib compared to DMSO by day 5 (Figure 1c); in contrast, for T47D cells, little and non-significant increase in HLA class I surface density was observed (Figure 1d). These results suggest that HLA class I surface expression is increased independently of the increase in cell surface size in MCF7 cells but is largely mediated through increases in cell size in T47D cells, an effect that may not have been taken into consideration in previous studies.¹³

The increase in HLA class I surface expression that was seen with CDK4/6i treatment could be due to a number of factors including increased transcription or translation of proteins involved in HLA expression, increased stabilization of HLA molecules on the cell surface,¹¹ or increased peptide transport to the endoplasmic reticulum. In order to gain insight into the mechanism underlying the observed phenomena, we performed qRT-PCR analysis on key gene products involved in antigen presentation. In MCF7 cells treated with 100 nM of abemaciclib, there was a 1.5–2 fold increase in the transcript levels of both *hla* and *beta-2-microglobulin (b2M)*, but little change in transcript levels of the transporter associated with antigen processing 1 and 2 (*tap1* and *tap2*) proteins when compared to DMSO (Figure 1e). This is in contrast to previous

studies which did show an upregulation of TAP proteins for MCF-7, MDA-MB453 and patient derived cancer cells at higher treatment concentrations compared to the concentrations used in this study.¹³ Moreover, in T47D cells treated with palbociclib, there were no significant changes in *hla*, *b2M*, or *tap1* transcript levels, when compared to DMSO (Figure 1f). These results imply that the increase in HLA class I surface protein levels observed in CDK4/6i treated breast cancer cells were not consistent with a broad upregulation in antigen presentation, which differs from previous observations which showed upregulation of various components of antigen presentation with CDK4/6 treatment.¹³

Mass spectrometry identified changes in the immunopeptidome after CDK4/6i treatment

To investigate how alterations in surface HLA levels affect the repertoire of presented HLA ligands, we biochemically isolated HLA class I (HLA-A, HLA-B and HLA-C) peptides from breast cancer cells treated with either abemaciclib, palbociclib, or DMSO, assigned them to their HLA alleles through the netMHCpan 4.0¹⁷ prediction algorithm and mapped the peptides to their proteins of origin (Supplementary Table 1).

In the MCF7 cell line, CDK4/6i treatment increased the number of unique identified HLA ligands 1.5 or 1.9-fold for palbociclib or abemaciclib, respectively resulting in 160 or 200 unique HLA class I ligands (Figure 2a, b). Compared to DMSO, results from abemaciclib and palbociclib combined induced the presentation, in total, of more than 200 new HLA class

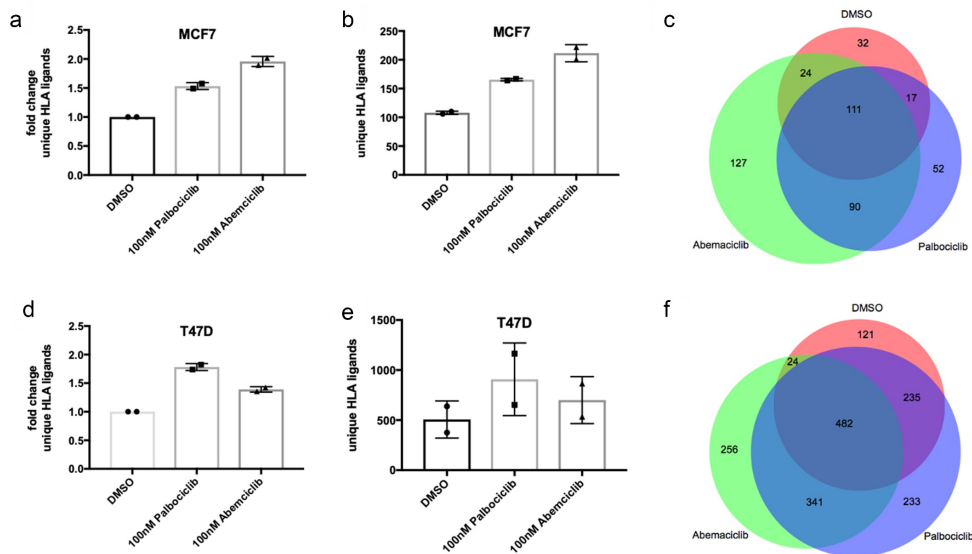


Figure 2. CDK4/6i induce changes in the immunopeptidome of breast cancer cells. Immunoprecipitation of HLA complexes and subsequent isolation and analysis of HLA-bound peptides by LC-MS/MS was performed after 7 day treatment with either 100 nM DMSO, Abemaciclib or Palbociclib. MCF and T47D cells respectively, showed relative (a,d) and absolute increases in unique HLA ligands (b, e) after drug treatment compared to DMSO treatment. Venn diagrams for MCF7 (c) and T47D (f) illustrate induction of HLA ligands. Error bars indicate mean and SD of two biological replicates.

I ligands at concentrations of 100 nM of either drug (Figure 2c). In the T47D cell line much higher total numbers of HLA ligands were detected, consistent with previously published data that determined that absolute HLA transcript levels are almost 3-fold higher in T47D compared to MCF7 cells.¹⁸ An average of 908 and 700 unique HLA ligands were identified in the palbociclib and abemaciclib treated cell lines respectively, compared to 506 in DMSO treated cells. The relative increase was about 1.7 and 1.4-fold, respectively (Figure 2d, e). This resulted in a total of more than 500 new HLA class I ligands induced by either drug CDK4/6i treatment (Figure 2f), demonstrating that though the increase in total HLA surface levels was highly influenced by the increase in cell size for T47D cells, the overall immunopeptidome still expanded notably. Although overall antigen presentation is not affected by CDK4/6i in this cell line, increased HLA surface area and changes to cellular states are sufficient to modulate the immunopeptidome. Of note, the numbers of identified HLA ligands matched or exceeded the amount of ligands recently reported on the same breast cancer cell lines¹⁸ and are in line with the relative amounts of HLA complex presented on their cell surface.¹⁹ The results showed a trend for the upregulation of HLA ligands ($p = .09$). While not at $p < .05$, the narrow distribution of the error bars support the validity of the findings.

Interestingly, further analysis of the HLA ligands showed that the increase in HLA ligand presentation changed neither the HLA allelic association (Supplementary Fig. S2A, S2B), nor the length distribution of the HLA ligands (Supplementary Fig. S2C, S2D) ensuring consistency of the approach and excluding

potential bias through different processing after drug treatment.

CDK4/6i-induced HLA ligands are derived from proteins enriched in G1/S cell cycle transition

To further understand if there was a correlation between the inhibition of the CDK4/6 complex and the change in the immunopeptidome, we analyzed the source proteins of the drug-induced HLA ligands. Results from biological replicates of the different treatment conditions were combined for every cell line individually and source proteins lists were generated from either all proteins in the DMSO samples or from all source proteins induced from CDK4/6i treatment (Figure 3 A, B, left panel, Supplementary Table 2). The network analysis was performed using GeneMANIA²⁰ and focused on physical interactions rather than co-expression or genetic interactions, to address the direct physical inhibition of the CDK4/6 complex and pathways by this drug class. Network analyses clearly demonstrated a strong enrichment for proteins from the G1/S transition of cell cycle (q values of 2.5×10^{-6} for MCF7 and 8.8×10^{-19} for T47D cells). The enrichment of this class of proteins was the top hit for both cell lines after drug treatment, and specifically not enriched in the cells after DMSO-treatment, suggesting a drug-specific effect that is consistent with the known mechanism of CDK4/6i leading to cell cycle arrest in G1 phase (Figure 3 A, B, right panel). Building a network of all the proteins identified in our study through CDK4/6i induction that are involved in the “G1/S transition of mitotic cell cycle” illustrated three subgroups relevant to the

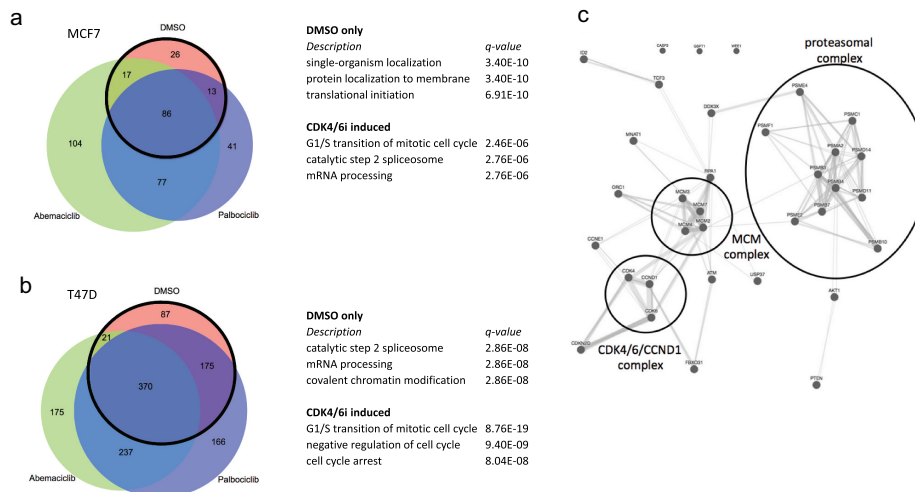


Figure 3. CDK4/6i induce MHC ligands enriched from source proteins contributing to “G1/S transition of mitotic cell cycle”. Source proteins from peptide sequences detected either in the DMSO sample (inside the bold lined circle) or source proteins from CDK4/6i induced peptides (outside the bold lined circle) were used for network analyses. GeneMANIA was used for analysis and only physical interactions were enabled. Top 3 enriched GO terms are shown for MCF7 cells (a) and T47D cells (b). (c) Network analysis of physical interactions from all proteins induced by CDK4/6i treatment contributing to the GO term “G1/S transition of mitotic cell cycle”. Circles indicate 3 clusters consisting of CDK4/CDK6/CCND1 complex (bottom left), MCM complex (middle) and proteasomal complex (upper right).

process: the CDK4/6/CCND1-complex (Figure 3c, lower left circle), the mcm-complex (Figure 3c, middle circle) and the proteasome (Figure 3c, upper right circle). Overall, a total of 60 unique HLA ligands (where post-translationally modified peptides are considered distinct from the unmodified counterpart) from various alleles and both cell lines were exclusively detected after drug treatment. These peptides were all derived from proteins from the G1/S cell cycle interactome. (Table 1). Of note, HLA ligands were repeatedly identified from the directly inhibited molecules CDK4 and CDK6, from the main interacting partner CCND1, and also from more distant physical interactors in the G1/S transition pathway, e.g. components of the mcm-complex. Other important proteins specifically induced after CDK4/6i treatment included the prognosis relevant proteins cyclin E1 (CCNE1) and many of the induced HLA ligands were derived from proteins that have not been reported to contribute to the immunopeptidome of

healthy tissues.²¹ Notably, such cell cycle HLA ligands were induced in the T47D cell line at least equally well compared to MCF7 cells, even though T47D showed no evidence of increased antigen presentation machinery when normalized to cell size (Figure 1–2). This demonstrates that such an effect is independent and more robust between cell lines than changes in antigen presenting machinery.

Increased degradation of pathway specific source proteins as potential mechanism for increased presentation as HLA ligands

In order to better understand the mechanism underlying the induction of so many HLA ligands derived from the inhibited pathway, we focused on CCND1 as an important target as it is important for carcinogenesis in many cancer types^{22,23} and proven to lead to immunogenic HLA ligands.^{24,25}

Table 1. CDK4/6i induced peptides derived from proteins contributing to the GO term G1/S transition of mitotic cell cycle.

Gene name	MCF7_DMSO	MCF7_Abemaciclib	MCF7_Palbociclib	T47D_DMSO	T47D_Abemaciclib	T47D_Palbociclib
CDK4			ALTPVVVTL (A02:01)		NPHKRISAF (B14:02)	
CDK6		ALTSVVVTL (A02:01) GEGAYGKVF (B44:02)				HRVVHRDL (B14:02)
CCND1		ALLESRLRQA (A02:01)			DRVLRAML (B14:02)	DRVLRAML (B14:02)
AKT1						SRHPFLTAL (B14:02)
ATM					DVHRVLVAR (A33:01)	
CASP2						STDVTEHSL (C08:02)
CCNE1					DAHNIQTHR (A33:01)	DAHNIQTHR (A33:01)
CDKN3					DSQSRSVSR (A33:01)	DSQSRSVSR (A33:01)
CDKN2D					DSQSRSVSR (A33:01)	DSQSRSVSR (A33:01)
DDX3X					NRFGKTAL (B14:02)	NRFGKTAL (B14:02)
FBXO31					DAYSFGSR (A33:01)	
GSPT1					DVYAKLLHR (A33:01)	
ID2		ALDSHTPTV (A02:01)			EAEPGGGSL (C08:02)	EAEPGGGSL (C08:02)
MCM2			AEAHARIHL (B44:02)		EAHARIHLR (A33:01)	
MCM3					HAQSIGMNR (A33:01)	HAQSIGMNR (A33:01)
					HAQSIGmNR (A33:01)	HAQSIGmNR (A33:01)
					DRTAIHEVM (B14:02)	
MCM4			RLAEAHAKV (A02:01)		HSMALIHNR (A33:01)	HSMALIHNR (A33:01)
					HSmALIHNR (A33:01)	HSmALIHNR (A33:01)
					DMRKIGSSR (A33:01)	DMRKIGSSR (A33:01)
					DmRKIGSSR (A33:01)	DmRKIGSSR (A33:01)
					KRLHREAL (B14:02)	KRLHREAL (B14:02)
MCM7	RLAQHITYV (A02:01)	RADSVGKLV (C05:01) RLAQHITYV (A02:01) KmQEHSQV (A02:01)	RLAQHITYV (A02:01) KmQEHSQV (A02:01)			GRYNPRSL (B14:02)
						TYTSARTLL (B14:02)
						VRLAHREQV (B14:02)
MNAT1					SSDLPVAL (C08:02)	
ORC1					NRVSSRLGL (B14:02)	
PSMA2					NYVNGKTF (B14:02)	
PSMB10					FRYQGHVGA (B14:02)	DRFQPNMTL (B14:02)
					DRFQPNMTL (B14:02)	DRFQPNmTL (B14:02)
					DRFQPNmTL (B14:02)	
PSMB3		GLATDVQTV (A02:01)			NRFQIATV (B14:02)	YADGESFL (C08:02)
PSMB4					YADGESFL (C08:02)	
PSMB7						FRYQGYIGA (B14:02)
PSMC1		IIDDNHAIIV (A02:01)			EHAPSIVFI (B14:02)	EHAPSIVFI (B14:02)
PSMD11					VEFQRAQSL (B14:02)	VEFQRAQSL (B14:02)
PSMD14			FVDDYTVRV (A02:01)			
PSME2		KVLERVNAV (A02:01)		YHISSNL (B14:02)		
PSME4					TRVDGRKL (B14:02)	TRVDGRKL (B14:02)
PSMF1					NNKDLYVLR (A33:01)	
PTEN					DFYGEVTR (A33:01)	
RPA1					VSDFGGRSL (B08:02)	VSDFGGRSL (B08:02)
TCF3		SLDTQPKV (A02:01)				
USP37					NRLPRVLIL (B14:02)	NRLPRVLIL (B14:02)
						DDLKRATEL (B14:02)
WEE1					DIKPSNIFISR (A33:01)	DIKPSNIFISR (A33:01)
					EVYAHAVL (B14:02)	

Underlined peptides were tested in ELISpot assays.

Furthermore, CCND1 is the direct interacting partner of CDK4/6.²⁶ We exclusively identified peptides derived from CCND1 after CDK4/6i treatment in both cell lines, (ALLESSLRQA in complex with HLA-A*02:01 on MCF7 cells and DRVLRAML in complex with B*14:02 on T47D cells). We first evaluated the transcript and protein expression levels of cyclin D1 in CDK4/6i treated cells compared to DMSO during a 7-day time course. As reported,^{27,28} we observed compensatory upregulation of *cyclin D1* transcript levels in both MCF7 and T47D cells treated with CDK4/6i which increased with longer exposure to drug (Figure 4a, 4b). Western blot analysis of the protein expression levels of Cyclin D1 in both breast cancer cell lines largely paralleled that of transcript, demonstrate slight increase in total intracellular Cyclin D1 (Figure 4c). This indicated that at the protein level, increased Cyclin D1 expression correlated with the exclusive detection of Cyclin D1 derived peptides in CDK4/6i treated breast cancer cells (Figure 4a-c, Table 1), suggesting that inhibition of this pathway might lead to a compensatory increase in protein levels and antigen presentation.

Next, we sought to determine if increased Cyclin D1 presentation in cells treated with CDK4/6i could be attributed to an increase in protein degradation through the multi-ubiquitin pathway. We immunoprecipitated multi-ubiquitinated proteins and then performed a western blot for Cyclin D1 at different time points. Similarly to the results observed for overall protein levels the amount of ubiquitinated cyclin D1

increased in CDK4/6i treated MCF7 and T47D cells compared to DMSO in a time dependent manner as indicated by higher molecular weight bands at later time points (Figure 4d arrows). Taken together, these results support a model whereby CDK4/6i led to compensatory upregulation of cell cycle proteins, followed by their degradation and presentation on HLA (Figure 5).

Drug-induced HLA ligands elicit T cell responses in healthy donors and have higher probability for T cell recognition

Finally, to demonstrate that CDK4/6i-induced HLA ligands were capable of eliciting T cell reactivity, we selected 8 peptides that were predicted to bind HLA-A*02:01 based on the netMHCpan4.0 algorithm including a CCND1- and CDK6-derived peptide. According to the T cell recognition score algorithm,²⁹ three of these eight peptides reached the threshold of 0.1, which suggests T cell recognition and reactivity; however, clear evidence of immunogenicity can only be given through T cell based functional assays. After T cell stimulation of four healthy donors with peptide-pulsed antigen presenting cells we repeatedly detected positive T cell responses by ELISpot for one of the three peptides predicted to have higher potential for reactivity and no responses for the remaining five peptides not being predicted to be immunogenic (Figure 4e, Table 2). The positive response was directed against IIDDNHAIIV from PSMC1 protein, a cell cycle interactome

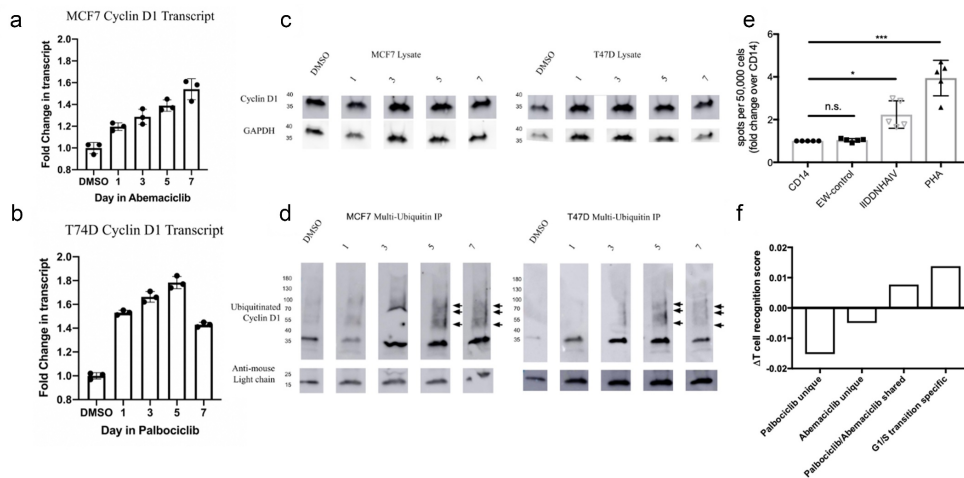


Figure 4. CDK4/6i alter cell cycle pathway for immunotherapeutic targeting. (a) MCF7 and (b) T47D breast cancer cells were treated with 100 nM abemaciclib or palbociclib, respectively, for indicated times. qRT-PCR of Cyclin D1 compared to Actin B was normalized to DMSO treated cells and technical replicates plotted. (c) Western blot for Cyclin D1 from lysates of MCF7 and T47D cells treated as described in (A) with times listed on top of each lane. Molecular weight is provided on the left axis (kD). (d) Ubiquitinated proteins were immunoprecipitated from cell lysates in (C), with times listed on top of each lane and Western blot was performed for Cyclin D1. Arrowheads denote higher molecular weight bands of Cyclin D1, indicative of increased ubiquitination. Molecular weight is provided on left axis (kD). Western blots were repeated twice with similar results. (e) ELISpot result from healthy donor's T cell stimulation with peptide loaded antigen presenting cells. CD14 positive cells and EW-peptide were used as negative control. PHA for positive control. Error bars indicate mean and SD of biological replicates. All data were normalized to the results of CD14 sample. Data are representative for 4 healthy donors and a total of 5 biological replicates. **P* < .05, ** *P* < .01, *** *P* < .001, **** *P* < .0001 (f) T cell recognition predictions for HLA ligands from two different breast cancer cell lines using the iedb online platform²⁸ were performed. Graph shows the differences (delta) of mean T cell recognition values compared to predictions from HLA ligands found in DMSO-treated samples. Data represent the merged results from 2 different cell lines and all replicates.

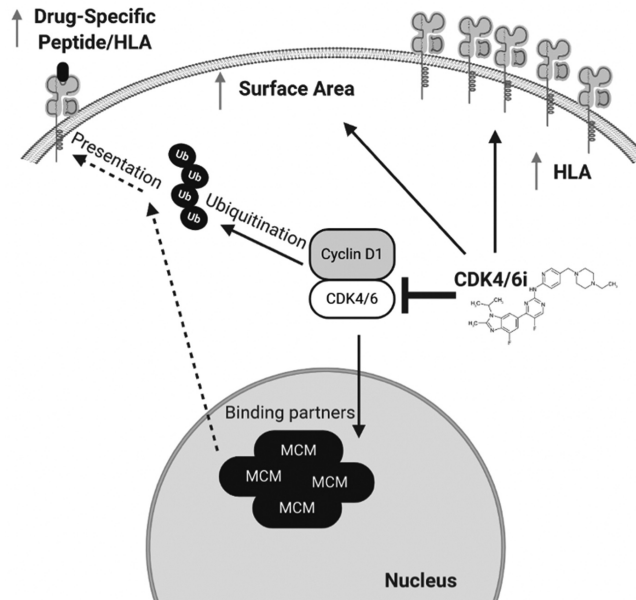


Figure 5. Proposed mechanism of increased CCND1 presentation after CDK4/6i treatment. CDK4/6i inhibit CDK4/6 and their binding partners, leading to ubiquitination. CDK4/6i also promotes compensatory upregulation of cell cycle proteins, HLA, and increased surface area. Together, these mechanisms lead to presentation of a wide variety of cancer-specific peptides derived from cell cycle effectors.

Table 2. Predictions and assays for T cell recognition in drug-induced A*02 ligands.

HLA ligand	Predicted binding affinity for HLA-A*02 [nM]	T cell recognition score	ELISpot result
ALLESLRQA	414.5	-0.260	negative
ALTSVVVTL	35.8	-0.018	negative
FVDDYTVRV	6.8	0.130	negative
GLATDVQTV	23.5	0.037	negative
IIDDNHAIV	115.8	0.160	positive
KVLERVNAV	19.4	0.200	negative
RLAEAHAKV	16.2	0.089	negative
SLDTQPKKV	1878.4	-0.380	negative

protein that in a recent study was shown not to give rise to any HLA ligands in healthy tissues.²¹ These published data support the idea of no preexisting tolerance against this peptide. However, as testing dozens of peptides for T cell recognition by T cell assays is cumbersome and potentially still biased by small numbers we performed T cell recognition predictions for all drug-induced peptides compared to DMSO-treated control cell lines using aforementioned algorithm²⁹ to determine tendencies for T cell reactivity within the different groups. We calculated the average of T cell recognition scores for peptides found in the DMSO-treated samples for each cell line separately to avoid bias introduced by different HLA types. Next, we calculated mean T cell recognition scores for different subsets of induced HLA ligands accordingly for each cell line

separately but including all replicate data. Following subsets of HLA ligands were used: palbociclib unique, abemaciclib unique, shared between palbociclib and abemaciclib samples and HLA ligands from proteins involved in the G1/S phase transition GO term, called “G1/S transition specific” which correspond to the HLA ligands listed in Table 1. Finally the difference between mean T cell recognition scores from DMSO and aforementioned induced subsets was calculated per cell line and then results for both cell lines added. Intriguingly, mean T cell recognition scores from induced HLA ligands found exclusively either in the palbociclib or abemaciclib samples showed lower scores compared to the DMSO mean resulting in a negative T cell recognition score (Figure 4f). In contrast, HLA ligands shared between both drugs and especially HLA ligands derived from proteins involved in the biological process most effectively targeted by CDK4/6i (G1/S phase transition) were assigned higher T cell recognition scores compared to the DMSO group (Figure 4f) suggesting that HLA ligands specifically induced in a drug class-specific manner of CDK4/6i have the highest probability of being recognized by T cells. Furthermore, even if the absolute difference of the T cell recognition score between these subgroups is small the biological impact can be more profound as immune responses against few peptides can lead to relevant biological differences and T cell reactivity for one target has already been demonstrated after testing only eight candidates.

Discussion

Immunotherapies, such as immune checkpoint blockade therapy are now standard of care for many cancer types.³⁰ However, for many cancer types, checkpoint blockade remains unsuccessful likely due to lack of presentation of suitable immunogenic epitopes, e.g. neoepitopes or tumor associated antigens on the cancer cell surface.^{31,32} Similarly, adoptive T cell therapies, ImmTacs, vaccines, or TCRmimic antibodies also depend on the reliable presentation of the HLA ligand for which they are specific, on the target cells.^{7,9,33,34}

CDK4/6 inhibitors, abemaciclib and palbociclib, led to an increase in total surface area of treated breast cancer cells, as well as transcriptional upregulation of HLA in the MCF7 cell line. Although increases in HLA may be due in part to the enlarged cell volume in the T47D cell line, we still observed quantitative and qualitative changes in the immunopeptidome by mass spectrometry in both the MCF7 and T47D cell lines. These results indicated that an increase in HLA complex levels may broaden the repertoire of detectable presented antigens even when higher HLA cell surface levels are due in part to an expanded cell surface area and not to an increase in antigen presentation. Though increasing cell size and granularity could suggest senescence related mechanisms for the observed effect we believe that these cells did not present a strong senescence phenotype as determined by negative staining for the newly identified senescence marker urokinase plasminogen activator receptor (³⁵, data not shown).

Additionally, in contrast to previous results, we did not observe significant changes in transcription of antigen presentation machinery, as a whole.¹³ This could be explained by the 3–5 times lower concentration of CDK4/6i that was used in our study compared to previous published work.

Lower doses of drug were further used in our experiments to avoid confounding biochemical changes in the cell as a result of toxicity or cell death processes. The exact mechanism of HLA upregulation and induction of antigen presentation by this class of inhibitors is still unknown. These results suggest that CDK4/6i has indirect effects on increased HLA surface expression, and a transcriptional program of antigen presentation does not seem to be induced, per se. Additionally, other studies showed induction of the immunopeptidome after treatment of MCF7 cells with abemaciclib.¹⁴ As we also saw peptides derived from the immuno-proteasome subunit PSMB10 presented on the cell surface after CDK4/6i treatment, we provided further evidence of the activation of the immunoproteasome that would then also contribute to the re-shaping of the immunopeptidome. Also, we hypothesize that the presentation of peptides from proteasomal proteins is mediated by their regular degradation after upregulation of this set of proteins. The upregulation of the proteasome components is needed as the CDK4/6 inhibition leaves many proteins from the inhibited pathway without function and subject to degradation. As insufficient proteasomal activity then can lead to autophagy²⁵ proteasomal proteins are upregulated to guarantee the sufficient degradation.

However, most importantly, many of the drug-induced antigens we found on the CDK4/6i treated groups were associated with proteins from the mitotic pathways, specifically the

G1/S phase transition, the phase in which cells arrest after CDK4/6i treatment.²⁶ This suggested that inhibition of the cellular process by the drugs led to preferential degradation of proteins and subsequent presentation on HLA peptides from proteins in the cell cycle pathway interactome. CDK4/6i gave rise to about 70 induced HLA ligands from the specific GO term “G1/S transition of mitotic cell cycle”, which represented about 10% of all treatment induced HLA ligands. Mass spectrometry analysis revealed the peptides “ALLESSLRQA” and “DRLVRAAML,” an HLA-A*02:01-presented and HLA-B*14:02-presented peptide, respectively from the Cyclin D1 protein, among other peptides. In a previous study, the ALLESSLRQA sequence was predicted to be an HLA-A*02:01 binder, but had never been validated for its immunogenicity as it was considered a suboptimal HLA binder.²³ By using Quantitative Reverse Transcriptase-PCR and Western blotting analysis we confirmed a compensatory upregulation of CDK4/6 binding partners, such as Cyclin D1, after CDK4/6i treatment. Additionally, Cyclin D1 exhibited higher levels of ubiquitination in CDK4/6i treated cells. Taken together, we propose a mechanism of increased immunopeptidome repertoire after CDK4/6i treatment whereby disruption of the CDK4/CDK6/CCND1 complex leads to upregulation and subsequent degradation and presentation of cell cycle proteins (Figure 5). Though changes in the immunopeptidome due to CDK4/6i treatment have recently been reported in melanoma cell lines after CDK4/6i treatment¹⁵ this is the first study to demonstrate pathway-dependent degradation and presentation of a directly inhibited protein complex and its downstream interacting partners. However, for future studies it should also be considered that CDK4/6i could lead to the induction of HLA ligands from non-coding regions as these drugs can induce expression of endogenous retroviral elements. Additionally, neoepitopes from germline or somatic mutations could also demonstrate a valuable source for HLA ligands with and without CDK4/6i treatment.

Furthermore, it still has to be determined if these effects can only be observed in cell lines fully dependent on the CDK4/6 pathway as CDK4/6 independent cell lines have not been used in this study. This is especially important as less CDK4/6-dependent cell lines are more likely to be treated with immune checkpoint inhibition in which our proposed mechanism can be particularly relevant. Also triple negative breast cancers should further be investigated for this mechanism as their cyclin E amplification allows them to bypass the CDK4/6 inhibition, but could still be subject to changes in the HLA ligandome, which then could be utilized therapeutically.

Still, many of these drug-induced HLA ligands offer the potential to be ideal targets for cancer immunotherapies. For example CCND1 is expressed in multiple cancers, e.g. mantle cell lymphoma²³ and native immunogenic peptides from this protein have been shown to induce CD4 and CD8+ cytotoxic T cell responses in HLA matched donors.^{24,25} Therefore, Cyclin D1 targeted immunotherapies may synergize with CDK4/6 inhibition in a variety of cancer types. Additionally, CCNE1 is a known negative prognostic marker in breast cancer³⁶ and an extensive study of HLA ligands in healthy tissues did not detect any peptides from CCNE1 presented on

the cell surface of nonmalignant cells.²¹ Given these characteristics CCND1 as well as CCNE1, together with the other induced CDK4/6i induced proteins, those targets should be considered promising targets for immunotherapy approaches. Additionally, we stimulated T cells from healthy donors with a selection of drug-induced A*02 restricted peptides and identified an epitope from the PSMC1 antigen which elicited T cell responses. Additionally, to consider all induced HLA ligands we performed predictions for the T cell recognition of HLA ligands identified in DMSO-treated samples and for subsets of CDK4/6i-induced peptides. Strikingly, HLA-ligands found to be induced by both drugs rather than only one of them showed much higher T cell recognition scores as well as higher scores compared to the HLA ligands found in DMSO-treated cell lines. As HLA ligands that were induced by both drugs are more likely to be induced due to the class specific characteristics rather than off-target effects of these kinase inhibitors, this suggests that the specific targeting of the CDK4/6 complex leads to induction of HLA ligands of higher probability of T cell recognition. This hypothesis is further supported by the fact that HLA ligands from the GO term G1/S phase transition, the subset of peptides that are most likely to be induced by the class specific inhibition of these drugs, demonstrated even higher T cell recognition scores.

Overall, we demonstrated that low doses (100 nM) of CDK4/6 inhibitors abemaciclib and palbociclib can induce substantial and reproducible changes in HLA surface levels and in the ligands that are bound to these complexes, potentially rendering them more susceptible to immune mediated killing by CD8 + T cells. Considering that CDK4/6i have considerable toxicity (i.e. diarrhea, nausea, dyspnea, arthralgia, neutropenia and lymphopenia) at clinically used antineoplastic therapeutic doses.³⁷ Our results suggested that using concentrations 3 to 5-fold lower than patient plasma concentrations can still achieve significant drug-induced peptide presentation changes. However, *in vivo* studies have to be performed in order to investigate if low concentration CDK4/6i treatment can positively influence the effects of immune checkpoint blockade in breast cancer cells. If this can be proven, using lower doses of CDK4/6i at some appropriate time point may mitigate toxicity while synergizing with immunotherapies.

Additionally, we provide the proof-of-concept how physical inhibition of a protein complex leads to the enhanced presentation of HLA ligands directly involved or associated with this complex. This approach could be used to combine the direct inhibition of a complex with a T cell immunotherapy-based approach that targets the specific degradation product of one of the proteins involved.

Therefore, this study provides additional evidence and rationale to combine low-dose CDK4/6i with immunotherapies, such as checkpoint blockade. More over, generating immunotherapeutics that can target cell-cycle derived peptides presented on HLA are attractive. For example adoptive T cell transfer, TCRmimic antibodies or vaccination therapies could allow for specific targeting of breast cancer cells in combination with CDK4/6i.

Materials and methods

Human cell lines

MCF7 (HLA-A*02:01, HLA-B*18:01, HLA-B*44:02, HLA-C*05:01) and T47D (HLA-A*33:01, HLA-B*14:02, HLA-C*08:02) cell lines were cultured in RPMI medium (Gibco) supplemented with 10% FBS (Gibco), penicillin and streptomycin, and 1% L-glutamate. All cell lines were obtained from ATCC, and tested negative for mycoplasma. HLA typing was performed by American Red Cross.

Antibodies and commercial reagents

APC anti-Human HLA-A, B, C (clone W6/32) from Biolegend (Cat. No. 311409), FITC Anti-Human HLA-A2 from BD Biosciences (Cat. No. 551285), were used for flow cytometry. Unlabeled clone W6/32 antibody from BioXcell (Cat. No. BE0079), was used for HLA class I/peptide immunoprecipitation for mass spectrometry. Anti-Human Cyclin D1 (ab134175) from Abcam, and anti-multi ubiquitin magnetic beads from MBL International, were used for Western blot. All antibodies were kept at 4°C. Abemaciclib and Palbociclib were purchased from Sellekchem. The drugs were diluted to 10 mM stocks in DMSO, and kept at -20°C.

Viability assays

15,000 cells were cultured in 96 well plates with serial dilutions of abemaciclib and palbociclib. After 4 days, cells were resuspended in Cell Titer-Glo Luminescent Cell Viability Assay from Promega for 10 minutes, and agitated at room temperature. Luminescence in the 96 well plates was read using a microtiter plate luminometer (PerkinElmer).

Flow cytometry

Cells were treated with 10, 100, or 1000 nM abemaciclib or palbociclib for 1, 3, 5, or 7 days. Cells were harvested, washed with PBS, and labeled with 1:50 dilution of APC Anti-Human HLA-ABC and FITC Anti-Human HLA-A2 in buffer (2% FBS, 0.1% sodium azide, in PBS) for 30 minutes. Cells were analyzed using a Fortessa Flow Cytometer from BD Biosciences or a Guava flow cytometer from Millipore.

Quantitative reverse-transcriptase PCR

Cells were treated with 100 nM Abemaciclib or Palbociclib for 1, 3, 5, or 7 days. Cells were harvested, washed with PBS, and RNA was extracted using Qiagen RNA Easy Plus (Qiagen; #74134). cDNA was created using qScript cDNA SuperMix (Quantabio; #95048) according to recommended cycling times and temperatures in thermocycler. qPCR was performed using PerfeCTa FastMix II (Quantabio; #95118) and TaqMan real-time probes purchased from Life Technologies: HLA-A (Hs01058806_g1), beta-2-microglobulin (Hs00187842_m1), TAP1 (Hs00388677_m1), and TAP2 (Hs00241060_m1),

Cyclin D1 (Hs00765553_m1), GAPDH (Hs02758991), Actin B (Hs99999903_m1). Data were normalized to baseline expression of GAPDH or Actin B.

Immunopurification of HLA class I ligands

HLA class I ligands (HLA-A,B and -C) were isolated as described previously.³⁸ In brief, 40 mg of Cyanogen bromide-activated-Sepharose 4B (Sigma-Aldrich, cat. # C9142) were activated with 1 mmol/L hydrochloric acid (Sigma-Aldrich, cat. # 320331) for 30 minutes. Subsequently, 0.5 mg of W6/32 antibody (Bio X Cell, BE0079; RRID: AB_1107730) was coupled to sepharose in the presence of binding buffer (150 mmol/L sodium chloride, 50 mmol/L sodium bicarbonate, pH 8.3; sodium chloride: Sigma-Aldrich, cat. # S9888, sodium bicarbonate: SigmaAldrich, cat. #S6014) for at least 2 hours at room temperature. Sepharose was blocked for 1 hour with glycine (Sigma-Aldrich, cat. # 410225). Columns were washed with PBS twice and equilibrated for 10 minutes. MCF7 and T47D breast cancer cells were treated with DMSO, 100 nmol/L Abemaciclib, or 100 nmol/L Palbociclib for seven days. Cells (1×10^7 per condition) were harvested with Cellstripper (Corning, cat. # 25-056-CI) and washed three times in ice-cold sterile PBS (Media preparation facility MSKCC). Afterward, cells were lysed in 1 mL 1% CHAPS (Sigma-Aldrich, cat. # C3023) in PBS, supplemented with 1 tablet of protease inhibitors (Complete, cat. # 11836145001) for 1 hour at 4°C. This lysate was spun down for 1 hour at 20,000 g at 4°C. Supernatant was run over the affinity column through peristaltic pumps at 1 mL/minute overnight at 4°C. Affinity columns were washed with PBS for 15 minutes, run dry, and HLA complexes subsequently eluted five times with 200 mL 1% trifluoroacetic acid (TFA, Sigma/Aldrich, cat. # 02031). For the separation of HLA ligands from their HLA complexes, tC18 columns (Sep-Pak tC18 1 cc VacCartridge, 100 mg Sorbent per Cartridge, 37–55 mm Particle Size, Waters, cat. # WAT036820) were prewashed with 80% acetonitrile (ACN, Sigma-Aldrich, cat. # 34998) in 0.1% TFA and equilibrated with two washes of 0.1% TFA. Samples were loaded, washed again with 0.1% TFA, and eluted in 400 mL 30% ACN in 0.1%TFA followed by 400 mL 40% ACN in 0.1%TFA, then 400 mL 50% ACN in 0.1%TFA. Sample volume was reduced by vacuum centrifugation for mass spectrometry analysis.¹¹

LC-MS/MS analysis of HLA ligands

Samples were analyzed by a high-resolution/high-accuracy LC-MS/MS (Lumos Fusion, Thermo Fisher). Peptides were desalted using ZipTips (Sigma Millipore; cat. #ZTC18S008) according to the manufacturer's instructions and concentrated using vacuum centrifugation prior to being separated using direct loading onto a packed-in-emitter C18 column (75 mm ID/12 cm, 3 mm particles, Nikkyo Technos Co., Ltd). The gradient was delivered at 300 nL/minute increasing linear from 2% Buffer B (0.1% formic acid in 80% acetonitrile)/98% Buffer A (0.1% formic acid) to 30% Buffer B/70% Buffer A, over 70 minutes. MS and MS/MS were operated at resolutions of 60,000 and 30,000, respectively. Only charge states 1, 2, and 3 were allowed. 1.6 Th was chosen as the isolation window and

the collision energy was set at 30%. For MS/MS, the maximum injection time was 100 ms with an AGC of 50,000.

Mass spectrometry data processing

Mass spectrometry data were processed using Byonic software (version 2.7.84, Protein Metrics) through a custom-built computer server equipped with 4 Intel Xeon E5-4620 8-core CPUs operating at 2.2 GHz, and 512 GB physical memory (Exxact Corporation). Mass accuracy for MS1 was set to 6 ppm and to 20 ppm for MS2, respectively. Digestion specificity was defined as unspecific and only precursors with charges 1, 2, and 3, and up to 2 kDa were allowed. Protein FDR was disabled to allow complete assessment of potential peptide identifications. Oxidization of methionine, N-terminal acetylation, phosphorylation of serine, threonine, and tyrosine were set as variable modifications for all samples. All samples were searched against the UniProt Human Reviewed Database (20,349 entries, <http://www.uniprot.org>, downloaded June 2017). Peptides were selected with a minimal log prob value of 2 corresponding to p -values < 0.01 for PSM in the given database and were HLA assigned by netMHC 4.0 with a 2% rank cutoff. Similar processing was performed with Mascot and PEAKS algorithm on a model leukemia cell line BV173 as it yields higher numbers of HLA ligands. Byonic demonstrated an overlap of 79.3% with Mascot (PEAKS overlapped with Mascot by 76.9%) and 84.3% with PEAKS with the highest sensitivity observed for Byonic. In T47D cells DMSO, Abemaciclib and Palbociclib samples showed an overlap between Byonic and PEAKS of 75%, 67%, and 69%, respectively. For all T47D derived HLA ligands the identity between the two algorithms was 79% (Supplementary Figure 3).

Source proteins of identified HLA ligands were divided into proteins that were identified in DMSO samples and proteins only identified in drug-treated samples. These protein lists were used for network analyses using GENEMANIA online platform.²⁰ Only physical interactions were enabled and no resultant genes were allowed. Automatically selected weighting method was used and all terms with q -values < 0.05 were considered significant.

Peptide stimulation and ELISpot assay

CD14+ monocytes were isolated from cell separation medium-purified (Fisher Scientific, Cat. Nr. 25072 Cl) PBMCs from HLA-A*02:01 healthy donors on Memorial Sloan Kettering Cancer Center (MSK) IRB-approved protocols by positive selection using mAb to human CD14 coupled with magnetic beads (Miltenyi Biotech, Cat. Nr. 130-050-201) and used for the first stimulation of T cells. The CD14- fraction of PBMCs was used for isolation of CD3 positive cells by negative immunomagnetic cell separation using a pan T cell isolation kit (Miltenyi Biotech, Cat. Nr. 130-096-535). The purity of the cells was regularly assessed in previous experiments and was always >98%. *In vitro* T cell stimulation and generation of monocyte-derived dendritic cells (DCs) from CD14+ cells was performed as previously described.¹¹ T cells were stimulated for 7 d in the presence of RPMI 1640 supplemented with 5% autologous plasma (AP), 20 ug/mL synthetic peptides, 1 ug/

mL B2-m, and 10 ng/mL IL-15. Monocyte-derived DCs were generated from CD14⁺ cells, by culturing the cells in RPMI 1640 medium supplemented with 1% AP, 500 units/mL recombinant IL-4, and 1,000 units/mL GM-CSF. On days 2 and 4 of incubation, fresh medium with IL-4 and GM-CSF was either added or replaced half of the culture medium. On day 6, maturation cytokine cocktail was added. On day 7 or 8, T cells were re-stimulated with mature DCs, with IL-15. In most cases, T cells were stimulated three times in the same manner, using either DCs or CD14⁺ cells as APCs. A week after final stimulation, the peptide-specific T cell response was examined by IFN-gamma enzyme-linked immunospot (ELISPOT) assay.

For the ELISpot assay HA-Multiscreen plates (Millipore) were coated with 100 μ L of mouse anti-human IFN-gamma antibody (10 μ g/mL; clone 1-D1K; Mabtech) in PBS, incubated overnight at 4°C, washed with PBS to remove unbound antibody, and blocked with RPMI 1640/10% autologous plasma (AP) for 2 h at 37°C. Purified CD3⁺ T cells were plated with either autologous CD14⁺ (10:1 E: APC ratio) or autologous DCs (30:1 E: APC ratio). Various test peptides were added to the wells at 20 μ g/mL. Negative control wells contained APCs and T cells without peptides or with irrelevant peptides. Positive control wells contained T cells plus APCs plus 20 μ g/mL phytohemagglutinin (PHA, Sigma). All conditions were done in triplicates. Microtiter plates were incubated for 20 h at 37°C and then extensively washed with PBS/0.05% Tween and 100 μ L/well biotinylated detection antibody against human IFN-g (2 μ g/mL; clone 7-B6-1; Mabtech) was added. Plates were incubated for an additional 2 h at 37°C and spot development was performed. Spot numbers were read and determined by Zellnet Consulting Inc.

Software and statistics

T cell recognition prediction were performed using an online tool found associated with iedb.²⁸ Only 9mer HLA ligands were considered as suggested by the inventors of the algorithm. For figure 4f mean T cell recognition scores from HLA ligands identified in the DMSO samples were calculated as baseline. Then mean T cell recognition scores were calculated for different subsets, e.g. Palbociclib unique, Palbociclib/Abemaciclib shared corresponding to Figure 2c and 2f or “G1/S phase specific” corresponding to Table 1. All calculations were initially made for each cell line separately to avoid confounding by different HLA types. Then, mean T cell recognition scores from above mentioned subsets were subtracted from DMSO baseline and results for both cell lines added to retrieve the final result. Figure 5 was created using Biorender.

Graphs except Venn diagrams were drawn with Graphpad Prism 7. For statistics built-in analyses from Graphpad Prism were used. Student's t test were used for qPCR and flow cytometry statistical analysis. Venn diagrams were prepared using the BioVenn online platform.³⁹ P values < .05 were considered significant.

Acknowledgments

We thank Alex Kentsis for access to the Byonic Software and the Proteomics Resource Center at The Rockefeller University for the performance of all LC/MS-MS experiments.

Disclosure of Potential Conflicts of Interest

D.A. Scheinberg has potential conflicts of interest, defined by *Oncoimmunology* by ownership in, income from, or research funds from: Pfizer, Sella Life Sciences, Iovance, Eureka Therapeutics, Sapience, Oncopep, Actinium, and Bristol Myers Squibb. All other authors declare no conflict of interest.

Funding

This work was supported by the Deutsche Forschungsgemeinschaft [KL3118/1-1]; Doris Duke Charitable Foundation [1]; National Institutes of Health [P30 CA008748]; National Institutes of Health [R35 CA241894]

ORCID

Christopher M. Bourne  <http://orcid.org/0000-0001-9290-4223>

Author's Contributions

A.C., C.M.B. Z.E.H.A., S.S.M., T.K., and M.G.K., performed and analyzed experiments. M.G.K. and D.A.S. designed experiments. A.C., C.M.B., and M.G.K. wrote the original draft of the manuscript. T.D., M.G.K. and D.A. S. supervised the project. D.A.S. provided funding and edited the manuscript. All authors reviewed and contributed to the manuscript.

Data availability

Mass spectrometry data have been deposited at the PRIDE archive with the dataset identifier PXD024965.

References

1. Fox P, Darley A, Furlong E, Miaskowski C, Patiraki E, Armes J, Ream E, Papadopoulou C, McCann L, Kearney N, et al. The assessment and management of chemotherapy-related toxicities in patients with breast cancer, colorectal cancer, and Hodgkin's and non-Hodgkin's lymphomas: a scoping review [Internet]. *Eur J Oncol Nurs*. 2017;26:63–82. doi:10.1016/j.ejon.2016.12.008.
2. Plummer C, Steingart RM, Jurczak W, Iakobishvili Z, Lyon AR, Plataras JP, Minotti G. Treatment specific toxicities: hormones, antihormones, radiation therapy. *Semin Oncol*. 2019;46(6):414–420. doi:10.1053/j.seminoncol.2019.01.006.
3. Sharpe AH, Pauken KE. The diverse functions of the PD1 inhibitory pathway [Internet]. *Nat Rev Immunol*. 2018;18(3):153–167. doi:10.1038/nri.2017.108.
4. Ribas A, Wolchok JD. Cancer immunotherapy using checkpoint blockade. *Science*. 2018;359:1350–1355.
5. Yin L, Dai S, Clayton G, Gao W, Wang Y, Kappler J, Marrack P. Recognition of self and altered self by T cells in autoimmunity and allergy. *Protein Cell*. 2013;4(1):8–16. doi:10.1007/s13238-012-2077-7.
6. Schumacher TN, Schreiber RD. Neoantigens in cancer immunotherapy. *Science*. 2015;348(6230):69–74. doi:10.1126/science.aaa4971.
7. Dubrovsky L, Dao T, Gejman RS, Brea EJ, Chang AY, Oh CY, Casey E, Pankov D, Scheinberg DA. T cell receptor mimic

- antibodies for cancer therapy. *Oncoimmunology*. 2016;5(1): e1049803. doi:10.1080/2162402X.2015.1049803.
8. Chandran SS, Klebanoff CA. T cell receptor-based cancer immunotherapy: emerging efficacy and pathways of resistance. *Immunol Rev*. 2019;290:127–147. doi:10.1111/immr.12772.
 9. Chang AY, Gejman RS, Brea EJ, Oh CY, Mathias MD, Pankov D, Casey E, Dao T, Scheinberg DA. Opportunities and challenges for TCR mimic antibodies in cancer therapy. *Expert Opin Biol Ther*. 2016;16(8):979–987. doi:10.1080/14712598.2016.1176138.
 10. Brea EJ, Oh CY, Manchado E, Budhu S, Gejman RS, Mo G, Mondello P, Han JE, Jarvis CA, Ulmert D, et al. Kinase regulation of human MHC class I molecule expression on cancer cells. *Cancer Immunol Res*. 2016;4(11):936–947. doi:10.1158/2326-6066.CCR-16-0177.
 11. Oh CY, Klatt MG, Bourne C, Dao T, Dacek MM, Brea EJ, Mun SS, Chang AY, Korontsvit T, Scheinberg DA, et al. ALK and RET inhibitors promote HLA class I antigen presentation and unmask new antigens within the tumor immunopeptidome. *Cancer Immunol Res*. 2019;7(12):1984–1997. doi:10.1158/2326-6066.CCR-19-0056.
 12. Planes-Laine G, Rochigneux P, Bertucci F, Chrétien A-S, Viens P, Sabatier R, et al. PD-1/PD-L1 targeting in breast cancer: the first clinical evidences are emerging: a literature review. *Cancers* [Internet]. 2019;11:1033. doi:10.3390/cancers11071033.
 13. Goel S, DeCristo MJ, Watt AC, BrinJones H, Sceney J, Li BB, Khan N, Ubellackker JM, Xie S, Metzger-Filho O, Hoog J, et al. CDK4/6 inhibition triggers anti-tumour immunity. *Nature*. 2017;548(7668):471–475. doi:10.1038/nature23465.
 14. Schaer DA, Beckmann RP, Dempsey JA, Huber L, Forest A, Amaladas N, Li Y, Wang YC, Rasmussen ER, Chin D, et al. The CDK4/6 inhibitor abemaciclib induces a T cell inflamed tumor microenvironment and enhances the efficacy of PD-L1 checkpoint blockade. *Cell Rep*. 2018;22(11):2978–2994. doi:10.1016/j.celrep.2018.02.053.
 15. Stopfer LE, Mesfin JM, Joughin BA, Lauffenburger DA, White FM. Multiplexed relative and absolute quantitative immunopeptidomics reveals MHC I repertoire alterations induced by CDK4/6 inhibition. *Nat Commun*. 2020;11(1):2760. doi:10.1038/s41467-020-16588-9.
 16. Pernas S, Tolaney SM, Winer EP, Goel S. CDK4/6 inhibition in breast cancer: current practice and future directions. *Ther Adv Med Oncol*. 2018;10:1758835918786451. doi:10.1177/1758835918786451.
 17. Jurtz V, Paul S, Andreatta M, Marcatili P, Peters B, Nielsen M. NetMHCpan-4.0: improved peptide-MHC class I interaction predictions integrating eluted ligand and peptide binding affinity data. *J Immunol*. 2017;199(9):3360–3368. doi:10.4049/jimmunol.1700893.
 18. Rozanov DV, Rozanov ND, Chiotti KE, Reddy A, Wilmarth PA, David LL, Cha SW, Woo S, Pevzner P, Bafna V, et al. MHC class I loaded ligands from breast cancer cell lines: a potential HLA-I-typed antigen collection. *J Proteomics*. 2018;176:13–23. doi:10.1016/j.jprot.2018.01.004.
 19. Klatt MG, Aretz ZEH, Curcio M, Gejman RS, Jones HF, Scheinberg DA. An input-controlled model system for identification of MHC bound peptides enabling laboratory comparisons of immunopeptidome experiments. *J Proteomics*. 2020;228:103921. doi:10.1016/j.jprot.2020.103921.
 20. Warde-Farley D, Donaldson SL, Comes O, Zuberi K, Badrawi R, Chao P, Franz M, Grouios C, Kazi F, Lopes CT, et al. The GeneMANIA prediction server: biological network integration for gene prioritization and predicting gene function. *Nucleic Acids Res*. 2010;38(Web Server issue):W214–20. doi:10.1093/nar/gkq537.
 21. Marcu A, Bichmann L, Kuchenbecker L, Backert L, Kowalewski DJ, Freudenmann LK, et al. The HLA Ligand Atlas. A resource of natural HLA ligands presented on benign tissues [Internet]. bioRxiv. 2019. 778944. [cited 2020 Apr 18]. Available from: <https://www.biorxiv.org/content/10.1101/778944v1>
 22. Chen J, Zurawski G, Zurawski S, Wang Z, Akagawa K, Oh S, Hideki U, Fay J, Banchemereau J, Song W, Palucka AK, et al. A novel vaccine for mantle cell lymphoma based on targeting cyclin D1 to dendritic cells via CD40. *J Hematol Oncol*. 2015;8(1):35. doi:10.1186/s13045-015-0131-7.
 23. Wang M, Sun L, Qian J, Han X, Zhang L, Lin P, Cai Z, Yi Q. Cyclin D1 as a universally expressed mantle cell lymphoma-associated tumor antigen for immunotherapy. *Leukemia*. 2009;23(7):1320–1328. doi:10.1038/leu.2009.19.
 24. Von Bergwelt-baldon MS, Shimabukuro-Vornhagen A, Wendtner CM, Kondo E. Identification of native, immunogenic peptides from cyclin D1. *Leukemia*. 2010;24(1):209–211. doi:10.1038/leu.2009.184.
 25. Dao T, Korontsvit T, Zakhaleva V, Haro K, Packin J, Scheinberg DA. Identification of a human cyclin D1-derived peptide that induces human cytotoxic CD4 T cells. *Plos One*. 2009;4(8):e6730. doi:10.1371/journal.pone.0006730.
 26. Vijayaraghavan S, Karakas C, Doostan I, Chen X, Bui T, Yi M, Raghavendra AS, Zhao Y, Bashour SI, Ibrahim NK, et al. CDK4/6 and autophagy inhibitors synergistically induce senescence in Rb positive cytoplasmic cyclin E negative cancers. *Nat Commun*. 2017;8(1):15916. doi:10.1038/ncomms15916.
 27. Scott SC, Lee SS, Abraham J. Mechanisms of therapeutic CDK4/6 inhibition in breast cancer. *Semin Oncol*. 2017;44:385–394. doi:10.1053/j.seminoncol.2018.01.006.
 28. Chen SH, Gong X, Zhang Y, Van Horn RD, Yin T, Huber L, Burke TF, Manro J, Iversen PW, Wu W, et al. RAF inhibitor LY3009120 sensitizes RAS or BRAF mutant cancer to CDK4/6 inhibition by abemaciclib via superior inhibition of phospho-RB and suppression of cyclin D1. *Oncogene*. 2018;37(6):821–832. doi:10.1038/ncr.2017.384.
 29. Calis JJ, Maybeno M, Greenbaum JA, Weiskopf D, De Silva AD, Sette A, Keşmir C, Peters B. Properties of MHC class I presented peptides that enhance immunogenicity. *PLoS Comput Biol*. 2013;9(10):e1003266. doi:10.1371/journal.pcbi.1003266.
 30. Vaddepally RK, Kharal P, Pandey R, Garje R, Chandra AB. Review of indications of FDA-approved immune checkpoint inhibitors per NCCN guidelines with the level of evidence. *Cancers* [Internet]. 2020;12(3):738. <http://dx.doi.org/10.3390/cancers12030738>
 31. Gejman RS, Chang AY, Jones HF, DiKun K, Hakimi AA, Schietinger A, Scheinberg DA. Rejection of immunogenic tumor clones is limited by clonal fraction. *Elife* [Internet]. 2018;7. <http://dx.doi.org/10.7554/eLife.41090>.
 32. Wolf Y, Bartok O, Patkar S, Eli GB, Cohen S, Litchfield K, Levy R, Jiménez-Sánchez A, Trabish S, Lee JS, et al. UVB-induced tumor heterogeneity diminishes immune response in melanoma. *Cell*. 2019;179(1):219–35.e21. doi:10.1016/j.cell.2019.08.032.
 33. Heemskerk B, Liu K, Dudley ME, Johnson LA, Kaiser A, Downey S, Zheng Z, Shelton TE, Matsuda K, Robbins PF, et al. Adoptive cell therapy for patients with melanoma, using tumor-infiltrating lymphocytes genetically engineered to secrete interleukin-2. *Hum Gene Ther*. 2008;19(5):496–510. doi:10.1089/hum.2007.0171.
 34. Rafiq S, Purdon TJ, Daniyan AF, Koneru M, Dao T, Liu C, Scheinberg DA, Brentjens RJ. Optimized T-cell receptor-mimic chimeric antigen receptor T cells directed toward the intracellular Wilms Tumor 1 antigen. *Leukemia*. 2017;31(8):1788–1797. doi:10.1038/leu.2016.373.
 35. Amor C, Feucht J, Leibold J, Ho YJ, Zhu C, Alonso-Curbelo D, Mansilla-Soto J, Boyer JA, Li X, Giavridis T, et al. Senolytic CAR T cells reverse senescence-associated pathologies. *Nature*. 2020;583(7814):127–132. doi:10.1038/s41586-020-2403-9.
 36. Zhao Z-M, Yost SE, Hutchinson KE, Li SM, Yuan Y-C, Noorbakhsh J, Liu Z, Warden C, Johnson RM, Wu X, et al. CCNE1 amplification is associated with poor prognosis in patients with triple negative breast cancer. *BMC Cancer*. 2019;19(1):96. doi:10.1186/s12885-019-5290-4.

37. Choo JR-E, Lee S-C. CDK4-6 inhibitors in breast cancer: current status and future development. *Expert Opin Drug Metab Toxicol.* 2018;14:1123-1138. doi:10.1080/17425255.2018.1541347.
38. Klatt MG, Mack KN, Bai Y, Aretz ZE, Nathan LI, Mun SS, Dao T, Scheinberg DA. Solving an MHC allele specific bias in the reported immunopeptidome. *JCI Insight.* 2020. doi:10.1172/jci.insight.141264.
39. Hulsen T, De Vlieg J, Alkema W. Biovenn – a web application for the comparison and visualization of biological lists using area-proportional Venn diagrams. *BMC Genomics.* 2008;9(1):488. doi:10.1186/1471-2164-9-488.

2.4. Entwicklung einer tumoragnostischen TZR-imitierenden CAR-T-Zelle

Originalarbeit 5

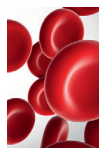
Klatt MG, Dao T, Yang Z, Liu J, Mun SS, Dacek MM, Luo H, Gardner TJ, Bourne C, Peraro L, Aretz ZEH, Korontsvit T, Lau M, Kharas MG, Liu C, Scheinberg DA. A TCR mimic CAR T cell specific for NDC80 is broadly reactive with solid tumors and hematologic malignancies. *Blood*. 2022;140(8):861-874.

Die Verbindung der Erkenntnisse der bisherigen Arbeiten mündete schließlich in diese abschließende Publikation, in welcher das Ziel in der Entwicklung einer TZR-imitierenden CAR-T-Zelle bestand, deren Target durch die Analyse von Immunpeptidomen unterschiedlicher Tumorentitäten definiert wurde. Zusätzlich sind konventionelle CAR-T-Zell-Therapien aufgrund der begrenzten Verfügbarkeit von krebsspezifischen Zelloberflächenproteinen nur schwer auf ein breites Spektrum von Krebsarten anwendbar. Ein intrazelluläres tumoragnostisches Target zu definieren und dieses mittels einer TZR-imitierenden CAR-T-Zelle anzugreifen, stellt insbesondere für nicht-immunogene HLA Liganden einen neuen Therapieansatz dar.

Die Immunpeptidome von acht unterschiedlichen hämatologischen und nicht-hämatologischen Neoplasien wiesen all das HLA-A*02 restringierte Targetpeptid ALNEQIARL auf, welches aus dem Kinetochor-assoziierten Protein NDC80 stammt. Zusätzlich ließ sich das entsprechende Peptid nur in gesundem Knochenmark und Ovarien nachweisen, was aus unserer Sicht zu tolerabler Toxizität führen würde.

Mittels einer Phagenbibliothek wurde ein single chain variable fragment (scFv) isoliert, welches gute Sensitivität und Spezifität gegen das Zielpeptid aufwies. Darüber hinaus war eine mit diesem scFv generierte TZR-imitierende CAR-T-Zelle dazu in der Lage mehrere Tumorzelllinien hochspezifisch und effizient abzutöten. Insbesondere wurde keine relevante Toxizität gegenüber Knochenmarkszellen aus Nabelschnurblut, aktivierten T-Zellen oder Zellen des Herzens beobachtet. Auch die Testung für möglich off-Targets erbrachte keine relevanten Hinweise auf eine zu befürchtende Toxizität. Schließlich konnte diese Arbeit in zwei Mausmodellen für akute lymphatische Leukämie sowie für ein Mesotheliom die Tumorlast signifikant gegenüber Kontroll-CAR-T-Zellen kontrollieren und das Überleben verlängern.

Insgesamt zeigte diese Arbeit in sehr stringenter Weise die effektive Definition eines Targets für eine T-Zell basierte Immuntherapie mittels Massenspektrometrie und wie dieses Wissen dann systematisch in die Entwicklung der entsprechenden Therapie einfließen kann. Die hohe Sensitivität und Spezifität dieses Konstrukts unterstreicht dabei die Robustheit dieser Herangehensweise, welche sich inzwischen auch in anderen Projekten sehr bewährt hat. Zusätzlich evaluieren wir in laufenden Projekten die pharmakologische Modulation des Zielpeptides zur Optimierung dieser Therapie.



IMMUNOBIOLOGY AND IMMUNOTHERAPY

A TCR mimic CAR T cell specific for NDC80 is broadly reactive with solid tumors and hematologic malignancies

Martin G. Klatt,¹ Tao Dao,¹ Zhiyuan Yang,² Jianying Liu,² Sung Soo Mun,¹ Megan M. Dacek,¹ Hanzhi Luo,¹ Thomas J. Gardner,¹ Christopher Bourne,^{1,3} Leila Peraro,¹ Zita E. H. Aretz,^{1,4} Tanya Korontsvit,¹ Michael Lau,⁵ Michael G. Kharas,¹ Cheng Liu,² and David A. Scheinberg^{1,6}

¹Molecular Pharmacology Program, Sloan Kettering Institute, New York, NY; ²Eureka Therapeutics, Emeryville, CA; ³Immunology and Microbial Pathogenesis Program and ⁴Physiology, Biophysics and Systems Biology Program, Weill Cornell Medicine, New York, NY; ⁵Department of Pediatrics, Memorial Sloan Kettering Cancer Center, New York, NY; and ⁶Pharmacology Program, Weill Cornell Medicine, New York, NY

KEY POINTS

- HLA-A*02:ALNEQIARL derived from NDC80 is a broadly presented cancer immunotherapy target with high abundance in hematologic malignancies.
- CAR T cells designed for this target exhibit high sensitivity and specificity with no relevant toxicity toward hematopoietic stem cells.

Target identification for chimeric antigen receptor (CAR) T-cell therapies remains challenging due to the limited repertoire of tumor-specific surface proteins. Intracellular proteins presented in the context of cell surface HLA provide a wide pool of potential antigens targetable through T-cell receptor mimic antibodies. Mass spectrometry (MS) of HLA ligands from 8 hematologic and nonhematologic cancer cell lines identified a shared, non-immunogenic, HLA-A*02-restricted ligand (ALNEQIARL) derived from the kinetochore-associated NDC80 gene. CAR T cells directed against the ALNEQIARL:HLA-A*02 complex exhibited high sensitivity and specificity for recognition and killing of multiple cancer types, especially those of hematologic origin, and were efficacious in mouse models against a human leukemia and a solid tumor. In contrast, no toxicities toward resting or activated healthy leukocytes as well as hematopoietic stem cells were observed. This shows how MS can inform the design of broadly reactive therapeutic T-cell receptor mimic CAR T-cell therapies that can target multiple cancer types currently not druggable by small molecules, conventional CAR T cells, T cells, or antibodies.

Introduction

Chimeric antigen receptor (CAR) T cells are immunotherapies approved by the US Food and Drug Administration that have shown remarkable results in patients with hematologic cancers.^{1,2} However, CAR T-cell products are currently only approved for a small subset of cancer patients because a major limitation in the design of new CAR T-cell candidates is the lack of known cancer-specific cell surface proteins that will provide high sensitivity with limited toxicity to normal tissues.³ Although target identification for CAR T cells against other malignancies seems feasible,^{4,5} even highly evolved screening strategies cannot always provide single tumor-specific antigens.⁶ In addition, these target identification strategies are typically designed for a single cancer type, offering few options for a highly desirable, broadly usable, tumor-agnostic approach.

We hypothesized that intracellular proteins that are degraded through the proteasome and presented as peptides on HLA class I molecules can be a valuable source to identify more broadly presented antigens enabling a tumor-agnostic target strategy. Traditionally, such peptide:HLA class I complexes are recognized by T cells through their T-cell receptor (TCR),

but as a consequence of thymic selection, self-antigens cannot typically be recognized by TCR T cells.⁷ In contrast, TCR mimic antibodies offer the unique opportunity to specifically target peptide:HLA complexes in a manner comparable to that of TCRs but independent of the immunogenicity of the presented HLA ligand. Furthermore, TCR mimic antibodies with their respective single-chain variable fragments (scFvs) can be engineered into multiple therapeutic formats, including CAR T cells, which have been proven effective against several targets.⁸⁻¹⁷

To identify an HLA-A*02-bound peptide present in multiple cancer types, we affinity-purified peptide:HLA complexes from different cancer cell lines with varying HLA-A*02 abundances and performed liquid chromatography-tandem mass spectrometry (LC-MS/MS) to identify the eluted peptide sequences. Network analyses of source proteins from which the HLA ligands were derived, and identification of shared biological functions between the cell lines,¹⁸ facilitated the selection of a suitable HLA ligand candidate. This candidate was ALNEQIARL from the “kinetochore NDC80 protein homolog” (referred to as NDC80), an essential and highly expressed protein in tumors, especially within poor prognosis subgroups.¹⁹⁻²¹

We discovered a TCR mimic scFv (NDC80-clC) that specifically recognized the ALNEQIARL:HLA-A*02 complex and engineered it into a second-generation CAR T-cell format. We describe here the *in vitro* killing of NDC80-clC CAR T cells against multiple cancer cell lines in a peptide- and HLA-specific manner. Moreover, these CAR T cells suppressed tumor growth and prolonged survival in a hematologic and nonhematologic mouse model while sparing stimulated and unstimulated healthy A*02-positive blood leukocytes, fibroblasts, and cardiomyocytes, as well as hematopoietic stem cells (HSCs) *in vitro*. Overall, our study shows how non-immunogenic peptide:HLA complexes can be an invaluable source for tumor-specific antigens that are undruggable by conventional therapeutic approaches. The NDC80-clC CAR T cell is a candidate for development into a tumor-agnostic drug capable of targeting highly proliferative HLA-A*02-positive cancer cells such as leukemias or aggressive lymphomas.

Materials and methods

Immunopurification and LC-MS/MS analysis of HLA class I ligands

HLA class I ligands were isolated as described previously.^{22,23} W6/32 (Bio X Cell, BE0079; RRID: AB_1107730), BB7.2 (MSKCC Antibody Core Facility), or clone C or murine immunoglobulin G1 (migG1; Eureka Therapeutics) antibody was used for respective experiments.

scFv clones specific for peptide/HLA-A0201 complexes

A human scFv antibody E-ALPHA phage display library was used for the selection of monoclonal antibody clones specific to ALNEQIARL:HLA-A*02 as described previously.¹⁴ In brief, T2 cells pulsed with 50 µg/mL irrelevant control peptides were used to remove any clones that potentially bind to HLA-A*02:01 in the library. Remaining clones were screened for T2 cells pulsed with 50 µg/mL ALNEQIARL peptides. Positive clones were determined by their binding to T2 cells pulsed with ALNEQIARL peptides but not to T2 cells pulsed with control peptides by flow cytometry.

Generation of NDC80-CAR T cells

scFvs were grafted onto a second-generation CAR with CD28 and CD3ζ signaling domains engineered *in cis* to provide intracellular T-cell stimulation signals. The CAR sequence was cloned into a pCDH lentiviral vector (Systems Biosciences) for delivery into T cells. Human T cells were activated with CD3/CD28 Dynabeads (Thermo Fisher Scientific; 11-161-D). One day after activation, human T cells were transduced with concentrated lentivirus in plates coated with RetroNectin (Takara). Transduced T cells were then expanded in the presence of 100 U/mL interleukin-2 (Sigma) for 8 to 12 days. Transduction efficiency was assessed by direct staining using anti-myc clone 71D10-Al647 (Cell Signaling; #63730).

Animals and *in vivo* models

Eight- to 10-week-old NOD.Cg-Prkdc^{scid} IL2rg^{tm1Wj}/SzJ mice (NSG) were purchased from The Jackson Laboratory. Female mice were used for all experiments. For the BV173 model, mice were injected first with 1 million BV173 cells and after 5 days with phosphate-buffered saline, 2 million 4H11 CAR T cells, or

2 million NDC80-clC CAR T cells (8 days after transduction) via tail vein. Starting with day 14, we cheek bled mice and stained the samples for HLA-A*02 as well as murine CD45 to determine the fraction of blast cells in the peripheral blood. For the JMN model, mice were injected intraperitoneally with 300 000 GFP-Luc-transduced JMN cells. Tumor burden was assessed by bioluminescence imaging twice per week before treatment and then after injection of 150 000 NDC80-clC CAR T cells, 4H11 CAR T cells, or phosphate-buffered saline.

Additional and more detailed methods are presented in the supplemental Materials and Methods (available on the *Blood* Web site).

Results

LC-MS/MS analysis defines the NDC80-derived peptide ALNEQIARL as a highly tumor-associated HLA-A*02 ligand

To discover a tumor-associated HLA-A*02-restricted HLA ligand, we immunopurified HLA complexes from 4 hematologic cancer cell lines (BV173, OCI-AML02, SUDHL6, and MAC2A) and 4 nonhematologic cancer cell lines (JMN, TPC-1, MDA-MB231, and PANC-1) and analyzed the immunopeptidome of the complexes via LC-MS/MS (Figure 1A). We identified >11 000 unique HLA class I-assigned peptides, of which 3289 were considered HLA-A*02:01 binders (supplemental Table 1). Using source proteins from which the HLA ligands were derived (supplemental Table 2), we performed network analyses via the GeneMANIA algorithm through a Cytoscape plugin.²⁴ Of 923 Gene Ontology terms resulting from the analyses of the 8 different cell lines, only 3 processes were shared among all lines: kinetochore, chromosome centromeric region, and protein DNA complex. Finally, from all the proteins involved in these 3 Gene Ontology terms, only peptides from the NDC80 protein were presented in all 8 cell lines. Similarly, three HLA-A*02-restricted HLA ligands from NDC80 were detected at the cell surface (ALNEQIARL, GLNEEIARV, and HLEEQIAKV), but only the ALNEQIARL peptide ligand was shared between all the tested cancer lines. Of note, although the HLA ligand GLNEEIARV also exhibited high presentation frequency (7 of 8 cell lines), we considered it a less suitable candidate because public immunopeptidome data from healthy human tissues showed that the GLNEEIARV ligand was presented in multiple essential healthy tissues, including lung, esophagus, ovary, uterus, cerebellum, and colon.²⁵ In the same study, the ALNEQIARL peptide was only detected in ovary, thymus, and bone marrow, which we considered potentially acceptable off-tumor targets; these reactivities were investigated later in this study.

Encouragingly, NDC80 is overexpressed in a plethora of different cancer types, especially within subgroups with a poor prognosis.¹⁹⁻²¹ To underline its strong tumor association, we retrieved expression data from 934 cancer cell lines from the Cancer Cell Line Encyclopedia²⁶ and calculated mean transcripts per million (TPM) for all cancer types in which ≥5 cell lines were available (Figure 1B). These mean TPM were significantly higher compared with the NDC80 expression levels of the corresponding healthy tissues published by the GTEx consortium²⁷ (Figure 1C; supplemental Figure 1A). However, because cancer cell lines are preselected for high proliferation capacity, we

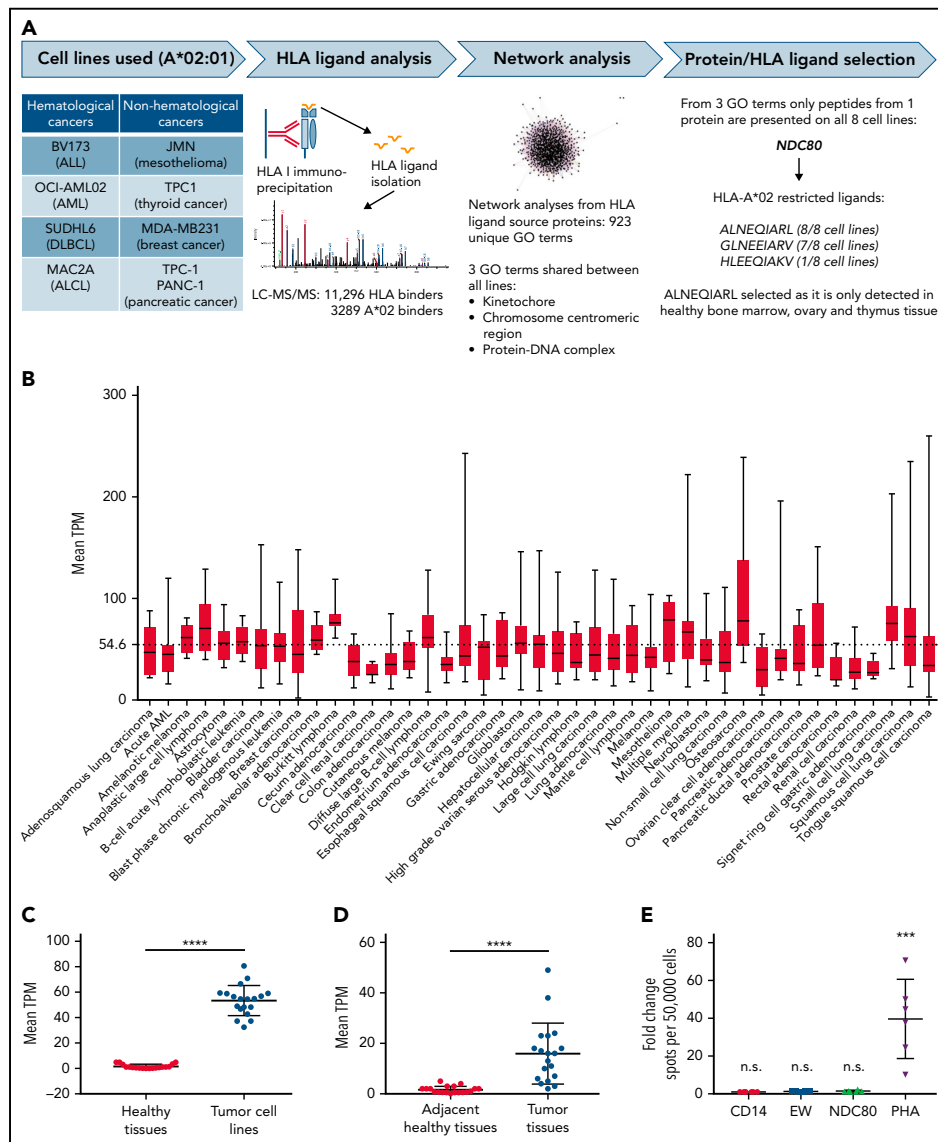


Figure 1. Identification of the NDC80-derived ALNEQIARL peptide as a tumor-associated HLA ligand. (A) Experimental strategy. (B) Mean *NDC80* expression levels in different cancer cell lines. Only cancer types with at least 5 data points were considered. Whiskers indicate minimum to maximum. (C) Mean *NDC80* expression of healthy tissues and corresponding cancer cell lines. (D) Mean *NDC80* expression of adjacent healthy tissues and corresponding primary cancer tissues. (E) ELISpot results from 3 healthy donors and 2 biological replicates per donor. Data were normalized to results from CD14⁺ cells alone. EW served as control peptide. Error bars in panels C, D, and E denote standard deviation. *****P* < .001 (Mann-Whitney test), *****P* < .0001 (Wilcoxon matched-pairs signed-rank test). ALCL, anaplastic large cell lymphoma; ALL, acute lymphoblastic leukemia; DLBCL, diffuse large B-cell lymphoma; GO, Gene Ontology; EW, Ewing sarcoma-derived HLA-A0201-binding peptide; EW, QLQNPYSYDK; PHA, phytohemagglutinin.

additionally analyzed data from cancer tissues and matched adjacent healthy tissues from the PCAWG (Pan-Cancer Analysis of Whole Genomes) project²⁸ and found a similar, highly significant overexpression of NDC80 (Figure 1D; supplemental Figure 1B). Of note, NDC80 overexpression reached up to 1300-fold in glioblastoma and astrocytoma cell lines vs healthy brain tissue and >100-fold for pancreatic adenocarcinoma vs adjacent healthy tissue (supplemental Figure 1C-D). Nevertheless, the mean TPM of NDC80 in cancer cell lines was significantly higher compared with that of cancer tissues, suggesting an artificial enhancement in the cancer cell lines (supplemental Figure 1E). In line with this broad and high expression of NDC80 in cancer cells, a literature search for MS identification of NDC80 peptides and testing of additional cell lines and primary tissues via MS in our laboratory (>90% positivity rate for A*02-positive cell lines) confirmed the frequent presentation of the ALNEQIARL peptide on the cell surface (Table 1).

Furthermore, we investigated 12 publicly available pairs of colorectal carcinoma (CRC) and nonmalignant colon (NMC) samples for a quantitative comparison of HLA ligand presentation.²⁹ Using Skyline software (MacCoss Lab Software; version 21.1) and the known retention times from successful MS/MS identifications, we calculated absolute and relative precursor intensities in these paired data sets that were normalized for equal peptide yields before acquisition. However, we note that even for unsuccessful MS/MS identifications, these intensities have been calculated to reflect baseline intensities; we assume in these instances, however, that the peptide is not presented at the surface. Using this approach, we observed significantly higher average intensities in the CRC compared with the NMC samples (supplemental Figure 2A). In 7 of 12 matched samples, the

relative intensities between CRC and NMC for our target peptide were 3- to 90-fold higher (supplemental Figure 2B).

Finally, to investigate whether the ALNEQIARL ligand could also be targeted by a human TCR-directed T cell, we tested T-cell reactivity in healthy A*02-positive blood donors. No reactivity was detected in several donors after multiple stimulations in line with previous published results (Figure 1E). Although the cited publication²⁹ described one successful attempt to prime T cells with this peptide, preexisting T-cell responses in 17 cancer patients or 15 healthy donors were not observed. Overall, these data suggest that the human immune system is largely tolerant to ALNEQIARL and that this peptide is a highly tumor-associated HLA ligand, which ideally could be targeted by a TCR mimic-based strategy.

Phage library screen identifies an ALNEQIARL:HLA-A*02-reactive clone

We used an established phage library screening platform (E-ALPHA Phage Display, Eureka Therapeutics; diversity, 1×10^{11} clones) comprising both naive and semisynthetic human scFv B-cell antibodies to select clones reactive with the ALNEQIARL:HLA-A*02 complex (Figure 2A). First, the library was screened for clones that selectively bound T2 cells pulsed with the ALNEQIARL peptide but not T2 cells pulsed with a mixture of 20 irrelevant endogenous HLA-A2 peptides derived from various disease-related and housekeeping proteins. After 3 rounds of panning to ALNEQIARL:HLA-A*02 complex, 347 positive clones were identified by using flow cytometry, which correspond to 60 unique clones by sequence. These 60 unique clones were further screened for selectively binding to T2 cells pulsed with the ALNEQIARL peptide but not T2 cells pulsed with 4 homologous peptides (ALNEKLVNL, ALNELLQHV, MLANDIARL, and TLADIARL)

Table 1. MS evidence of HLA-A*02:ALNEQIARL in cell lines and primary tissue samples

Tumor type	Cell line	Primary tissue	References
Hematologic malignancies			
AML	AML14, OCI-AML02, THP-1	Yes	39; authors' own data for cell lines and primary samples
B-ALL	JY, BV173, Nalm6, ALL-3	Yes	40-42
Multiple myeloma	U266	NT	Authors' own data
DLBCL	DB, SUDHL4	NT	Authors' own data
T-cell lymphoma	MAC2A	NT	Authors' own data
MCL	—	Yes	43
Nonhematologic malignancies			
Melanoma	A375, SKMEL5, MEWO, MEL624	Yes	44-47
Breast cancer	MDA-MB231	Yes	48; authors' own data for cells and primary tissue
Colon cancer	—	Yes	29
Prostate cancer	LnCAP	NT	Authors' own data
Pancreatic cancer	PANC-1	NT	Authors' own data
Thyroid cancer	TPC-1	NT	Authors' own data
Mesothelioma	JMN, MESO37	NT	Authors' own data
Glioblastoma	—	Yes	49

B-ALL, B-cell acute lymphoblastic leukemia; DLBCL, diffuse large B-cell lymphoma; MCL, myeloid cell leukemia; NT, not tested.

from widely expressed proteins (EIF3F, TLN1, EHD1, and NYNR1), which have been identified in our MS experiments as well as multiple healthy tissues.²⁵ Using this approach, we aimed to avoid cross-reactivity with these peptides and to ensure binding of the

scFvs to central amino acid positions #3 to #8. Ultimately, 6 clones (ie, clones A-F) (supplemental Figure 3A) were selected based on these binding data and engineered into lentiviral second-generation CAR T-cell constructs.

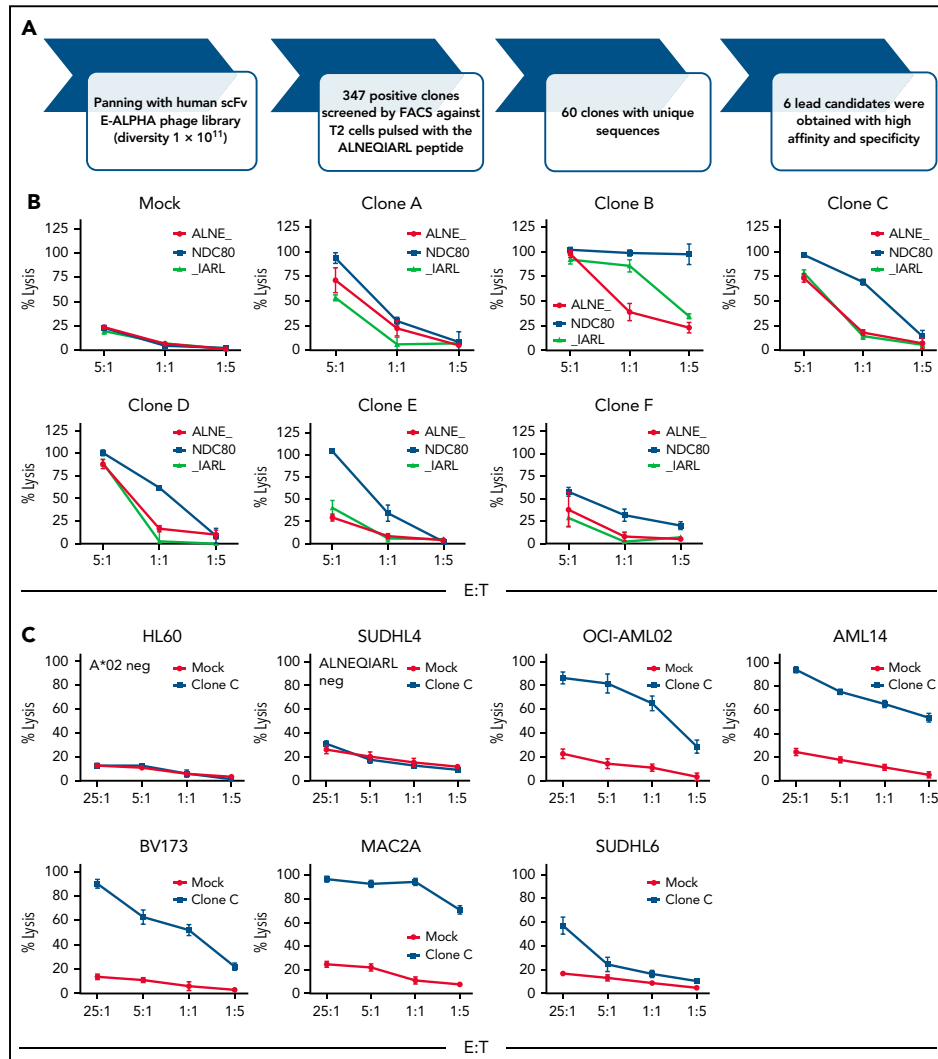


Figure 2. Phage library screen discovers an ALNEQIARL-specific scFv with efficacy against various cancer cell lines in CAR T-cell format. (A) Phage library screen procedure. (B) Characterization of six NDC80 CAR T-cell clones (ie, A-F) against peptide pulsed T2 cells. (C) Efficacy and specificity of NDC80-clC CAR T cells against hematologic cancer cell lines. (D) Efficacy and specificity of NDC80-clC CAR T cells against nonhematologic cancer cell lines. Error bars in panels B through D denote standard deviation. FACS, fluorescence-activated cell sorter; E:T, effector-to-target ratio.

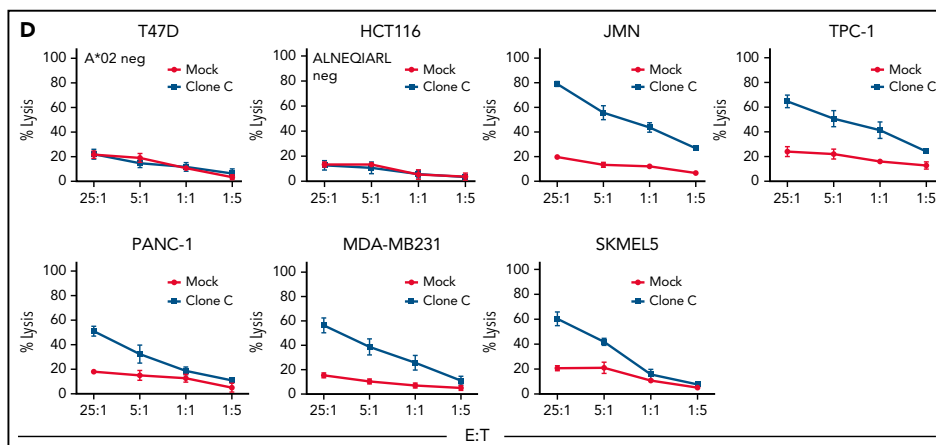


Figure 2 (continued)

CAR T cells were generated with high efficiency for clones A to F (supplemental Figure 3B). Then, killing against T2 cells pulsed with either the target peptide ALNEQIARL or control peptides ALNEKLVNL and MLANDIARL was assessed (Figure 2B). Clones A, B, and D were sorted out due to cross-reactivity toward either the ALNEKLVNL peptide (clones A and D) or the MLANDIARL peptide (clone B). Although also showing some reactivity to the ALNEKLVNL peptide, clone F was not considered further due to lower reactivity toward the target peptide. These decisions were mostly made based on the data points with an effector-to-target ratio of 1:1 and the areas under the curve, as the 5:1 setting generally led to substantial killing in most of the clone/peptide combinations. Therefore, clones C and E proceeded to additional evaluation.

We selected 7 cell lines each from hematologic and non-hematologic origin and HLA type based on MS data and HLA type (Table 2). Of note, 5 of the cell lines in each group were ALNEQIARL:HLA-A*02 positive, one in each group was HLA-A*02 positive but negative by MS for ALNEQIARL (SUDHL4 and HCT116), and one cell line each was negative for both HLA-A*02 and the target peptide (HL60 and T47D). Strikingly, clone C (NDC80-clC) CAR T cells were able to kill all cell lines in a dose-dependent and target-specific manner (Figure 2C-D). In contrast, clone E (NDC80-clE), although also showing the same high specificity, exhibited much lower efficacy compared with NDC80-clC (supplemental Figure 4A-B). Both clones exhibited more effective killing against cell lines of hematologic origin, probably due to higher antigen density of HLA-A*02 molecules on the cell surface (supplemental Figure 4C). This hypothesis was also supported by the observation that after engineering scFv clone C into a murine IgG1 format, binding against cancer cell lines by flow cytometry was only observed for cell lines of very high antigen density (eg, BV173, AML14, or MAC2A) (supplemental Figure 4D) but not for nonhematologic cell lines. IgG binding to some cell lines allowed an estimate of target complexes on a per-cell level using quantitation beads: 503 sites

per cell on MAC2A cells, 876 sites per cell on AML14 cells, and 1356 sites on BV173 cells. Taken together, these data illustrated high sensitivity of the NDC80-clC CAR T cells toward multiple cancer cell lines independent of their cancer type. However, as we showed earlier, primary tissues have, on average, lower levels of NDC80; we thus now wanted to test the ability of NDC80-clC CAR T cells to eliminate patient-derived HLA-A*02-positive or -negative but CD33-positive (PDX) acute myeloid leukemia (AML) cells in vitro (supplemental Figure 5A). Target cells were labeled with carboxyfluorescein diacetate succinimidyl ester (CFSE) and after 24 hours of coincubation with either MOCK-transduced T cells or NDC80-clC CAR T cells at an effector-to-target ratio of 5:1, killing was assessed by using flow cytometry. Again, HLA-A*02-positive PDX tumor cells were efficiently eliminated in contrast to HLA-A*02-negative tumor cells (supplemental Figure 5B).

NDC80-clC CAR T cells exhibit high target specificity

Although we performed a strict screening process, there was a risk that NDC80-clC CAR T cells could still mediate additional off-target binding. To further investigate the specificity of our NDC80-clC CAR T cell, we first characterized its binding characteristics through an alanine screening assay on peptide-pulsed T2 cells (Figure 3A). These peptides were also tested for T2 stabilization, which was determined by HLA-A*02 staining. As expected, alanine substitutions at the anchor positions 2 and 9 of the peptide only allowed moderate stabilization of the HLA-A*02 complexes on T2 cells, although all other peptides stabilized the A*02 protein to similar levels as the unmodified peptide (supplemental Figure 6A). The murine IgG1 (mIgG1) antibody derived from clone C exhibited binding to the center of the peptide, as peptides substituted at positions 3, 4, and 5 decreased binding ~50%. In addition, modifications at positions 6, 7, and 8 abrogated binding completely. For clone E, antibody binding was similarly impaired by the substitutions, although

position 7 seemed to be irrelevant for antibody binding (supplemental Figure 6B).

To highlight the functional effects, we repeated alanine screens using CAR T cells of the respective clones and assessed killing by using a lactate dehydrogenase assay. NDC80-cIE CAR T cells exhibited an almost identical pattern to the antibody binding, with no relevant effect from modifications at position 7 but clearly centralized engagement of the CAR T cells with the ALNEQIARL:HLA-A*02 complex (supplemental Figure 6B). For NDC80-cIC CAR T cells, the killing assay also confirmed the importance of positions 3 to 8 for CAR T-cell binding and killing, as all peptide modifications at these sites led to a decrease in killing compared with the unmodified peptide sequence (Figure 3A). Furthermore, we also observed no relevant cross-reactivity of the mlgG1 antibodies with T2 cells pulsed with the target ALNEQIARL or the potential off-target peptides ALNEKLVNL or MLANDIARL (supplemental Figure 6C).

Target sequence specificity was further shown by NDC80 knockdown experiments. Because NDC80 plays an essential role in chromosome segregation and cell division, stable knockout cell lines cannot be maintained. Therefore, we turned to small interfering RNA-based knockdown experiments as they have been described successfully for NDC80.³⁰ After validating successful knockdown of NDC80 in JMN cells in a dose-dependent manner (Figure 3B), we showed complete abrogation of JMN cell line killing at the highest small interfering RNA dose (Figure 3C). Importantly, we know from JMN cell MS experiments that peptides with potential for off-target binding by NDC80-cIC CAR T cells (ALNEKLVNL, ALNELLQHV, ALNEEAGRLL, YLDEYIARM, and LLFEGIARI) were also presented at the cell surface of these target cells but did not mediate killing after knockdown of NDC80. These specificity data were corroborated by immunoprecipitation combined with MS. We prepared a lysate of 3×10^7 BV173 cells, divided it into 3 equal parts, and performed pull-downs with either nonspecific mlgG1 control antibody, NDC80 clone C antibody, or the HLA-

A*02-specific BB7.2 antibody. LC-MS/MS analysis of these samples yielded ~300 HLA-A*02-specific HLA ligands, of which 1 peptide (ILMEHIHKL) was found in the IgG control sample and 5 peptides in the NDC80-specific pull-down. Strikingly, these 5 peptides contained the NDC80-derived ALNEQIARL as well as 4 other HLA ligands with homologous amino acid sequences (ALNEKLVNL, KVLERVNAV, RLAEAHAKV, and MLANDIARL) (Figures 3D; supplemental Figure 6D). However, the risk of these 4 potential off-targets being functionally relevant seems limited as the signal intensity for the off-targets compared with ALNEQIARL was at least 3-fold lower in the MS experiment. After pulsing T2 cells with these 5 peptides (ALNEQIARL plus 4 off-targets) and the other NDC80-derived epitopes (GLNEEIARV and HLEEIQIAKV) as controls, binding was only observed for T2 cells pulsed with the ALNEQIARL peptide (Figure 3E).

Overall, these data suggest that NDC80-cIC CAR T cells and the clone C mlgG1 bind the ALNEQIARL peptide in the context of HLA-A*02 with very high specificity. No evidence for a functionally or physiologically relevant off-target was detected.

NDC80-cIC CAR T cells and clone C antibody reactivity with healthy human cells

Because our new cellular therapy showed encouraging sensitivity and specificity, we next evaluated risks for on-target off-tumor toxicity to different healthy human cells. First, because leukocytes express the highest levels of HLA class I within the different cell types in the body,³¹ we tested if these cells would stain positive with the mlgG1 clone C antibody, as we have seen positivity for several cancer cell lines. For all tested subsets (T cells [CD3⁺], B cells [CD19⁺], and myelomonocytic cells [CD33⁺ and CD15⁺]), no positive staining over the IgG background was observed (Figure 4A). However, because CAR T cells were the preferred therapeutic option for our model, and because we have seen discrepancies between antibody binding and killing, we investigated the potential of the NDC80-cIC CAR T cell to kill healthy A*02-positive peripheral blood mononuclear

Table 2. Cell line killing based on MS evidence of HLA-A*02:ALNEQIARL

Cell line	HLA-A*02/MS	NDC80-cIC killing	NDC80-cIE killing
Hematologic malignancies			
AML14	+/+	+++	+
OCI-AML02	+/+	+++	+
BV173	+/+	+++	+
SUDHL6	+/+	+	-
MAC2A	+/+	+++	+
SUDHL4	+/-	-	-
HL60	-/-	-	-
Nonhematologic malignancies			
JMN	+/+	+++	+
TPC-1	+/+	++	-
MDA-MB231	+/+	++	-
PANC-1	+/+	+	-
SKMEL-5	+/+	+	-
HCT116	+/-	-	-
T47D	-/-	-	-

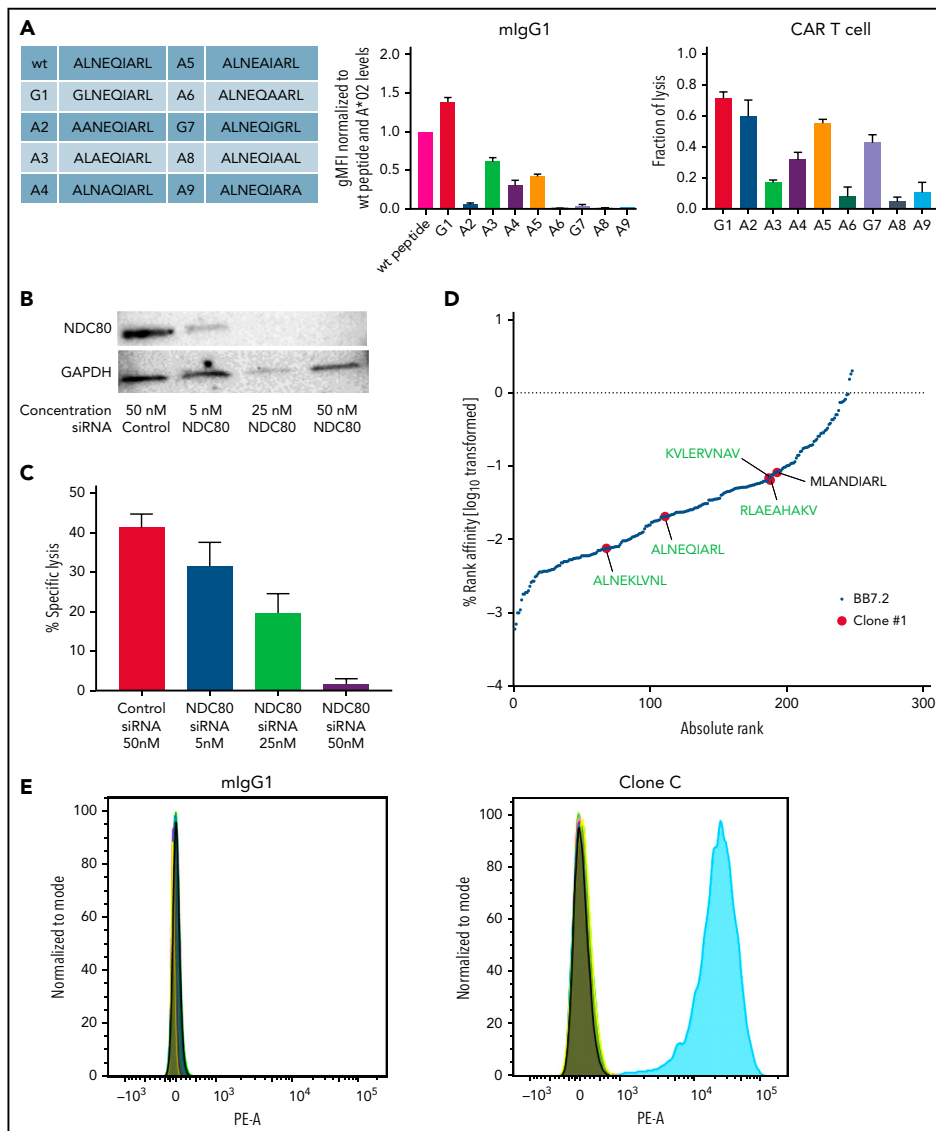


Figure 3. Clone C CAR T cells recognize the ALNEQIARL peptide with high specificity. (A) Alanine screen: peptides used for T2 pulsing (left), mlgG1 binding (middle), and CAR T-cell killing (right). (B) Western blot of NDC80 knockdown using small interfering RNA (siRNA). (C) CAR T-cell killing against JMN NDC80 knockdown cells corresponding to panel B. (D) HLA ligands identified via MS after immunoprecipitation with either HLA-A*02-specific BB7.2 antibody (black) or mlgG1 clone C (red). Peptides are ranked by predicted binding to HLA-A*02 using netMHCpan 4.0 in EL mode. Peptides in green were identified in 2/2 MS runs; peptide in black was identified in 1/2 runs. (E) Flow cytometry of clone C or mlgG1 isotype binding of T2 cells pulsed with either the ALNEQIARL peptide or the potential off-targets from panel D. Two NDC80-derived peptides (GLNEEIARV and HLEEIQIAKV) were used as internal negative controls. Error bars denote standard deviation in panels A and C. GAPDH, glyceraldehyde-3-phosphate dehydrogenase; gMFI, geometric mean fluorescence intensity. PE-A, phycoerythrin.

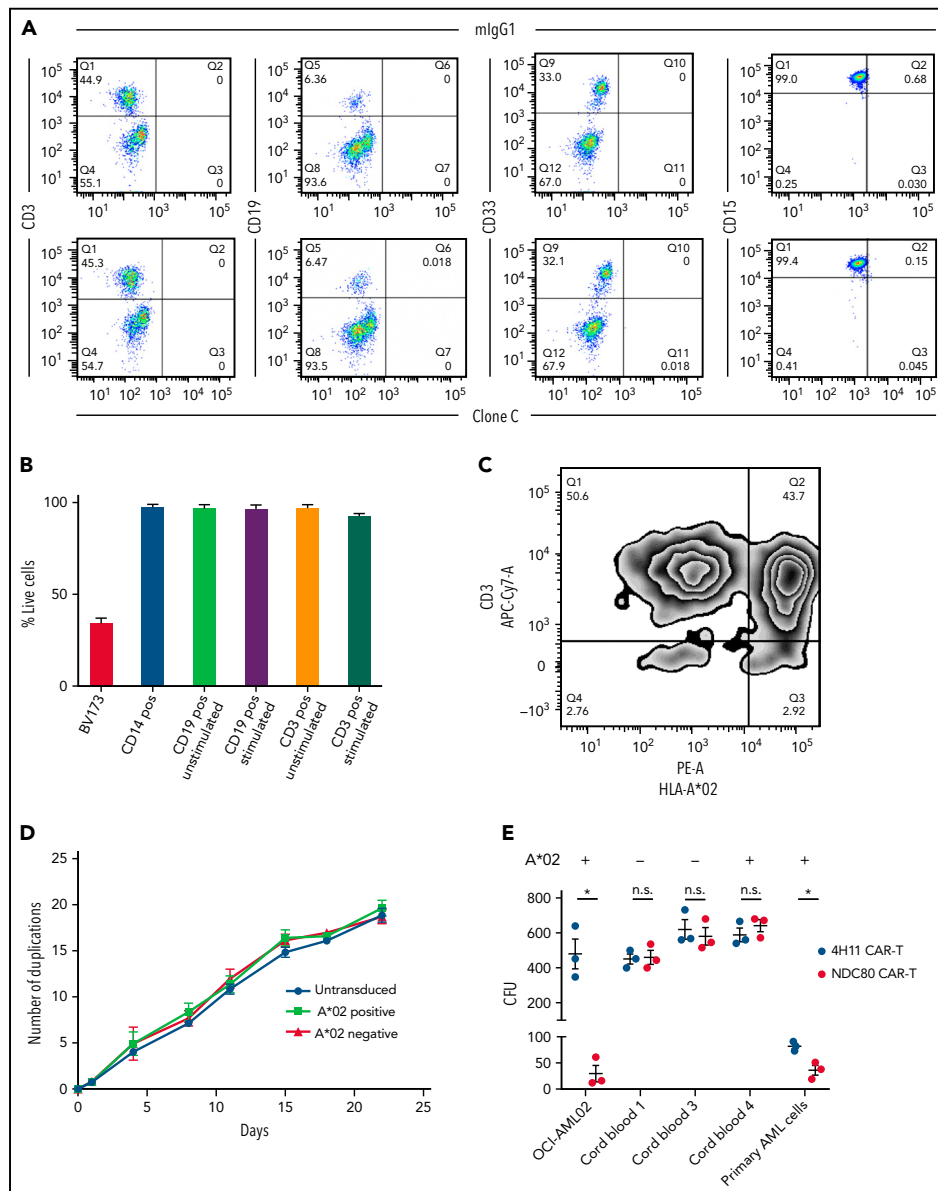


Figure 4.

Downloaded from <http://ashpublications.org/blood/article-pdf/140/8/861/19167230/blood.2021.012882.pdf> by guest on 27 November 2023

cells. Mitogen-stimulated T and B cells were also included in this assay as their increased proliferation could lead to greater expression of NDC80 as well as processing and presentation of the ALNEQIARL HLA ligand. Little to no killing of sorted hematopoietic cells was observed (Figure 4B). Alternatively, we investigated killing of peripheral blood mononuclear cells via flow cytometry with CFSE-labeled cells without prior sorting and also observed minimal killing; in this assay, however, proliferation effects of different cell populations could have biased the results (supplemental Figure 7).

Because recognition and killing of activated T cells could strongly affect the production and efficacy of A*02-positive NDC80-specific CAR T cells, we next tested these NDC80-c1C CAR T cells for their potential to mitigate fratricide. In an overnight 1:1 mixed lymphocyte culture of A*02-positive and A*02-negative NDC80-c1C CAR T cells, only a slight reduction of A*02-positive CAR T cells was observed relative to the A02-negative cells (Figure 4C). To address the potential long-term fratricide effects of HLA-A*02-positive NDC80-c1C CAR T cells, HLA-A*02-positive and HLA-A*02-negative CAR T cells were cultivated over 3 weeks, and viability as well as cell numbers were monitored. Again, no signs of significant differences in cell proliferation or viability were observed between these 2 groups, indicating no relevant fratricidal effects (Figure 4D).

Although no toxicities were seen in our experiments with mature hematopoietic cells, the question remained if other important proliferative cells such as HSCs would be affected by the NDC80-c1C CAR T cells. This is especially important as MS analysis of the HLA ligandome of healthy individuals showed presentation of the ALNEQIARL peptide in one bone marrow sample.²⁵ We therefore used colony-forming unit assays from cord blood-isolated HLA-A*02-positive and -negative CD34⁺ HSCs with OCI-AML02 cancer cells and one primary HLA-A*02 AML sample as positive controls. OCI-AML02 cancer cells as well as the primary AML cells formed significantly fewer colonies when treated with the NDC80-c1C CAR T cells compared with a control CAR T cell (Figure 4E). In contrast, no differences were observed in cord blood-isolated HSCs independent of their HLA-A*02 status. Furthermore, cell numbers as well as lineage development were likewise not affected by the NDC80-c1C CAR T cells (supplemental Figure 8A-C). We corroborated the results from colony-forming unit assays using lactate dehydrogenase assays showing no toxicity for either HLA-A*02-positive or -negative cord blood-derived HSCs (supplemental Figure 8D). Together, these data indicate that NDC80-c1C CAR T cells do not cause relevant toxicity toward the CAR T cells themselves, healthy leukocytes, or HSCs.

To expand the list of tissues tested for on-target off-tumor toxicity, we analyzed human thymic fibroblasts, cardiac fibroblasts, and cardiomyocytes. None of these cells stained positively for our NDC80 TCR mimic antibody independent of their HLA-A*02

status, which further highlights its specificity (supplemental Figure 9A). Identical results were obtained after culturing these cells for ~10 days, although cardiomyocytes did not survive this culture period. In addition, only baseline killing of CFSE-labeled cells was observed after 24 hours of coculture with either MOCK T cells or NDC80-c1C CAR T cells (supplemental Figure 9B). We compared our results vs the ratio of remaining target cells observed when this assay was performed with unpulsed T2 cells, which served as a true negative control (supplemental Figure 9C-D).

NDC80-c1C CAR T cells control human leukemia and mesothelioma tumor growth in mouse models, leading to prolonged survival

Because our new agent has been proven to selectively identify its target and to mediate killing in a cancer-specific manner, we tested its potency in 2 mouse models: an intravenous BV173 leukemia model and an intraperitoneal JMN mesothelioma solid tumor model. We injected 1 million BV173 cells per mouse intravenously followed by 2 million CAR T cells on day 5; disease burden was monitored through weekly cheek bleeds and subsequently by flow cytometry to determine the fraction of leukemia cells vs CD45⁺ mouse leukocytes as described previously³² (Figure 5A; gating strategy provided in supplemental Figure 10). MUC16-specific CAR T cells as well as tumor cell injection alone served as controls. We observed significant control of peripheral blast count of the NDC80-c1C CAR T cells over controls (Figure 5B; supplemental Figure 11A), which was monitored until day 56 and then followed up by overall survival, which also showed superiority of the NDC80-c1C CAR T cells over the control groups (Figure 5C). Diminished killing of GFP-Luc transduced cells compared with wild-type BV173 cells was noted, which positively correlated to the degree of GFP expression (supplemental Figure 11B). Therefore, in these experiments, we chose cheek bleeds over a bioluminescence model, to reduce the risk of biasing the *in vivo* experiments by this reduction in killing capacity. Wild-type cells were used instead.

JMN cells luciferase positive cells were used in the intraperitoneal model experiment. Notably, luciferase transduction of JMN cells did not affect killing by NDC80-c1C CAR T cells compared with untransduced JMN cells *in vitro* (supplemental Figure 11C). Then, 0.3 million JMN cells were injected intraperitoneally and imaged on day 3; this was then followed by the injection of 0.15 million NDC80-c1C CAR T cells or MUC16-specific CAR T cells on day 4 (Figure 5D). Bioluminescence imaging revealed profound tumor control, with a 10- to 200-fold decrease in tumor signal in individual NDC80-c1C CAR T cell-treated mice and an average 10-fold decrease in tumor signal from day 14 onward in the entire group (Figure 5E-G). This significant tumor control also translated into a survival benefit, with 100% survival of mice to day 60; in contrast, no survivors remained in the control CAR T cell-treated group after 42 days (Figure 5H).

Figure 4. Clone C CAR T cells do not mediate toxicity toward healthy leukocytes, activated lymphocytes, or HSCs. (A) Flow cytometry of clone C or mlgG1 isotype binding of healthy A*02-positive CD3, CD19, CD33, and CD15 positive cells. Data are representative of 3 donors. (B) Lactate dehydrogenase-killing assay with clone C CAR T cells and magnetic-activated cell-sorted CD3, CD14, and CD19 positive cells. CD13 and CD19 positive cells were also tested after 48 hours of activation. BV173 cells served as positive control. (C) Zebra plot after coculture of clone C CAR T cells produced from cells of A*02-positive and -negative blood donors. Flow cytometry was performed after 18 hours' coculture at 1:1 ratio. Plot is representative of 3 biological replicates. (D) Cell proliferation capacity of simulated but untransduced T cells and HLA-A*02-positive and -negative clone C CAR T cells. (E) Colony-forming unit (CFU) assays of cord blood-isolated CD34⁺ HSCs, OCI-AML02 cell line as positive control, and N3 primary AML cells. Cells were plated after 18-hour 1:1 coculture of CAR T cells and target cells. MUC16-specific 4H11 CAR T cells served as control. Error bars in panels B, D, and E denote standard deviation. **P* < .05 (unpaired *t* test). APC-Cy7, allophycocyanin-cyanin 7; n.s., not significant; PE-A, phycoerythrin; Q, quadrant.

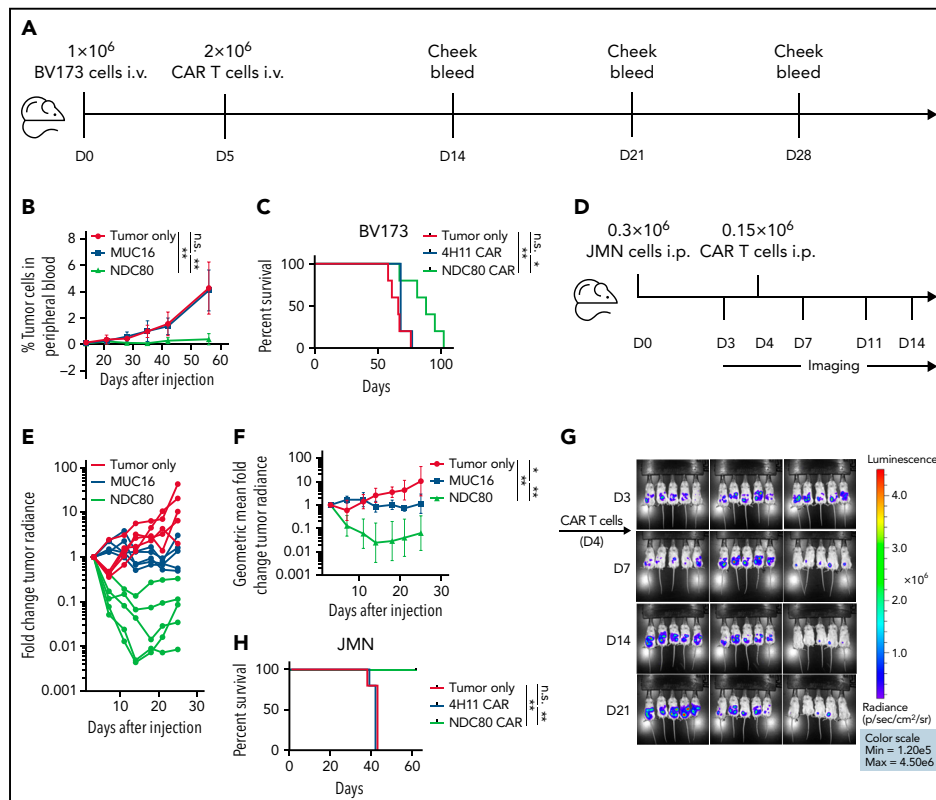


Figure 5. Clone C CAR T cells control tumor growth and prolong survival in leukemia and mesothelioma mouse models. (A) Experimental design for BV173 intravenous (i.v.) leukemia model. (B) Mean tumor burden as defined by percentage of A*02-positive blast cells in mouse blood. Five mice per group. ***P* < .01 (Mann-Whitney test). Error bars denote standard deviation. (C) Overall survival in BV173 leukemia model. **P* < .05, ***P* < .01 (log-rank test). Experiment was conducted twice, with comparable results. (D) Experimental design for JMN intraperitoneal (i.p.) mesothelioma model. (E) Spaghetti plot depicting individual tumor burden relative to day 3. (F) Geometric mean of average tumor burden spaghetti plot depicting individual tumor burden relative to day 3. Five mice per group. **P* < .05, ***P* < .01 (Mann-Whitney test). Error bars denote 95% confidence interval. (G) Bioluminescence imaging using luciferase pre- and post-CAR T-cell treatment. (H) Overall survival in JMN mesothelioma model. ***P* < .01 (log-rank test). Experiment was conducted twice, with comparable results. D, day; n.s., not significant.

Discussion

Most protein targets within cancer cells are not druggable by conventional small molecule drugs, and cell surface proteins that may be addressable by therapeutic antibodies are mostly not tumor specific. Therefore, the discovery of new targets that may be approached by immunologic agents is urgently needed. In this study, we showed that MS can be used to rationally discover broadly presented tumor-associated HLA ligands that can serve as targets for therapeutic TCR mimic CAR T cells. In addition, the use of HLA ligands found abundantly presented on cancer cells, but not with, or with limited amounts on, normal cells, broadens the spectrum of potential cancer-specific targets tremendously. As a target, this class of antigen does not require that the individual peptide is immunogenic, because engineering of TCR mimic antibodies bypasses the need to have

antigens that are immunogenic to the host. This gives them another advantage over conventional TCR T-cell therapies, as naturally occurring TCRs are usually limited in their targeting capacity by negative thymic selection, which rules out a wide range of self-proteins as potential targets. Of note, alternative strategies to target non-immunogenic self-proteins have also been developed in the TCR T-cell field (eg, through allo-restricted T cells^{33,34} or mouse models with humanized TCR repertoires³⁵). Nevertheless, these strategies are restricted to some degree and do not allow targeting of any stable peptide:HLA combinations as is theoretically possible with a TCR mimic drug.

This approach also opens the door to epitopes that may be found widely among different cancer types compared with the tumor- and patient-specific mutational neoantigens. TCR mimics against various targets have usually focused on well-known immunogenic

CD8 T-cell epitopes.⁸⁻¹⁷ Some of these neoantigen epitopes are presented in cell lines at an abundance of only a dozen molecules per cell or less.^{11,13} In contrast, we detected ~500 to 1300 copies of the NDC80 ALNEQIARL peptide on cancer cell lines by flow cytometry, thus reducing the requirement for development of ultrapotent agents. Notably, as the NDC80 epitope was first identified by MS in the immunopeptidome of several unmatched cancer cell lines, adequate cell surface presentation for the target was validated from the start of the discovery process.

Furthermore, most of the described targets of TCR-based agents are cancer-germline antigens, oncofetal antigens, viral antigens, or neoantigens, which are generally limited to selected cancer types. Importantly, we detected the NDC80 target antigen in >90% of the A*02-positive cell lines tested by MS. Hence, this target is much more prevalent than these other public and private neoantigens. Interestingly, the ALNEQIARL peptide has also been identified by MS on different A*02 suballeles (A*02:02; 03; 04; 07; 11),^{36,37} thus broadening target patient populations considerably. Finally, because the NDC80 protein is essential for chromosome segregation and cell division, tumor escape by downregulation of the protein or by functionally relevant mutations would be a less likely event.

Using the E-ALPHA phage library platform, we successfully identified an scFv, which in a CAR T-cell format was able to effectively and selectively bind to the ALNEQIARL:A*02 complex, kill cancer target cells *in vitro*, and mediate tumor control in mice, resulting in prolonged survival in leukemia and solid tumor models. Importantly, although the ALNEQIARL:A*02 complex also might be presented on healthy HLA-A*02-positive dividing cells, we did not observe relevant killing of healthy leukocytes, HSCs, mitogen-stimulated T and B cells, or thymic and cardiac fibroblasts. In the case of HSCs, the reduced expression of HLA on these cells is a possible explanation for this finding.³¹ In peripheral leukocytes, which are generally not proliferating, there is much lower expression of NDC80 compared with tumor cell lines or primary tissues. Interestingly, although the parent protein NDC80 is an essential protein in dividing cells, and its expression can be measured in many different tissue types, it seems that NDC80 peptides can be cancer-selective targets due to the additional restriction for HLA presentation. This process appears to be associated with the oncogenic state. The lack of normal cell presentation might also in part be explained by the constraints of having sufficient HLA complexes, rather than their ligands, in HLA:peptide formation.³⁸ Therefore, many peptides, although properly processed and transported to the endoplasmic reticulum, might not be presented if they are of lower abundance (eg, in terminally differentiated cells) or if the available rate of HLA complexes is highly limited (eg, observed in HSCs). Still, due to limitations in current methods, we cannot definitively rule out presentation of the ALNEQIARL peptide on all healthy tissues, similar to the GLNEEIARV peptide, which is also derived from NDC80. Although a reasonable therapeutic index seems to be achievable, additional extensive toxicity studies should be performed to ensure safety of this drug before it could be introduced into clinical development. Testing for cross-reactivity in transgenic mice might be useful; however, the production of murine CAR T cells with human constructs was not feasible, and HLA-A*02 transgenic mouse toxicity studies are confounded by graft-versus-host disease effects when using human cells. Future studies of cross-reactivity might require use of a TCR mimic antibody or a bispecific format.

Overall, our study highlights the importance of considering non-immunogenic, broadly expressed, tumor-associated HLA ligands identified by MS as targets for cancer immunotherapy druggable through TCR mimic CAR T cells. This expansion of the potential antigen repertoire thus enabled us to develop the NDC80-cC CAR T-cell construct with broad applicability and strong reactivity against highly proliferative cancers often found among hematologic malignancies.

Acknowledgments

The authors thank Alex Kentsis for access to the Byonic Software and providing the AML PDX cells for killing assays. They also thank the Proteomics Resource Center at The Rockefeller University for the performance of all LC/MS-MS experiments.

This study was supported by the Leukemia and Lymphoma Society, the National Institutes of Health, National Cancer Institute (P30CA 008748, R01 CA55349, P01 CA23766, and R35 CA241894); The Experimental Therapeutics Center of MSK; and Tudor Funds. M.G.K. is supported by the German Research Foundation (DFG) with an individual Research Grant (KL3118/11) and is a fellow of the Berlin Institute of Health Clinician Scientist Program.

Authorship

Contribution: M.G. Klatt, T.D. Z.Y., J.L., S.S.M., M.M.D., H.L., T.J.G., C.B., L.P., Z.E.H.A., T.K., and M.L. performed and analyzed experiments; M.G. Klatt, T.D., M.G. Kharas, C.L., and D.A.S. designed experiments; M.G. Klatt and T.D. wrote the original draft of the manuscript; T.D. and D.A.S. supervised the project; and D.A.S. provided funding and edited the manuscript. All authors reviewed and contributed to the manuscript.

Conflict-of-interest disclosure: D.A.S. has ownership in, income from, or research funds from: Pfizer, Sellas Life Sciences, Iovance, Eureka Therapeutics, Sapience, OncoPep, Actinium, Colmmune, and Repertoire. T.D. worked as a consultant to Eureka Therapeutics. C.L., Z.Y., and J.L. are employees of Eureka Therapeutics. M.G. Klatt is a consultant to Ardigen. M.G. Kharas received speaker honorarium from AstraZeneca and Kumquat; and serves on the scientific advisory board of 858 Therapeutics. MSKCC has filed for patent protection for some components developed in this study. The remaining authors declare no competing financial interests.

ORCID profiles: M.G.K., 0000-0001-8703-7305; S.S.M., 0000-0002-3735-6057; M.M.D., 0000-0003-1731-1502; C.B., 0000-0001-9290-4223; L.P., 0000-0002-7301-0379; Z. E.H.A., 0000-0001-9851-8796; M.L., 0000-0001-7698-7452; M.G.K., 0000-0002-1165-6991.

Correspondence: Martin G. Klatt, Department of Hematology, Oncology and Tumorimmunology, Charité - University Medicine Berlin, Hindenburgdamm 30, 12203 Berlin, Germany; e-mail: martin.klatt@charite.de; and David A. Scheinberg, Molecular Pharmacology and Center for Experimental Therapeutics, Memorial Sloan Kettering Cancer Center, 1275 York Avenue, Box 531, New York, NY 10065; e-mail: scheinbd@mskcc.org.

Footnotes

Submitted 8 June 2021; accepted 25 March 2022; prepublished online on *Blood* First Edition 16 April 2022. DOI 10.1182/blood.2021012882.

The online version of this article contains a data supplement.

The publication costs of this article were defrayed in part by page charge payment. Therefore, and solely to indicate this fact, this article is hereby marked "advertisement" in accordance with 18 USC section 1734.

REFERENCES

- Chong EA, Ruella M, Schuster SJ; Lymphoma Program Investigators at the University of Pennsylvania. Five-year outcomes for refractory B-cell lymphomas with CAR T-cell therapy. *N Engl J Med*. 2021;384(7):673-674.
- Munshi NC, Anderson LD Jr, Shah N, et al. Idecabtagene vicleucel in relapsed and refractory multiple myeloma. *N Engl J Med*. 2021;384(8):705-716.
- Guedan S, Calderon H, Posey AD Jr, Maus MV. Engineering and design of chimeric antigen receptors. *Mol Ther Methods Clin Dev*. 2018;12:145-156.
- Sauer T, Parikh K, Sharma S, et al. CD70-specific CAR T cells have potent activity against acute myeloid leukemia without HSC toxicity. *Blood*. 2021;138(4):318-330.
- Schäfer D, Tomiuk S, Küster LN, et al. Identification of CD318, TSPAN8 and CD66c as target candidates for CAR T cell based immunotherapy of pancreatic adenocarcinoma. *Nat Commun*. 2021;12(1):1453.
- Perna F, Berman SH, Soni RK, et al. Integrating proteomics and transcriptomics for systematic combinatorial chimeric antigen receptor therapy of AML. *Cancer Cell*. 2017;32(4):506-519.e5.
- Rammensee HG, Bevan MJ. Evidence from in vitro studies that tolerance to self antigens is MHC-restricted. *Nature*. 1984;308(5961):741-744.
- Chang AY, Dao T, Gejman RS, et al. A therapeutic T cell receptor mimic antibody targets tumor-associated PRAME peptide/HLA-I antigens. *J Clin Invest*. 2017;127(7):2705-2718.
- Dao T, Pankov D, Scott A, et al. Therapeutic bispecific T-cell engager antibody targeting the intracellular oncoprotein WT1. *Nat Biotechnol*. 2015;33(10):1079-1086.
- Dao T, Yan S, Veomett N, et al. Targeting the intracellular WT1 oncogene product with a therapeutic human antibody. *Sci Transl Med*. 2013;5(176):176ra33.
- Douglass J, Hsiue EH, Mog BJ, et al. Bispecific antibodies targeting mutant RAS neoantigens. *Sci Immunol*. 2021;6(57):eabd5515.
- Herrmann AC, Im JS, Pareek S, et al. A novel T-cell engaging bi-specific antibody targeting the leukemia antigen PR1/HLA-A2. *Front Immunol*. 2019;9:3153.
- Hsiue EH, Wright KM, Douglass J, et al. Targeting a neoantigen derived from a common TP53 mutation. *Science*. 2021;371(6533):eabc8697.
- Liu H, Xu Y, Xiang J, et al. Targeting alpha-fetoprotein (AFP)-MHC complex with CAR T-cell therapy for liver cancer. *Clin Cancer Res*. 2017;23(2):478-488.
- Paul S, Pearlman AH, Douglass J, et al. TCR β chain-directed bispecific antibodies for the treatment of T cell cancers. *Sci Transl Med*. 2021;13(584):eabd3595.
- Rafiq S, Purdon TJ, Daniyan AF, et al. Optimized T-cell receptor-mimic chimeric antigen receptor T cells directed toward the intracellular Wilms tumor 1 antigen. *Leukemia*. 2017;31(8):1788-1797.
- Zhao Q, Ahmed M, Tassev DV, et al. Affinity maturation of T-cell receptor-like antibodies for Wilms tumor 1 peptide greatly enhances therapeutic potential. *Leukemia*. 2015;29(11):2238-2247.
- Klatt MG, Kowalewski DJ, Schuster H, et al. Carcinogenesis of renal cell carcinoma reflected in HLA ligands: a novel approach for synergistic peptide vaccination design. *Oncimmunology*. 2016;5(8):e1204504.
- Chen W, Liao L, Lai H, Yi X, Wang D. Identification of core biomarkers associated with pathogenesis and prognostic outcomes of laryngeal squamous-cell cancer using bioinformatics analysis. *Eur Arch Otorhinolaryngol*. 2020;277(5):1397-1408.
- Liu ZK, Zhang RY, Yong YL, et al. Identification of crucial genes based on expression profiles of hepatocellular carcinomas by bioinformatics analysis. *PeerJ*. 2019;7:e7436.
- Zhang H, Zou J, Yin Y, et al. Bioinformatic analysis identifies potentially key differentially expressed genes in oncogenesis and progression of clear cell renal cell carcinoma. *PeerJ*. 2019;7:e8096.
- Klatt MG, Aretz ZEH, Curcio M, Gejman RS, Jones HF, Scheinberg DA. An input-controlled model system for identification of MHC bound peptides enabling laboratory comparisons of immunopeptidome experiments. *J Proteomics*. 2020;228:103921.
- Klatt MG, Mack KN, Bai Y, et al. Solving an MHC allele-specific bias in the reported immunopeptidome. *JCI Insight*. 2020;5(19):141264.
- Montejo J, Zuberi K, Rodriguez H, et al. GeneMANIA Cytoscape plugin: fast gene function predictions on the desktop. *Bioinformatics*. 2010;26(22):2927-2928.
- Marcu A, Bichmann L, Kuchenbecker L, et al. HLA Ligand Atlas: a benign reference of HLA-presented peptides to improve T-cell-based cancer immunotherapy. *J Immunother Cancer*. 2021;9(4):e002071.
- Barretina J, Caponigro G, Stransky N, et al. The Cancer Cell Line Encyclopedia enables predictive modelling of anticancer drug sensitivity. *Nature*. 2012;483(7391):603-607.
- Aguet F, Barbeira AN, Bonazzola R, et al; GTEx Consortium. The GTEx Consortium atlas of genetic regulatory effects across human tissues. *Science*. 2020;369(6509):1318-1330.
- Goldman MJ, Zhang J, Fonseca NA, et al. A user guide for the online exploration and visualization of PCAWG data. *Nat Commun*. 2020;11(1):3400.
- Löffler MW, Kowalewski DJ, Backert L, et al. Mapping the HLA ligandome of colorectal cancer reveals an imprint of malignant cell transformation. *Cancer Res*. 2018;78(16):4627-4641.
- Ju LL, Chen L, Li JH, et al. Effect of NDC80 in human hepatocellular carcinoma. *World J Gastroenterol*. 2017;23(20):3675-3683.
- Boegel S, Löwer M, Bukur T, Som P, Castle JC, Sahin U. HLA and proteasome expression body map. *BMC Med Genomics*. 2018;11(1):36.
- Gopalakrishnapillai A, Kolb EA, Dhanan P, et al. Generation of pediatric leukemia xenograft models in NSG-B2m mice: comparison with NOD/SCID mice. *Front Oncol*. 2016;6:162.
- Gao L, Bellantuono I, Elsässer A, et al. Selective elimination of leukemic CD34(+) progenitor cells by cytotoxic T lymphocytes specific for WT1. *Blood*. 2000;95(7):2198-2203.
- Wilde S, Sommermeier D, Frankenberger B, et al. Dendritic cells pulsed with RNA encoding allogeneic MHC and antigen induce T cells with superior antitumor activity and higher TCR functional avidity. *Blood*. 2009;114(10):2131-2139.
- Obenaus M, Leitão C, Leisegang M, et al. Identification of human T-cell receptors with optimal affinity to cancer antigens using antigen-negative humanized mice. *Nat Biotechnol*. 2015;33(4):402-407.
- Abelin JG, Keskin DB, Sarkizova S, et al. Mass spectrometry profiling of HLA-associated peptidomes in mono-allelic cells enables more accurate epitope prediction. *Immunity*. 2017;46(2):315-326.
- Sarkizova S, Klaeger S, Le PM, et al. A large peptidome dataset improves HLA class I epitope prediction across most of the human population. *Nat Biotechnol*. 2020;38(2):199-209.
- Komov L, Kadosh DM, Barnea E, Milner E, Hendler A, Admon A. Cell surface MHC class I expression is limited by the availability of peptide-receptive "empty" molecules rather than by the supply of peptide ligands. *Proteomics*. 2018;18(12):e1700248.
- Pandey K, Mifsud NA, Lim Kam Sian TCC, et al. In-depth mining of the immunopeptidome of an acute myeloid leukemia cell line using complementary ligand enrichment and data acquisition strategies. *Mol Immunol*. 2020;123:7-17.
- Lanoix J, Durette C, Courcelles M, et al. Comparison of the MHC I immunopeptidome repertoire of B-cell lymphoblasts using two isolation methods. *Proteomics*. 2018;18(12):e1700251.
- Pearson H, Daouda T, Granados DP, et al. MHC class I-associated peptides derive from selective regions of the human genome. *J Clin Invest*. 2016;126(12):4690-4701.
- Kemps PG, Zondag TC, Steenwijk EC, et al. Apparent lack of BRAF V600E derived HLA class I presented neoantigens hampers neoplastic cell targeting by CD8⁺ T cells in Langerhans cell histiocytosis. *Front Immunol*. 2020;10:3045.
- Khodadoust MS, Olsson N, Wagar LE, et al. Antigen presentation profiling reveals

- recognition of lymphoma immunoglobulin neoantigens. *Nature*. 2017;543(7647):723-727.
44. Bassani-Sternberg M, Bräunlein E, Klar R, et al. Direct identification of clinically relevant neoepitopes presented on native human melanoma tissue by mass spectrometry. *Nat Commun*. 2016;7:13404.
45. Gloger A, Ritz D, Fugmann T, Neri D. Mass spectrometric analysis of the HLA class I peptidome of melanoma cell lines as a promising tool for the identification of putative tumor-associated HLA epitopes. *Cancer Immunol Immunother*. 2016;65(11):1377-1393.
46. Koumantou D, Barnea E, Martin-Esteban A, et al. Editing the immunopeptidome of melanoma cells using a potent inhibitor of endoplasmic reticulum aminopeptidase 1 (ERAP1). *Cancer Immunol Immunother*. 2019;68(8):1245-1261.
47. Stopfer LE, Mesfin JM, Joughin BA, Lauffenburger DA, White FM. Multiplexed relative and absolute quantitative immunopeptidomics reveals MHC I repertoire alterations induced by CDK4/6 inhibition. *Nat Commun*. 2020;11(1):2760.
48. Ternette N, Olde Nordkamp MJM, Müller J, et al. Immunopeptidomic profiling of HLA-A2-positive triple negative breast cancer identifies potential immunotherapy target antigens. *Proteomics*. 2018;18(12):e1700465.
49. Shraibman B, Barnea E, Kadosh DM, et al. Identification of tumor antigens among the HLA peptidomes of glioblastoma tumors and plasma [retracted in *Mol Cell Proteomics*. 2018;17(11):2132-2145]. *Mol Cell Proteomics*. 2019;18(6):1255-1268.

© 2022 by The American Society of Hematology

Downloaded from <http://ashpublications.org/blood/article-pdf/140/8/851/19167230/2021012882.pdf> by guest on 27 November 2023

3. Diskussion

3.1 Absolute Sensitivität und Spezifität von T-Zell basierten Therapien

Die hier vorgestellten Arbeiten der Immunpeptidomik und translationalen T-Zell Immuntherapie illustrieren die Wichtigkeit der Identifikation von tumorspezifischen oder zumindest tumorassoziierten HLA Liganden. Sie bilden die Grundlage für die Effektivität dieser Therapien, denn ohne eine suffiziente Präsentation des Targets sind sämtliche therapeutische Ansätze nicht zielführend. Umso überraschender ist es, dass diese Grundvoraussetzung teilweise noch immer bei der Entwicklung von T-Zell basierten Therapien nicht beachtet wird (46). Zusätzlich illustriert meine erste diskutierte Arbeit, dass selbst etablierte Methoden nicht vor einem systematischen Bias geschützt sind. Der Nachweis, dass relevante Anteile des Immunpeptidoms auf Grund technischer Aspekte nicht eluiert wurden und somit seit der Entwicklung der HLA Liganden Isolation Jahre HLA Liganden hoher Hydrophobizität nicht in die Analyse möglicher Targets und off-Targets eingegangen sind, unterstreicht die Wichtigkeit der vorgestellten Arbeit. Dennoch ist es nicht ausgeschlossen, dass weitere Aspekte der biochemischen Isolation die Analyse des Immunpeptidoms weiter beeinflussen. So konnte ich in einer noch unveröffentlichten Arbeit zeigen, dass HLA Liganden mit starker mehrfach positiver Ladung (4+, 5+ etc.), welche normalerweise massenspektrometrisch nicht erfasst werden, detektierbar sind, wenn diese Ladungen mittels chemischer Modifikation der positiv geladenen Seitengruppen supprimiert werden. Gerade unter dem Aspekt von stark basischen Proteinen mit einem hohen Anteil von Arginin und Lysin ist diese Methode hochrelevant und kann zur Entdeckung neuer HLA Liganden führen.

Dennoch muss in der Betrachtung von möglichen Zielepitopen ein Aspekt berücksichtigt werden, welcher bisher wenig beleuchtet wurde. Die Sensitivität von TZR-basierten Therapien aber noch viel mehr von TZR-imitierenden Wirkstoffen ist stark von der Abundanz der präsentierten HLA Liganden abhängig. Selbstverständlich ist es inzwischen möglich, die Sensitivität eines Medikamentes für die Erkennung eines HLA Liganden durch

Affinitätsoptimierung deutlich zu steigern (47,48). Es muss dabei jedoch beachtet werden, dass diese Verstärkung der Bindung an das Target auch die Wahrscheinlichkeit steigert, an off-Targets mit ähnlicher Sequenz oder dreidimensionaler Ausrichtung zu binden. Aus diesem Grund wurden zahlreiche Methoden entwickelt, welche die Spezifitäten von TZR-basierten Therapien gegen Tausende mehr oder wenig zufällig generierte Peptide zu evaluieren, um so das Risiko von off-Target Toxizitäten zu minimieren (49-51). Was jedoch alle diese High-Throughput Plattformen außer Acht lassen sind die Erkenntnisse der Immunpeptidomik, denn die Spezifität eines T-Zell Rezeptors gegen Peptide zu testen, welche nicht an der Oberfläche auf HLA Komplexen präsentiert werden, ist ebenso wenig sinnvoll wie die Entwicklung eines Wirkstoffs gegen ein nicht präsentierten HLA Liganden. Die Verbindung des High-Throughput Screening mit der Immunpeptidomik wäre daher einer der wichtigsten Schritte für die weitere Evaluation von TZR basierten Therapien. Ein weiterer Aspekt, welchen diese Plattformen nicht berücksichtigen, ist die bereits erwähnte Abundanz der HLA Liganden, da diese nicht nur die Effektivität, sondern auch die Toxizität dieser Therapien entscheidend beeinflussen kann. Ein konkretes Beispiel aus der letzten vorgestellten eigenen Arbeit macht dies deutlich. Die in dieser Arbeit entwickelte TZR-imitierende CAR-T-Zelle ist gegen das Peptid ALNEQIARL gerichtet. Während unserer Charakterisierung konnte wir zeigen, dass dieses Konstrukt u.a. auch die Sequenzen ALNEKLVNL und MLANDIARL mit N- und C-terminaler Homologie zum Zielpetid binden kann. Es ist hierbei auch wichtig zu betonen, dass die Präsentation dieser beiden Sequenzen ebenfalls massenspektrometrisch validiert wurde. Die Bindung und Abtötung von Zellen, welche diese off-Targets tragen, findet allerdings erst ab einer Abundanz von ca. 3.000-5.000 Molekülen pro Zelle statt, einer Menge, welche in physiologischen Settings für ein einzelnes Peptid nicht erreicht wird. Somit würden Screeninguntersuchungen diese Sequenzen als mögliche off-Targets erkennen, eine physiologische Relevanz bestünde allerdings nicht und Nebenwirkungen auf Basis dieser Kreuzreaktivität sind nicht zu erwarten. Um also die exakte Sensitivität und Spezifität einer spezifischen Immuntherapie definieren zu können, wäre es ideal, die Grenzwerte der Erkennung des Targets und möglicher off-targets in Molekülen pro Zelle benennen zu können.

Daher liegt es nahe, in Zukunft die Targetidentifikation durch Immunpeptidomik nicht nur qualitativ durchzuführen, sondern diese auch viel mehr mit quantitativen Daten zu untermauern. So wurde z.B. nachgewiesen, dass die Mutation R175H im Protein p53 als Sequenz HMTEVVRHC in den meisten Zelllinien nur mit 1-3 Molekülen pro Zelle auf dem Komplex HLA-A*02:01 präsentiert wird und die hiergegen entwickelten Agenzien nur eine limitierte Aktivität aufweisen (52). Zusätzlich steigt das Risiko für off-Target Effekte, wenn die Aktivität des Medikamentes so stark sein muss, dass es ein einzelnes Molekül pro Zelle erkennen muss. Gerade auf dem Gebiet der TZR-imitierenden Wirkstoffe postulieren wir daher, dass Targets mit hoher Abundanz *a priori* bessere Zielstrukturen darstellen, da die Abschätzung von off-Target Effekten immer als sehr schwer gilt und bis zur klinischen Testung es beinahe unmöglich ist diese auszuschließen. Die in der zweiten Arbeit dargestellte Methode der Normalisierung der Immunpeptidomexperimente stellt dabei eine sehr wertvolle Herangehensweise vor, welche diese quantitativen Analysen weiter unterstützt. Zusammenfassend belegen diese Daten jedoch, dass die Immunpeptidomik unabdingbar ist für die Definition von Targets aber auch relevanter off-Targets der T-Zell basierten Immuntherapie und das für eine genaue Bestimmung der Sensitivität und Spezifität dieser Wirkstoffe die quantitative Immunpeptidomik wertvolle Hinweise liefern kann. Dennoch sollten wir uns vor Augen halten, dass selbst bei einer idealen Entwicklung und präklinischen Testung Mechanismen untersucht werden müssen, welche in vivo die Effektivität beeinträchtigen können und welche nun im folgenden Abschnitt diskutiert werden.

3.2 Limitationen der Therapie und der Wirkstoffentwicklung

Jede onkologische Therapie ist neben ihrer Wirkung und verbundenen Nebenwirkungen auch von Mechanismen des Therapieversagens und der Resistenzmechanismen betroffen. In Bezug auf TZR-basierte Immuntherapien liegt es hierbei auf der Hand, dass Tumorzellen sämtliche Strategien anwenden, um die die Präsentation der angegriffenen HLA Liganden zu verhindern. Ein möglicher Schritt besteht in der Downregulation oder dem Verlust des Antigens, aus welchem das präsentierte Peptid stammt. Klassische Beispiele sind hier die

CGAs, welche oft durch Downregulation mittel Hypermethylierung der Erkennung durch das Immunsystem entgehen. Hypomethylierende Agenzien wie Azacitidin dagegen können diesen Effekt umkehren und so die Präsentation wiederherstellen (53,54). Unter diesem Aspekt ist auch nochmals die Wichtigkeit der dritten und vierten diskutierten Arbeit zur pharmakologischen Modulation des Immunpeptidoms hervorzuheben. Im Gegensatz zu den Targets der konventionellen CAR-T-Zellen lassen sich HLA Liganden als Zielstrukturen gezielt steuern und geben uns so die Möglichkeit die Effektivität der TZR-basierten Therapien zu verbessern. Im Idealfall kommen hier Substanzen zum Einsatz, welche selektiv auf Tumorzellen wirken, um eine vermehrte Präsentation im Normalgewebe zu verhindern, wie es bei den vorgestellten EZH2 Inhibitoren der Fall ist. Diese Herangehensweise kann wie bereits dargestellt auch beinahe komplett supprimierte Immunpeptidome wiederherstellen und so die Immunevasion umkehren. Dies kann jedoch selbst dann von Nutzen sein, wenn die pharmakologische Modulation auch im gesunden Gewebe stattfindet, denn sehr häufig lassen sich dennoch HLA Liganden identifizieren, welche eine absolute Spezifität für die Tumoren aufweisen auch wenn auf Grund der Komplexität und vielen Variablen der Präsentation die exakte Ursache hierfür nicht immer klar gefunden werden kann. Wie bereits im Vorfeld erwähnt stellen in Bezug auf die Immunevasion die public neoepitopes eine spezielle Gruppe dar, da hier die mutierten HLA Liganden aus essenziellen Onkogenen stammen und so ein Verlust dieser Proteine zu einem Untergang des Tumors führen würde. Dementsprechend verlagert sich hier der Evasionsmechanismus hin zu dem noch weiter verbreiteten, der Downregulation oder dem Verlust der Antigenpräsentationsmaschinerie und insbesondere des HLA Komplexes.

Hierbei tritt als wohl häufigster Mechanismus der Immunevasion nicht der komplette Verlust des HLA-Komplexes auf, da dies mit einer erhöhten Aktivität von natürlichen Killerzellen einherginge. Stattdessen verlieren Tumorzellen gezielt ein HLA-Allel, was als „HLA loss of heterozygosity (HLA-LOH)“ beschrieben wurde und unter anderem das klinische Ansprechen auf Immuncheckpointblockade beeinflusst (55). Obwohl inzwischen Wirkstoffe identifiziert

wurden, welche eine solche HLA Downregulation umkehren können (56), ist der komplette genetische Verlust des HLA Alleles oder Teile der Antigenpräsentationsmaschinerie ein Schritt, welcher die Wirkung einer TZR-basierten Immuntherapie vollständig eliminiert. Eine mögliche Strategie diesen Mechanismus zu umgehen, ist die Kombination von konventionellen CAR-T-Zellen mit TZR-imitierenden CAR-T-Zellen. Hierbei werden in eine T-Zelle sowohl ein CAR mit TZR-imitierendem scFv gegen einen tumorspezifischen HLA Liganden eingebracht und ein CAR gegen ein Oberflächenprotein, wobei dieses CAR eine truncierte CD28 Domäne aufweist. Durch diese Kombination kommt es nur bei der gleichzeitigen Aktivierung des TZR-imitierendem scFv und des zweiten CAR gegen das Oberflächenprotein zu einer Aktivierung der CAR-T-Zellen. Dies erhöht nicht nur die Spezifität des Konstrukts, da das gleichzeitige Vorkommen beider Antigene nur auf den Tumorzellen zu erwarten ist, sondern es reduziert auch die Wahrscheinlichkeit der Immunevasion, da durch den zeitgleichen Angriff auf zwei Targets mit unterschiedlichem Präsentationsmechanismus das Risiko eines doppelten Verlustes beider Antigene weniger wahrscheinlich wird (57).

Neben den reaktiven biologischen Mechanismen, welche eine spezifische Therapie gegen pHLA verhindert, soll jedoch noch ein wichtiger Punkt angesprochen werden, welcher nur selten bei der Entwicklung dieser Wirkstoffe zur Sprache kommt: die Limitation der Therapie auf Bevölkerungsgruppen mit häufigen HLA Allel Subtypen. Wie bereits angesprochen ist der HLA Genpool hochpolymorph und im Rahmen der Evolution haben sich bestimmte HLA Allele weiter verbreitet als anderen. Zusätzlich ist die systematische HLA Typisierung von Bevölkerungen kostspielig und wird nur im Rahmen der Suche nach Knochenmarkspendern für allogene Stammzelltransplantationen regelhaft durchgeführt. Hierdurch sind insbesondere Bevölkerungsteile des globalen Südens in den entsprechenden Karteien kaum vertreten und die Forschung und Entwicklung von TZR-Produkten fokussiert sich in erster Linie auf die HLA Komplexe A*02:01 und A*03:01, welche sich besonders häufig in der kaukasischen Bevölkerung finden (5). Lediglich das Allel A*24:02 wird häufiger in die Forschung miteinbezogen, da dieser Genotyp im (südost)asiatischen Raum weit verbreitet ist und daher

eine sehr große Bevölkerungspopulation von einem Medikament mit dieser Restriktion profitieren könnte (58). Insgesamt zeigt sich aber eine systematische Benachteiligung von Bevölkerungsgruppen mit selteneren oder weniger systematisch erfassten HLA Typen. Dieses Problem könnte zum Beispiel umgangen werden, wenn für ein definiertes Antigen parallel nicht nur TZR-basierte Wirkstoff für ein HLA Allel identifiziert werden würden, sondern für ein breites Set an HLA Allelen. Da diese Strategien die Entwicklung deutlich aufwändiger machen, könnten als Alternative Targets identifiziert werden, welche nachweislich auf mehreren Allelen desselben HLA Supertyps präsentiert werden, was die Wahrscheinlichkeit erhöht, dass der Wirkstoff das Peptid im Kontext mehrerer unterschiedlicher HLA Komplexe erkennt. Eine wirklich breite Abdeckung von zahlreichen HLA Typen liefert bisher nur eine Bank aus EBV-spezifischen T-Zelllinien, welche für die Therapie von EBV-assoziierten Lymphomen nach einer Knochenmarktransplantation eingesetzt werden (59).

Insgesamt müssen TZR-basierten Immuntherapien auf dem Weg zum erfolgreichen klinischen Einsatz viele Hürden überwinden und eine vorausschauende Planung kann hier helfen mögliche Limitationen zu umgehen. Eine der besten Lösungen, welche die Entwicklung, Testung und der Einsatz von TZR-basierten Immuntherapien deutlich vereinfachen würde, wird nun im Folgenden diskutiert werden.

3.3. Zukünftige Herausforderungen

Zahlreiche Faktoren beeinflussen die Präsentation von HLA Liganden: die Expression der Antigene aus welchen sich die Peptide ableiten, die Abundanz der präsentierenden HLA Komplexe, die Effektivität der Antigenpräsentationsmaschinerie, die Konkurrenz durch anderen Peptide, welche auf der Zelloberfläche präsentiert werden und noch viele andere. Zusätzlich unterliegen diese Faktoren stetigen Veränderungen durch die Tumorbilogie aber auch die einwirkenden Therapien und die Veränderungen, welche das Immunsystem im Laufe einer Erkrankung erfährt. Hier stellt die letzte vorgestellte Arbeit zu einer TZR-imitierenden CAR-T Zelle hier eine interessante Ausnahme dar. Das genutzte Target ist direkt an die Proliferation der Tumorzellen geknüpft, wodurch dieses auch nach Vortherapien und

Veränderungen der Tumorbiologie weiterhin relevant sein sollte, denn die Fähigkeit der Krebszellen sich zu teilen, bleibt im Laufe der Tumorevolution essenziell. Somit beinhaltet dieses in mehreren Gesichtspunkten neue Therapeutikum die einzigartige Eigenschaft sofern die HLA Expression gewährleistet ist immer einen Angriffspunkt zu liefern und insbesondere bei hochproliferativen Subgruppen von Tumoren eine hohe Effektivität zeigt. Um dem Aspekt der sich unter Therapie verändernden Tumorzellen jedoch allgemein gerecht zu werden, wäre die ideale Ergänzung von TZR-basierten Therapien die Etablierung von therapiebegleitenden Diagnostika. Da bisher nur Surrogatparameter für die Präsentation der HLA Liganden Target verwendet werden wie die Expression des HLA Komplexes und des Antigens, würde der direkte Nachweis des HLA Liganden auf Tumorzellen von Patient*innen eine deutlich höhere Sicherheit bei der Selektion der Patient*innen mit sich bringen.

Um die Belastung für Patient*innen möglichst gering zu halten, bietet sich die Analyse von zirkulierenden Tumorzellen (circulating tumor cells, CTCs) für den Nachweis der Zielepitope an. Da CTCs jedoch nur in sehr geringer Anzahl von durchschnittlich 100/ml zu finden sind (60), ist eine effektive Isolation gepaart mit hochsensitiver Immunpeptidomik unerlässlich für die Entwicklung eines solchen therapiebegleitenden Diagnostikums. Wir postulieren jedoch, dass die Verbesserungen der Isolationsstrategie für HLA Liganden in Verbindung mit neuen massenspektrometrischen Analysemethoden und technischen Weiterentwicklungen der Massenspektrometer selbst, es bald ermöglichen werden, diese technische Herausforderung anzugehen und zu meistern. Dies würde nicht nur die Patientenauswahl deutlich vereinfachen und somit womöglich zu besseren klinischen Resultaten im Bereich der TZR Immuntherapien führen, sondern auch ein Therapiemonitoring erlauben, aus welchem sich ein Verlust der Präsentation des Targetepitops ablesen ließe.

4. Zusammenfassung

Die in dieser Arbeit zusammengeführten Publikationen illustrieren in anschaulicher Art und Weise wie TZR-basierte Immuntherapien einen immer größeren Stellenwert in der Therapie von malignen Erkrankungen einnehmen. In den ersten Arbeiten wurde sehr deutlich der Stellenwert der Immunpeptidomik unterstrichen, welche vor allem durch technische Weiterentwicklungen in der Isolation und Analyse von HLA Liganden die eigene Sensitivität weiter verbesserte. Hierdurch wird die Immunpeptidomik zum idealen Werkzeug, welches tumorspezifische Targets definieren kann, indem es nicht nur die Abundanz von HLA Liganden abschätzt, sondern auch deren Veränderungen nach unterschiedlichen biologischen oder pharmakologischen Stimuli nachverfolgen kann. Dieser Aspekt wurde im dritten und vierten Manuskript sehr klar erläutert, da es hier gelang das Immunpeptidom mittels epigenetischer Modulatoren so zu verändern, dass es die Immunevasion umkehren konnte und neue Subgruppen von tumorspezifischen HLA Liganden definierte. Für Tyrosinkinaseinhibitoren dagegen konnten wir zeigen, dass deren spezifische Inhibition eines Signalweges auch zu einer definierten Präsentation von Peptiden aus dem Pathway nach sich zieht. Darüber hinaus liefert die Immunpeptidomik auch wertvolle Informationen über potenzielle off-Targets mit deren Hilfe die Spezifität einer TZR-basierten Therapie genauer eingeschätzt wird, um höhergradige Toxizitäten zu vermeiden. Daher ist der Einsatz der Immunpeptidomik bereits heute eine unumgängliche Methode, welche die Entwicklung eines jeden TZR-basierten spezifischen Therapeutikums begleiten sollte wie die erfolgreiche Umsetzung u.a. in meinen Arbeiten zur NDC80 spezifischen TZR-imitierenden CAR-T Zelle bereits belegt hat. Hier wurde erstmals systematisch ein tumoragnostischer HLA Ligand unabhängig von der Art des Quellproteins identifiziert, welcher eine spezifische Elimination von Tumorzellen erlaubt, obwohl NDC80 auch in gesunden Zellen nachgewiesen werden kann. Das große therapeutische Fenster durch die unterschiedliche Prozessierung in Tumorzellen und dem Normalgewebe erlaubt somit die Nutzung eines bisher unbeachteten Targets, welches erst durch die Immunpeptidomik klar definiert werden konnte.

Der Stellenwert der Immunpeptidomik wird vermutlich in den kommenden Jahren noch weiter zunehmen, da durch die immer bessere Sensitivität der Massenspektrometrie und optimierte Isolationsmethoden die benötigten Zellzahlen für derartige Analysen immer kleiner werden und somit auch immunpeptidomische Analysen aus zirkulierenden Tumorzellen schon bald möglich sein könnten.

Kurzum, die massenspektrometrische Analyse von HLA Liganden ist und bleibt der Goldstandard für die Entwicklung TZR-basierter Immuntherapien und sollte bei der Entwicklung dieser Therapeutika immer integriert werden. Die Erfolge der präklinischen, translationalen und klinischen Forschung der vergangenen Jahre zu welchen auch meine Arbeiten entscheidend beigetragen haben, belegen, dass die Zulassung weiterer TZR-basierter Wirkstoffe inklusive der TZR-imitierenden CAR T Zellen für die Behandlung maligner Erkrankungen nur eine Frage der Zeit ist.

5. Literaturverzeichnis (eigene diskutierte Arbeiten)

Originalarbeit 1

Klatt MG, Mack KN, Bai Y, Aretz ZEH, Nathan LI, Mun SS, Dao T, Scheinberg DA. Solving an MHC allele-specific bias in the reported immunopeptidome. *JCI Insight*. 2020;5(19). DOI: 10.1172/jci.insight.141264

Originalarbeit 2

Klatt MG, Aretz ZEH, Curcio M, Gejman RS, Jones HF, Scheinberg DA. An input-controlled model system for identification of MHC bound peptides enabling laboratory comparisons of immunopeptidome experiments. *J Proteomics*. 2020;228:103921. DOI: 10.1016/j.jprot.2020.103921

Originalarbeit 3

Bourne CM, Mun SS, Dao T, Aretz ZEH, Molvi Z, Gejman RS, Daman A, Takata K, Steidl C, **Klatt MG***, Scheinberg DA*. Unmasking the suppressed immunopeptidome of EZH2-mutated diffuse large B-cell lymphomas through combination drug treatment. *Blood Adv*. 2022;6(14):4107-4121. *geteilte Letztautorenschaft
DOI: 10.1182/bloodadvances.2021006069

Originalarbeit 4

Charles A, Bourne CM, Korontsvit T, Aretz ZEH, Mun SS, Dao T, **Klatt MG***, Scheinberg DA*. Low-dose CDK4/6 inhibitors induce presentation of pathway specific MHC ligands as potential targets for cancer immunotherapy. *Oncoimmunology*. 2021;10(1):1916243. *geteilte Letztautorenschaft
DOI: 10.1080/2162402X.2021.1916243

Originalarbeit 5

Klatt MG, Dao T, Yang Z, Liu J, Mun SS, Dacek MM, Luo H, Gardner TJ, Bourne C, Peraro L, Aretz ZEH, Korontsvit T, Lau M, Kharas MG, Liu C, Scheinberg DA. A TCR mimic CAR T cell specific for NDC80 is broadly reactive with solid tumors and hematologic malignancies. *Blood*. 2022;140(8):861-874. DOI: 10.1182/blood.2021012882

6. Literaturverzeichnis (andere Arbeiten)

1. Hodi, F. S., O'Day, S. J., McDermott, D. F., Weber, R. W., Sosman, J. A., Haanen, J. B., Gonzalez, R., Robert, C., Schadendorf, D., Hassel, J. C., Akerley, W., Van Den Eertwegh, A. J. M., Lutzky, J., Lorigan, P., Vaubel, J. M., Linette, G. P., Hogg, D., Ottensmeier, C. H., Lebbé, C., ... Urban, W. J. (2010). Improved Survival with Ipilimumab in Patients with Metastatic Melanoma. *New England Journal of Medicine*, 363(8), 711–723. <https://doi.org/10.1056/NEJMoa1003466>
2. Nathan, P., Hassel, J. C., Rutkowski, P., Baurain, J.-F., Butler, M. O., Schlaak, M., Sullivan, R. J., Ochsenreither, S., Dummer, R., Kirkwood, J. M., Joshua, A. M., Sacco, J. J., Shoushtari, A. N., Orloff, M., Piulats, J. M., Milhem, M., Salama, A. K. S., Curti, B., Demidov, L., ... Piperno-Neumann, S. (2021). Overall Survival Benefit with Tebentafusp in Metastatic Uveal Melanoma. *New England Journal of Medicine*, 385(13), 1196–1206. <https://doi.org/10.1056/NEJMoa2103485>
3. Hassel, J. C., Piperno-Neumann, S., Rutkowski, P., Baurain, J.-F., Schlaak, M., Butler, M. O., Sullivan, R. J., Dummer, R., Kirkwood, J. M., Orloff, M., Sacco, J. J., Ochsenreither, S., Joshua, A. M., Gastaud, L., Curti, B., Piulats, J. M., Salama, A. K. S., Shoushtari, A. N., Demidov, L., ... Nathan, P. (2023). Three-Year Overall Survival with Tebentafusp in Metastatic Uveal Melanoma. *New England Journal of Medicine*, NEJMoa2304753. <https://doi.org/10.1056/NEJMoa2304753>
4. Neefjes, J., Jongsma, M. L. M., Paul, P., & Bakke, O. (2011). Towards a systems understanding of MHC class I and MHC class II antigen presentation. *Nature Reviews Immunology*, 11(12), 823–836. <https://doi.org/10.1038/nri3084>
5. Robinson, J., Barker, D. J., Georgiou, X., Cooper, M. A., Flicek, P., & Marsh, S. G. E. (2019). IPD-IMGT/HLA Database. *Nucleic Acids Research*, gkz950. <https://doi.org/10.1093/nar/gkz950>
6. Chandran, S. S., & Klebanoff, C. A. (2019). T cell receptor-based cancer immunotherapy: Emerging efficacy and pathways of resistance. *Immunological Reviews*, 290(1), 127–147. <https://doi.org/10.1111/imr.12772>
7. Falk, K., Rötzschke, O., Stevanović, S., Jung, G., & Rammensee, H.-G. (1991). Allele-specific motifs revealed by sequencing of self-peptides eluted from MHC molecules. *Nature*, 351(6324), 290–296. <https://doi.org/10.1038/351290a0>
8. Nguyen, A. T., Szeto, C., & Gras, S. (2021). The pockets guide to HLA class I molecules. *Biochemical Society Transactions*, 49(5), 2319–2331. <https://doi.org/10.1042/BST20210410>
9. Zajonc, D. M. (2020). Unconventional Peptide Presentation by Classical MHC Class I and Implications for T and NK Cell Activation. *International Journal of Molecular Sciences*, 21(20), 7561. <https://doi.org/10.3390/ijms21207561>
10. Kievits, F., Ivanyi, P., Krimpenfort, P., Berns, A., & Ploegh, H. L. (1987). HLA-restricted recognition of viral antigens in HLA transgenic mice. *Nature*, 329(6138), 447–449. <https://doi.org/10.1038/329447a0>
11. Falk, K., Rötzschke, O., & Rammensee, H.-G. (1990). Cellular peptide composition governed by major histocompatibility complex class I molecules. *Nature*, 348(6298), 248–251. <https://doi.org/10.1038/348248a0>
12. Rötzschke, O., Falk, K., Deres, K., Schild, H., Norda, M., Metzger, J., Jung, G., & Rammensee, H.-G. (1990). Isolation and analysis of naturally processed viral peptides as recognized by cytotoxic T cells. *Nature*, 348(6298), 252–254. <https://doi.org/10.1038/348252a0>
13. Klatt, M. G., Mack, K. N., Bai, Y., Aretz, Z. E. H., Nathan, L. I., Mun, S. S., Dao, T., & Scheinberg, D. A. (2020). Solving an MHC allele-specific bias in the reported immunopeptidome. *JCI Insight*, 5(19), e141264. <https://doi.org/10.1172/jci.insight.141264>

14. Purcell, A. W., Ramarathinam, S. H., & Ternette, N. (2019). Mass spectrometry–based identification of MHC-bound peptides for immunopeptidomics. *Nature Protocols*, 14(6), 1687–1707. <https://doi.org/10.1038/s41596-019-0133-y>
15. Pak, H., Michaux, J., Huber, F., Chong, C., Stevenson, B. J., Müller, M., Coukos, G., & Bassani-Sternberg, M. (2021). Sensitive Immunopeptidomics by Leveraging Available Large-Scale Multi-HLA Spectral Libraries, Data-Independent Acquisition, and MS/MS Prediction. *Molecular & Cellular Proteomics*, 20, 100080. <https://doi.org/10.1016/j.mcpro.2021.100080>
16. Tran, N. H., Qiao, R., Xin, L., Chen, X., Liu, C., Zhang, X., Shan, B., Ghodsi, A., & Li, M. (2019). Deep learning enables de novo peptide sequencing from data-independent-acquisition mass spectrometry. *Nature Methods*, 16(1), 63–66. <https://doi.org/10.1038/s41592-018-0260-3>
17. Zhang, J., Xin, L., Shan, B., Chen, W., Xie, M., Yuen, D., Zhang, W., Zhang, Z., Lajoie, G. A., & Ma, B. (2012). PEAKS DB: De Novo Sequencing Assisted Database Search for Sensitive and Accurate Peptide Identification. *Molecular & Cellular Proteomics*, 11(4), M111.010587. <https://doi.org/10.1074/mcp.M111.010587>
18. Bern, M., Kil, Y. J., & Becker, C. (2012). Byonic: Advanced Peptide and Protein Identification Software. *Current Protocols in Bioinformatics*, 40(1). <https://doi.org/10.1002/0471250953.bi1320s40>
19. Phulphagar, K. M., Ctortocka, C., Jacome, A. S. V., Klaeger, S., Verzani, E. K., Hernandez, G. M., Udeshi, N. D., Clauser, K. R., Abelin, J. G., & Carr, S. A. (2023). Sensitive, High-Throughput HLA-I and HLA-II Immunopeptidomics Using Parallel Accumulation-Serial Fragmentation Mass Spectrometry. *Molecular & Cellular Proteomics*, 22(6), 100563. <https://doi.org/10.1016/j.mcpro.2023.100563>
20. Hu, Q., Noll, R. J., Li, H., Makarov, A., Hardman, M., & Graham Cooks, R. (2005). The Orbitrap: A new mass spectrometer. *Journal of Mass Spectrometry*, 40(4), 430–443. <https://doi.org/10.1002/jms.856>
21. Ishihara, M., Kageyama, S., Miyahara, Y., Ishikawa, T., Ueda, S., Soga, N., Naota, H., Mukai, K., Harada, N., Ikeda, H., & Shiku, H. (2020). MAGE-A4, NY-ESO-1 and SAGE mRNA expression rates and co-expression relationships in solid tumours. *BMC Cancer*, 20(1), 606. <https://doi.org/10.1186/s12885-020-07098-4>
22. Marcu, A., Bichmann, L., Kuchenbecker, L., Kowalewski, D. J., Freudenmann, L. K., Backert, L., Mühlenbruch, L., Szolek, A., Lübke, M., Wagner, P., Engler, T., Matovina, S., Wang, J., Hauri-Hohl, M., Martin, R., Kapolou, K., Walz, J. S., Velz, J., Moch, H., ... Neidert, M. C. (2021). HLA Ligand Atlas: A benign reference of HLA-presented peptides to improve T-cell-based cancer immunotherapy. *Journal for ImmunoTherapy of Cancer*, 9(4), e002071. <https://doi.org/10.1136/jitc-2020-002071>
23. Morgan, R. A., Chinnasamy, N., Abate-Daga, D., Gros, A., Robbins, P. F., Zheng, Z., Dudley, M. E., Feldman, S. A., Yang, J. C., Sherry, R. M., Phan, G. Q., Hughes, M. S., Kammula, U. S., Miller, A. D., Hessman, C. J., Stewart, A. A., Restifo, N. P., Quezado, M. M., Alimchandani, M., ... Rosenberg, S. A. (2013). Cancer Regression and Neurological Toxicity Following Anti-MAGE-A3 TCR Gene Therapy. *Journal of Immunotherapy*, 36(2), 133–151. <https://doi.org/10.1097/CJI.0b013e3182829903>
24. Blatnik, R., Mohan, N., Bonsack, M., Falkenby, L. G., Hoppe, S., Josef, K., Steinbach, A., Becker, S., Nadler, W. M., Rucevic, M., Larsen, M. R., Salek, M., & Riemer, A. B. (2018). A Targeted LC-MS Strategy for Low-Abundant HLA Class-I-Presented Peptide Detection Identifies Novel Human Papillomavirus T-Cell Epitopes. *PROTEOMICS*, 18(11), 1700390. <https://doi.org/10.1002/pmic.201700390>
25. Wang, Q., Douglass, J., Hwang, M. S., Hsiue, E. H.-C., Mog, B. J., Zhang, M., Papadopoulos, N., Kinzler, K. W., Zhou, S., & Vogelstein, B. (2019). Direct Detection and Quantification of Neoantigens. *Cancer Immunology Research*, 7(11), 1748–1754. <https://doi.org/10.1158/2326-6066.CIR-19-0107>

26. Chandran, S. S., Ma, J., Klatt, M. G., Dündar, F., Bandlamudi, C., Razavi, P., Wen, H. Y., Weigelt, B., Zumbo, P., Fu, S. N., Banks, L. B., Yi, F., Vercher, E., Etxeberria, I., Bestman, W. D., Da Cruz Paula, A., Aricescu, I. S., Drilon, A., Betel, D., ... Klebanoff, C. A. (2022). Immunogenicity and therapeutic targeting of a public neoantigen derived from mutated PIK3CA. *Nature Medicine*, 28(5), 946–957. <https://doi.org/10.1038/s41591-022-01786-3>
27. Gurung, H. R., Heidersbach, A. J., Darwish, M., Chan, P. P. F., Li, J., Beresini, M., Zill, O. A., Wallace, A., Tong, A.-J., Hascall, D., Torres, E., Chang, A., Lou, K., Hei-W., Abdolazimi, Y., Hammer, C., Xavier-Magalhães, A., Marcu, A., Vaidya, S., Le, D. D., ... Rose, C. M. (2023). Systematic discovery of neoepitope–HLA pairs for neoantigens shared among patients and tumor types. *Nature Biotechnology*. <https://doi.org/10.1038/s41587-023-01945-y>
28. Montesion, M., Murugesan, K., Jin, D. X., Sharaf, R., Sanchez, N., Guria, A., Minker, M., Li, G., Fisher, V., Sokol, E. S., Pavlick, D. C., Moore, J. A., Braly, A., Singal, G., Fabrizio, D., Comment, L. A., Rizvi, N. A., Alexander, B. M., Frampton, G. M., ... Albacker, L. A. (2021). Somatic HLA Class I Loss Is a Widespread Mechanism of Immune Evasion Which Refines the Use of Tumor Mutational Burden as a Biomarker of Checkpoint Inhibitor Response. *Cancer Discovery*, 11(2), 282–292. <https://doi.org/10.1158/2159-8290.CD-20-0672>
29. Mohammed, F., Stones, D. H., Zarlring, A. L., Willcox, C. R., Shabanowitz, J., Cummings, K. L., Hunt, D. F., Cobbold, M., Engelhard, V. H., & Willcox, B. E. (2017). The antigenic identity of human class I MHC phosphopeptides is critically dependent upon phosphorylation status. *Oncotarget*, 8(33), 54160–54172. <https://doi.org/10.18632/oncotarget.16952>
30. Patskovsky, Y., Natarajan, A., Patskovska, L., Nyovanie, S., Joshi, B., Morin, B., Brittsan, C., Huber, O., Gordon, S., Michelet, X., Schmitzberger, F., Stein, R. B., Findeis, M. A., Hurwitz, A., Van Dijk, M., Chantzoura, E., Yague, A. S., Pollack Smith, D., Buell, J. S., ... Krosggaard, M. (2023). Molecular mechanism of phosphopeptide neoantigen immunogenicity. *Nature Communications*, 14(1), 3763. <https://doi.org/10.1038/s41467-023-39425-1>
31. Molvi, Z., Klatt, M. G., Dao, T., Urraca, J., Scheinberg, D. A., & O'Reilly, R. J. (2023). The landscape of MHC-presented phosphopeptides yields actionable shared tumor antigens for cancer immunotherapy across multiple HLA alleles. *Journal for ImmunoTherapy of Cancer*, 11(9), e006889. <https://doi.org/10.1136/jitc-2023-006889>
32. Ouspenskaia, T., Law, T., Clauser, K. R., Klaeger, S., Sarkizova, S., Aguet, F., Li, B., Christian, E., Knisbacher, B. A., Le, P. M., Hartigan, C. R., Keshishian, H., Apffel, A., Oliveira, G., Zhang, W., Chen, S., Chow, Y. T., Ji, Z., Jungreis, I., ... Regev, A. (2022). Unannotated proteins expand the MHC-I-restricted immunopeptidome in cancer. *Nature Biotechnology*, 40(2), 209–217. <https://doi.org/10.1038/s41587-021-01021-3>
33. Goyal, A., Bauer, J., Hey, J., Papageorgiou, D. N., Stepanova, E., Daskalakis, M., Scheid, J., Dubbelaar, M., Klimovich, B., Schwarz, D., Märklin, M., Roerden, M., Lin, Y.-Y., Ma, T., Mücke, O., Rammensee, H.-G., Lübbert, M., Loayza-Puch, F., Krijgsveld, J., ... Plass, C. (2023). DNMT and HDAC inhibition induces immunogenic neoantigens from human endogenous retroviral element-derived transcripts. *Nature Communications*, 14(1), 6731. <https://doi.org/10.1038/s41467-023-42417-w>
34. Oh, C. Y., Klatt, M. G., Bourne, C., Dao, T., Dacek, M. M., Brea, E. J., Mun, S. S., Chang, A. Y., Korontsvit, T., & Scheinberg, D. A. (2019). ALK and RET Inhibitors Promote HLA Class I Antigen Presentation and Unmask New Antigens within the Tumor Immunopeptidome. *Cancer Immunology Research*, 7(12), 1984–1997. <https://doi.org/10.1158/2326-6066.CIR-19-0056>
35. Jones, H. F., Molvi, Z., Klatt, M. G., Dao, T., & Scheinberg, D. A. (2021). Empirical and Rational Design of T Cell Receptor-Based Immunotherapies. *Frontiers in Immunology*, 11, 585385. <https://doi.org/10.3389/fimmu.2020.585385>

36. Walter, S., Weinschenk, T., Stenzl, A., Zdrojowy, R., Pluzanska, A., Szczylik, C., Staehler, M., Brugger, W., Dietrich, P.-Y., Mendrzyk, R., Hilf, N., Schoor, O., Fritsche, J., Mahr, A., Maurer, D., Vass, V., Trautwein, C., Lewandrowski, P., Flohr, C., ... Singh-Jasuja, H. (2012). Multipeptide immune response to cancer vaccine IMA901 after single-dose cyclophosphamide associates with longer patient survival. *Nature Medicine*, 18(8), 1254–1261. <https://doi.org/10.1038/nm.2883>
37. Rojas, L. A., Sethna, Z., Soares, K. C., Olcese, C., Pang, N., Patterson, E., Lihm, J., Ceglia, N., Guasp, P., Chu, A., Yu, R., Chandra, A. K., Waters, T., Ruan, J., Amisaki, M., Zeboudj, A., Odgerel, Z., Payne, G., Derhovanessian, E., ... Balachandran, V. P. (2023). Personalized RNA neoantigen vaccines stimulate T cells in pancreatic cancer. *Nature*, 618(7963), 144–150. <https://doi.org/10.1038/s41586-023-06063-y>
38. Cameron, B. J., Gerry, A. B., Dukes, J., Harper, J. V., Kannan, V., Bianchi, F. C., Grand, F., Brewer, J. E., Gupta, M., Plesa, G., Bossi, G., Vuidepot, A., Powlesland, A. S., Legg, A., Adams, K. J., Bennett, A. D., Pumphrey, N. J., Williams, D. D., Binder-Scholl, G., ... Jakobsen, B. K. (2013). Identification of a Titin-Derived HLA-A1–Presented Peptide as a Cross-Reactive Target for Engineered MAGE A3–Directed T Cells. *Science Translational Medicine*, 5(197). <https://doi.org/10.1126/scitranslmed.3006034>
39. Hong, D. S., Van Tine, B. A., Biswas, S., McAlpine, C., Johnson, M. L., Olszanski, A. J., Clarke, J. M., Araujo, D., Blumenschein, G. R., Kebriaei, P., Lin, Q., Tipping, A. J., Sanderson, J. P., Wang, R., Trivedi, T., Annareddy, T., Bai, J., Rafail, S., Sun, A., ... Butler, M. O. (2023). Autologous T cell therapy for MAGE-A4+ solid cancers in HLA-A*02+ patients: A phase 1 trial. *Nature Medicine*, 29(1), 104–114. <https://doi.org/10.1038/s41591-022-02128-z>
40. Ishihara, M., Kitano, S., Kageyama, S., Miyahara, Y., Yamamoto, N., Kato, H., Mishima, H., Hattori, H., Funakoshi, T., Kojima, T., Sasada, T., Sato, E., Okamoto, S., Tomura, D., Nukaya, I., Chono, H., Mineno, J., Kairi, M. F., Diem Hoang Nguyen, P., ... Shiku, H. (2022). NY-ESO-1-specific redirected T cells with endogenous TCR knockdown mediate tumor response and cytokine release syndrome. *Journal for ImmunoTherapy of Cancer*, 10(6), e003811. <https://doi.org/10.1136/jitc-2021-003811>
41. Rohaan, M. W., Borch, T. H., Van Den Berg, J. H., Met, Ö., Kessels, R., Geukes Foppen, M. H., Stoltenborg Granhøj, J., Nuijen, B., Nijenhuis, C., Jedema, I., Van Zon, M., Scheij, S., Beijnen, J. H., Hansen, M., Voermans, C., Noringriis, I. M., Monberg, T. J., Holmstroem, R. B., Wever, L. D. V., ... Haanen, J. B. A. G. (2022). Tumor-Infiltrating Lymphocyte Therapy or Ipilimumab in Advanced Melanoma. *New England Journal of Medicine*, 387(23), 2113–2125. <https://doi.org/10.1056/NEJMoa2210233>
42. Kirkey, D. C., Loeb, A. M., Castro, S., McKay, C. N., Perkins, L., Pardo, L., Leonti, A. R., Tang, T. T., Loken, M. R., Brodersen, L. E., Loeb, K. R., Scheinberg, D. A., Le, Q., & Meshinchi, S. (2023). Therapeutic targeting of PRAME with mTCRCAR T cells in acute myeloid leukemia. *Blood Advances*, 7(7), 1178–1189. <https://doi.org/10.1182/bloodadvances.2022008304>
43. Douglass, J., Hsiue, E. H.-C., Mog, B. J., Hwang, M. S., DiNapoli, S. R., Pearlman, A. H., Miller, M. S., Wright, K. M., Azurmendi, P. A., Wang, Q., Paul, S., Schaefer, A., Skora, A. D., Molin, M. D., Konig, M. F., Liu, Q., Watson, E., Li, Y., Murphy, M. B., ... Zhou, S. (2021). Bispecific antibodies targeting mutant RAS neoantigens. *Science Immunology*, 6(57), eabd5515. <https://doi.org/10.1126/sciimmunol.abd5515>
44. Liu, H., Xu, Y., Xiang, J., Long, L., Green, S., Yang, Z., Zimdahl, B., Lu, J., Cheng, N., Horan, L. H., Liu, B., Yan, S., Wang, P., Diaz, J., Jin, L., Nakano, Y., Morales, J. F., Zhang, P., Liu, L., ... Liu, C. (2017). Targeting Alpha-Fetoprotein (AFP)–MHC Complex with CAR T-Cell Therapy for Liver Cancer. *Clinical Cancer Research*, 23(2), 478–488. <https://doi.org/10.1158/1078-0432.CCR-16-1203>

45. Mansilla-Soto, J., Eyquem, J., Haubner, S., Hamieh, M., Feucht, J., Paillon, N., Zucchetti, A. E., Li, Z., Sjöstrand, M., Lindenbergh, P. L., Saetersmoen, M., Dobrin, A., Maurin, M., Iyer, A., Garcia Angus, A., Miele, M. M., Zhao, Z., Giavridis, T., Van Der Stegen, S. J. C., ... Sadelain, M. (2022). HLA-independent T cell receptors for targeting tumors with low antigen density. *Nature Medicine*, 28(2), 345–352. <https://doi.org/10.1038/s41591-021-01621-1>
46. Immisch, L., Papafotiou, G., Popp, O., Mertins, P., Blankenstein, T., & Willimsky, G. (2022). H3.3K27M mutation is not a suitable target for immunotherapy in HLA-A2⁺ patients with diffuse midline glioma. *Journal for ImmunoTherapy of Cancer*, 10(10), e005535. <https://doi.org/10.1136/jitc-2022-005535>
47. Crean, R. M., MacLachlan, B. J., Madura, F., Whalley, T., Rizkallah, P. J., Holland, C. J., McMurrin, C., Harper, S., Godkin, A., Sewell, A. K., Pudney, C. R., Van Der Kamp, M. W., & Cole, D. K. (2020). Molecular Rules Underpinning Enhanced Affinity Binding of Human T Cell Receptors Engineered for Immunotherapy. *Molecular Therapy - Oncolytics*, 18, 443–456. <https://doi.org/10.1016/j.omto.2020.07.008>
48. Border, E. C., Sanderson, J. P., Weissensteiner, T., Gerry, A. B., & Pumphrey, N. J. (2019). Affinity-enhanced T-cell receptors for adoptive T-cell therapy targeting MAGE-A10: Strategy for selection of an optimal candidate. *Oncot Immunology*, 8(2), e1532759. <https://doi.org/10.1080/2162402X.2018.1532759>
49. Bentzen, A. K., Such, L., Jensen, K. K., Marquard, A. M., Jessen, L. E., Miller, N. J., Church, C. D., Lyngaa, R., Koelle, D. M., Becker, J. C., Linnemann, C., Schumacher, T. N. M., Marcatili, P., Nghiem, P., Nielsen, M., & Hadrup, S. R. (2018). T cell receptor fingerprinting enables in-depth characterization of the interactions governing recognition of peptide–MHC complexes. *Nature Biotechnology*, 36(12), 1191–1196. <https://doi.org/10.1038/nbt.4303>
50. Birnbaum, M. E., Mendoza, J. L., Sethi, D. K., Dong, S., Glanville, J., Dobbins, J., Özkan, E., Davis, M. M., Wucherpfennig, K. W., & Garcia, K. C. (2014). Deconstructing the Peptide-MHC Specificity of T Cell Recognition. *Cell*, 157(5), 1073–1087. <https://doi.org/10.1016/j.cell.2014.03.047>
51. Gejman, R. S., Jones, H. F., Klatt, M. G., Chang, A. Y., Oh, C. Y., Chandran, S. S., Korontsvit, T., Zakahleva, V., Dao, T., Klebanoff, C. A., & Scheinberg, D. A. (2020). Identification of the Targets of T-cell Receptor Therapeutic Agents and Cells by Use of a High-Throughput Genetic Platform. *Cancer Immunology Research*, 8(5), 672–684. <https://doi.org/10.1158/2326-6066.CIR-19-0745>
52. Hsiue, E. H.-C., Wright, K. M., Douglass, J., Hwang, M. S., Mog, B. J., Pearlman, A. H., Paul, S., DiNapoli, S. R., Konig, M. F., Wang, Q., Schaefer, A., Miller, M. S., Skora, A. D., Azurmendi, P. A., Murphy, M. B., Liu, Q., Watson, E., Li, Y., Pardoll, D. M., ... Zhou, S. (2021). Targeting a neoantigen derived from a common TP53 mutation. *Science*, 371(6533), eabc8697. <https://doi.org/10.1126/science.abc8697>
53. Srivastava, P., Paluch, B. E., Matsuzaki, J., James, S. R., Collamat-Lai, G., Blagitko-Dorfs, N., Ford, L. A., Naqash, R., Lübbert, M., Karpf, A. R., Nemeth, M. J., & Griffiths, E. A. (2016). Induction of cancer testis antigen expression in circulating acute myeloid leukemia blasts following hypomethylating agent monotherapy. *Oncotarget*, 7(11), 12840–12856. <https://doi.org/10.18632/oncotarget.7326>
54. Almstedt, M., Blagitko-Dorfs, N., Duque-Afonso, J., Karbach, J., Pfeifer, D., Jäger, E., & Lübbert, M. (2010). The DNA demethylating agent 5-aza-2'-deoxycytidine induces expression of NY-ESO-1 and other cancer/testis antigens in myeloid leukemia cells. *Leukemia Research*, 34(7), 899–905. <https://doi.org/10.1016/j.leukres.2010.02.004>
55. Chowell, D., Morris, L. G. T., Grigg, C. M., Weber, J. K., Samstein, R. M., Makarov, V., Kuo, F., Kendall, S. M., Requena, D., Riaz, N., Greenbaum, B., Carroll, J., Garon, E., Hyman, D. M., Zehir, A., Solit, D., Berger, M., Zhou, R., Rizvi, N. A., & Chan, T. A. (2018). Patient HLA class I genotype influences cancer response to checkpoint blockade immunotherapy. *Science*, 359(6375), 582–587. <https://doi.org/10.1126/science.aao4572>

56. Demel, U. M., Böger, M., Yousefian, S., Grunert, C., Zhang, L., Hotz, P. W., Gottschlich, A., Köse, H., Isaakidis, K., Vonficht, D., Grünschläger, F., Rohleder, E., Wagner, K., Dönig, J., Igl, V., Brzezicha, B., Baumgartner, F., Habringer, S., Löber, J., ... Keller, U. (2022). Activated SUMOylation restricts MHC class I antigen presentation to confer immune evasion in cancer. *Journal of Clinical Investigation*, 132(9), e152383. <https://doi.org/10.1172/JCI152383>
57. Dao, T., Xiong, G., Mun, S. S., Meyerberg, J., Korontsvit, T., Xiang, J., Cui, Z., Chang, A. Y., Jarvis, C. A., Cai, W., Luo, H., Pierson, A. J., Daniyan, A. F., Yoo, S., Takao, S., Kharas, M. G., Kentsis, A., Liu, C., & Scheinberg, D. A. (2023). Dual-receptor T cell platform with Ab-TCR and costimulatory receptor achieves specificity and potency against AML. *Blood Journal*, blood.2023021054. <https://doi.org/10.1182/blood.2023021054>
58. Li, Z., Gong, H., Liu, Q., Wu, W., Cheng, J., Mei, Y., Chen, Y., Zheng, H., Yu, X., Zhong, S., & Li, Y. (2020). Identification of an HLA-A*24:02-restricted α -fetoprotein signal peptide-derived antigen and its specific T-cell receptor for T-cell immunotherapy. *Immunology*, 159(4), 384–392. <https://doi.org/10.1111/imm.13168>
59. Prockop, S., Doubrovina, E., Suser, S., Heller, G., Barker, J., Dahi, P., Perales, M. A., Papadopoulos, E., Sauter, C., Castro-Malaspina, H., Boulad, F., Curran, K. J., Giralt, S., Gyurkocza, B., Hsu, K. C., Jakubowski, A., Hanash, A. M., Kernan, N. A., Kobos, R., ... O'Reilly, R. J. (2020). Off-the-shelf EBV-specific T cell immunotherapy for rituximab-refractory EBV-associated lymphoma following transplantation. *Journal of Clinical Investigation*, 130(2), 733–747. <https://doi.org/10.1172/JCI121127>
60. Sarioglu, A. F., Aceto, N., Kojic, N., Donaldson, M. C., Zeinali, M., Hamza, B., Engstrom, A., Zhu, H., Sundaresan, T. K., Miyamoto, D. T., Luo, X., Bardia, A., Wittner, B. S., Ramaswamy, S., Shioda, T., Ting, D. T., Stott, S. L., Kapur, R., Maheswaran, S., ... Toner, M. (2015). A microfluidic device for label-free, physical capture of circulating tumor cell clusters. *Nature Methods*, 12(7), 685–691. <https://doi.org/10.1038/nmeth.3404>

7. Danksagung

Zuerst gilt mein Dank Herrn Prof. Dr. med. Ulrich Keller, der als Direktor der Klinik für Hämatologie, Onkologie und Tumorimmunologie am Campus Benjamin Franklin sowie als ärztlicher Zentrumsleiter meine Forschungsarbeit stets mit allen Mitteln unterstützt hat. Ebenso danke ich Prof. Dr. med. Lothar Kanz, ehemaliger ärztlicher Direktor der Medizinischen Universitätsklinik Tübingen Abteilung für Onkologie, Hämatologie, Immunologie, Rheumatologie und Pulmologie, welcher mich in den ersten Jahren meiner Ausbildung für die Hämatologie und Onkologie begeisterte.

Zu größtem Dank bin ich meinen wissenschaftlichen Mentoren verpflichtet, welche nicht nur durch wissenschaftliche Exzellenz, sondern auch durch ihre persönlichen Qualitäten und Offenheit meine Kreativität förderten und mir halfen, meine Faszination für Tumorimmunologie immer weiter vertiefen zu können: Ich danke aus der Abteilung für Immunologie der Universität Tübingen dem langjährigen Direktor Prof. Dr. rer. nat. Hans-Georg Rammensee sowie dem ehemaligen Leiter des Wirkstoffpeptidlabors Prof. Dr. rer. nat. Stefan Stevanović für die Einführung in die Immunpeptidomik (als diese noch gar nicht diesen Namen trug) und dass sie ihr unendliches Wissen über T-Zell Immunologie mit mir teilten. Ich danke Prof. Nicholas (Nick) Haining, ehemaliger Arbeitsgruppenleiter am Dana-Farber Cancer Institute in Boston, dass er mir beigebracht hat, wie man große und großartige Experimente plant. Ich danke Prof. David (Dave) Scheinberg vom Memorial Sloan Kettering Cancer Center (MSKCC) in New York, dass er mir die Freiheit gegeben und das Vertrauen geschenkt hat mein eigenes kleines Labor innerhalb seines Labors aufzubauen und die Immunpeptidomik am „Tri-Institutional Campus“ zu etablieren und weiter bekannt zu machen. Ich danke Prof. Christopher (Chris) Klebanoff, ebenfalls MSKCC, für seine kreativen Ideen zu mutierten HLA Liganden und unsere langjährige, spannende und sehr erfolgreiche Kollaboration, welche hoffentlich noch viele Jahre bestehen wird. Insbesondere danke ich aber den unzähligen Wissenschaftlerinnen und Wissenschaftlern, welche mich auf meinem Weg unterstützt haben und die Forschung zu einer so wundervollen, kreativen und bereichernden Arbeit machen.

Nicht zuletzt und ganz besonders danke ich meiner Familie, meiner Frau und meinen zwei Kindern, welche mir immer wieder die nötige Kraft, Ausdauer und Rückhalt geben und mich motivieren gemeinsam alle Ziele zu erreichen. Ich bin unendlich dankbar, dass ich euch habe!

8. Erklärung

§ 4 Abs. 3 (1) der HabOMed der Charité

Hiermit erkläre ich, dass

- 1) weder früher noch gleichzeitig ein Habilitationsverfahren durchgeführt oder angemeldet wurde,
- 2) die vorgelegte Habilitationsschrift ohne fremde Hilfe verfasst, die beschriebenen Ergebnisse selbst gewonnen sowie die verwendeten Hilfsmittel, die Zusammenarbeit mit anderen Wissenschaftlern/ Wissenschaftlerinnen und mit technischen Hilfskräften sowie die verwendete Literatur vollständig in der Habilitationsschrift angegeben wurden,
- 3) mir die geltende Habilitationsordnung bekannt ist.

Ich erkläre ferner, dass mir die Satzung der Charité – Universitätsmedizin Berlin zur Sicherung Guter Wissenschaftlicher Praxis bekannt ist und ich mich zur Einhaltung dieser Satzung verpflichte.

.....
Ort, Datum

.....
Unterschrift